

BAT MICROBIOME RESISTANCE THROUGH FUNCTIONAL REDUNDANCY IN  
RESPONSE TO A FUNGAL PATHOGEN

by

Matthew S. Grisnik

A Dissertation Submitted in Partial Fulfillment of the Requirements for the Degree of  
Doctor of Philosophy in Molecular Biosciences

Middle Tennessee State University

April 2021

Dissertation Committee:

Dr. Donald Walker, Committee Chair

Dr. Mary Farone, Committee Member

Dr. Chris Herlihy, Committee Member

Dr. John Munafo, Committee Member

Dr. Joshua Grinath, Committee Member

## ACKNOWLEDGMENTS

First and foremost, I would like to thank my mentor and advisor Dr. Donald Walker for his guidance and support over the many years we have worked together, I could not have asked for a better advisor.

Next, I want to thank the rest of my committee, Dr. Mary Farone, Dr. Chris Herlihy, Dr. John Munafo, and Dr. Joshua Grinath. Your advice and guidance strengthened the quality of my work. In particular I would like to thank Dr. Joshua Grinath for imparting what I can assume is only a fraction of his statistical knowledge.

Lastly, I want to thank Jake Leys, Olivia Bowers, Ryan Hanscom, and the rest of the graduate and undergraduate students that have provided assistance and support throughout my degree.

## ABSTRACT

Planet Earth is currently experiencing a loss of biodiversity characterized by population declines that exceed the accepted background extinction rates. One of the drivers of this decline are emerging pathogens, with fungi representing a disproportionate percentage of pathogens causing decline. In 2006, *Pseudogymnoascus destructans* was introduced into the United States and has rapidly spread, threatening extinction of multiple bat species. The threat of emerging fungal pathogens has led to increased interest in understanding how the host associated cutaneous microbial assemblage interacts with fungal pathogens, particularly within the context of host health. In order to understand how the host associated microbial assemblage interacts with fungal pathogens, it is imperative to understand how assemblages are structured and maintained across the landscape. Metacommunity theory provides a way to understand local patterns within the context of interactions at the regional scale. The overall objective of my work is to understand how the bat cutaneous microbial assemblage interacts with *P. destructans* across the landscape. Previous work has suggested that there is a decoupling of taxonomy and function within microbial assemblages, therefore, I am interested in understanding how both taxonomic and functional assemblages respond to the presence of *P. destructans*. To address these objectives, I sampled bat cutaneous microbial assemblages across Tennessee and used high-throughput DNA sequencing techniques to characterize bat cutaneous microbial assemblages both taxonomically and functionally across the landscape in the presence/absence of *P. destructans*. Results indicate that the presence of *P. destructans* correlates with a shift in taxonomic microbial assemblage

structure but not necessarily function. Additionally, at the landscape scale, results suggest that the environment is one of the main drivers of the bat cutaneous microbial assemblage structure, and that the presence of *P. destructans* influences this relationship. I also tested and found that microorganisms composing the bat skin microbiome have antifungal activity against *P. destructans*.

## TABLE OF CONTENTS

LIST OF FIGURES.....	vii
LIST OF TABLES.....	ix
CHAPTER I: INTRODUCTION.....	1
References.....	10
CHAPTER II: THE CUTANEOUS MICROBIOTA OF BATS HAS <i>IN VITRO</i> ANTIFUNGAL ACTIVITY AGAINST THE WHITE NOSE PATHOGEN.....	13
Abstract.....	13
Introduction.....	14
Methods.....	17
Results.....	27
Discussion.....	38
Acknowledgments.....	42
References.....	43
CHAPTER III: HOST MICROBIOME FUNCTIONAL RESISTANCE TO FUNGAL PATHOGENICITY.....	47
Abstract.....	47
Introduction.....	48
Methods.....	51
Results.....	59
Discussion.....	67
References.....	73

CHAPTER IV: THE PRESENCE OF <i>PSEUDOGYMNOASCUS DESTRUCTANS</i> , A FUNGAL PATHOGEN OF BATS, CORRELATES WITH CHANGES IN MICROBIAL METACOMMUNITY STRUCTURE.....	78
Abstract.....	78
Introduction.....	79
Methods.....	85
Results.....	93
Discussion.....	104
Acknowledgments.....	110
References.....	111
CHAPTER V: OVERALL CONCLUSIONS.....	115
References.....	119
APPENDICES.....	120
Appendix A: Mothur Commands .....	121
Appendix B: qPCR Results.....	123
Appendix C: Mothur Commands .....	125
Appendix D: IACUC Approval .....	127

## LIST OF FIGURES

Figure 1. Conceptual diagram of the spatial extent of sampling of bat skin, cave soil, and roost microbial assemblages.....	8
Figure 2. Basic metacommunity structure of study.....	9
Figure 3. Comparison of the number of culturable antifungal bacteria on bat skin, the roost, or in the soil.....	30
Figure 4. Relative abundance of antifungal bacteria within each sample type.....	30
Figure 5. Comparison of the number of culturable antifungal bacteria on bat skin based on <i>P. destructans</i> status.....	31
Figure 6. Comparison of the abundance of culturable antifungal bacteria on bat skin based on <i>P. destructans</i> status.....	31
Figure 7. Non-metric multidimensional scaling ordination showing beta diversity patterns of the bat cutaneous microbiota compared to the cave roost and cave soil microbial assemblages.....	33
Figure. 8. Capscale analysis modeling <i>P. destructans</i> fungal load on Bray-Curtis dissimilarity values from the microbial assemblage of <i>P. destructans</i> positive and <i>P. destructans</i> negative bats.....	35
Figure 9. Comparison of functional gene categories between <i>P. destructans</i> positive (inside circle) and <i>P. destructans</i> negative (outside circle) bats.....	37
Figure 10. Heatmap comparing the abundance and presence/absence of bins across <i>P. destructans</i> status.....	59

Figure 11. Comparison of <i>P. destructans</i> negative indicator taxa (A) and punitive function (B) across <i>P. destructans</i> status. Non-metric multidimensional scaling ordination for taxonomic assemblage structure (C), and functional assemblage (D) across <i>P. destructans</i> positive and negative bats.....	60
Figure 12. Broadscale functional redundancy across functional pathways.....	62
Figure 13. Fine scale functional variability across functional orthologs.....	64
Figure 14. Broadscale functional redundancy regardless of bacterial taxonomy.....	65
Figure 15. Fine scale functional variation within a phylogenetic context.....	66
Figure 16. The elements of metacommunity structure and their resulting patterns.....	82
Figure 17. Distance decay analysis.....	94
Figure 18. Visual representation of microbial metacommunities across <i>P. destructans</i> status.....	96
Figure 19. Nestedness analysis.....	100
Figure 20. Comparison of beta diversity measured as multivariate dispersion across the interaction of ecoregion and <i>P. destructans</i> status.....	101
Figure 21. Non-metric multidimensional scaling ordination for <i>P. destructans</i> positive and negative bats.....	102

## LIST OF TABLES

Table 1. Heat map showing the identities of antifungal bacteria isolated from bat cutaneous swabs.....	29
Table 2. Analysis of average assemblage similarity across sample type.....	34
Table 3. Analysis of average assemblage similarity across <i>P. destructans</i> status.....	34
Table 4. Results for the EMS analysis of bats across <i>P. destructans</i> status.....	97
Table 5. Analysis of average assemblage similarity across <i>P. destructans</i> status and Ecoregion.....	103

## CHAPTER I: INTRODUCTION

A disturbance is a discrete event that causes a change or disruption in ecosystem or community structure (White and Pickett 1985). The agents of ecosystem disturbance can be either physical or biological in nature. Physical agents of disturbance include events such as fires, storms, and floods, whereas, biological agents include predation, grazing, or nonpredatory behaviors that displace other organisms (Sousa 1984). The frequency that a community is exposed to such events can allow for the evolution of disturbance reliant or resistant communities. Microbial community response to disturbance is understudied, however, researchers assume that these microbes respond to disturbance by being resistant, resilient, and/or with functional redundancy (Allison and Martiny 2008). A resistant community can experience disturbance with no impact on the community composition or function, whereas, resilience is the ability of a community to return to a pre-disruption state (Shade *et al.* 2012). Functional redundancy is defined as the ability of a community to maintain its original function despite its composition changing (Allison and Martiny 2008). A microbial community is considered stable in the face of disturbance if resistance/resilience is observed at both the community and functional levels (Pimm 1984). Disturbances can be both naturally occurring (i.e. hurricanes) or anthropogenically sourced. Anthropogenically sourced disturbance can include events such as deforestation (Friedman and Reich 2005) or the introduction of nonnative species (Sanders *et al.* 2003).

Nonnative species occur outside of a natural geographic distribution and are not naturally found within an ecosystem or habitat. The majority of introduced nonnative species are unable to successfully reproduce or are outcompeted (Zenni and Nuñez 2013),

however, those that do mate can form populations outside of their endemic range (Richardson *et al.* 2000). Invasive species often dominate over native species and frequently have negative impacts on native biodiversity (Crooks 2002). Well known examples include invasive species' ability to outcompete native species for resources (Petren and Case 1998), direct consumption of native species (Savidge 1987), and introduction of pathogens/parasites (i.e. *Cryphonectria parasitica*, the fungal agent of chestnut blight). Impacts to native biodiversity can affect both the structure and function of macro- and microorganism communities (Kourtev *et al.* 2002; Carlsson *et al.* 2004).

*Pseudogymnoascus destructans*, the causative fungal agent of white-nose syndrome (WNS), was introduced into Howes Cave, New York in 2006, and has since caused declines in bat populations across the eastern United States (Blehert *et al.* 2009). As of April 2021, bats with WNS have been identified in 35 states and seven Canadian provinces. *Pseudogymnoascus destructans*, but not WNS, has been found in four additional states (whitenosesyndrome.org). *Pseudogymnoascus destructans* infects bats during winter and causes them to increase the frequency of arousal from hibernation, which ultimately can lead to death (Reeder *et al.* 2012). Declines within hibernacula are rapid, with reports as high as 90% occurring yearly (Frick *et al.* 2010). White-nose syndrome has severely impacted bats, causing population declines of three federally listed bat species (*Myotis sodalis* [Indiana bat], *Myotis grisescens* [Gray bat], and *Myotis septentrionalis* [Northern long-eared myotis], Blehert *et al.* 2009; Leopardi *et al.* 2015). Furthermore, research predicts that WNS may cause the regional extinction of *Myotis lucifugus* (Little Brown Bats) by 2026 (Frick *et al.* 2010). The loss of bats concerns both conservation biologists and the farming industry, due to the important role that bats play

in cave ecosystems, and on the landscape in pest control (Boyles *et al.* 2011; Kunz *et al.* 2011). As a result, there has been interest in understanding ways to mitigate bat declines.

Patterns in host microbial community structure have been correlated with phylogenetic (Carrillo-Araujo *et al.* 2015), environmental determinants (Avena *et al.* 2016; Lemieux-Labonté *et al.* 2016), interspecific interactions (Song *et al.* 2013), social behaviors (Tung *et al.* 2015), and disease state (Cho and Blaser 2012; Lemieux-Labonté *et al.* 2017). The processes that drive microbial assembly patterns are thought to be similar to those governing macro-communities, namely selection, drift, speciation, and dispersal (Vellend 2010; Nemergut *et al.* 2013). Understanding processes that influence disease outcome for the host has both theoretical and applied implications.

The concept of the disease triangle was created in order to understand the relationship between various factors that result in disease outbreaks (Scholthof 2007). The three main factors influencing disease outcome include a susceptible host, virulent pathogen, and a favorable environment (McNew 1960). A diverse community of microbes survive on the cutaneous layer of vertebrates and are known to influence disease dynamics (Belden and Harris 2007; Grice and Segre 2011). Bacterial species in the microbiome compete with pathogenic or transient invaders, through the production of antimicrobial compounds, and prevent colonization of non-community members (Rollins-Smith 2009; Cornelison *et al.* 2014). Numerous studies have found antifungal bacterial species within the cutaneous microbial assemblage of bats (Cornelison *et al.* 2014; Hoyt *et al.* 2015; Cheng *et al.* 2016; Grisnik *et al.* 2020), as well as, within the microbiome of non-mammal organisms, including amphibians (Lauer *et al.* 2007; Harris *et al.* 2009) and reptiles (Hill *et al.* 2017). The identification of antifungal taxa within the

bat microbiome has led to an interest in using the microbiome to treat *P. destructans* infection. *Pseudomonas* species are known to have anti-*P. destructans* activity both *in vitro* and *in vivo* (Hoyt *et al.* 2015; Cheng *et al.* 2016). Bats that are *P. destructans* positive have a microbiome enriched with *Pseudomonas* species, as well as, other bacterial genera that have been reported to exhibit antifungal activity (Lemieux-Labonté *et al.* 2017).

One of the major risks involved with using antifungal taxa as a treatment for disease is the possibility of introducing a potentially harmful bacterial strain into a nonnative environment. This is of particular concern when introducing bacteria into caves, which are fragile ecosystems that are highly susceptible to numerous sources of degradation (Parise and Pascali 2003; Barton 2006). In order to minimize potential damage to this ecosystem, it is important that any candidate antifungal species be both a member of the bat cutaneous microbiome and found in the cave environment.

Understanding the factors that influence the bat and cave microbiome is important for determining the potential use of antifungal bacteria for disease treatment (Avena *et al.* 2016). The cutaneous microbiomes of *M. lucifugus* in *P. destructans* positive caves are enriched with antifungal bacteria relative to *M. lucifugus* found in *P. destructans* naïve caves (Lemieux-Labonté *et al.* 2017). Ecological processes like selection and environmental filtering are thought to drive skin enrichment of bacterial species that inhibit the growth of *P. destructans* and provide an innate immune response for bats (Grice and Segre 2011; Lemieux-Labonté *et al.* 2017). The potential implications of these microbe-pathogen interactions on host health is not fully understood.

Coupling of community assemblage structure with microbial function is a rapidly developing area in microbial community ecology. Metagenomic shotgun sequencing has allowed for researchers to determine functional differences within microbial communities using a collection of reference databases (Sharpton 2014). Functional community profiling can serve as a proxy for gene expression to approximate community function (Greenblum *et al.* 2011). Metagenomic shotgun sequencing has shown utility in determining differences between healthy and diseased human gut microbiome metabolic pathways (Morgan *et al.* 2012), however, our understanding of microbiome function over space and time in non-model organisms like bats is poorly understood.

In order to understand dynamic systems, it is important to consider scale of measurement, including both temporal and spatial aspects (Wiens 1989). Fine scale studies (those within a single patch or microsite) allow for a mechanistic understanding of system processes, however, without sampling at the broader scale (metacommunity level), these patterns cannot be translated into ecosystem processes (Wiens 1989). A classic example was observed between two bird species, the Least Flycatchers (*Empidonax minimus*) and American Redstarts (*Setophaga ruticilla*). At the fine scale (4-hectare plots) Least Flycatchers negatively influence the distribution of American Redstart territories, suggesting competitive exclusion of American Redstarts by Least Flycatchers, however, when looking to the regional scale, these two species are positively associated with one another (Sherry and Holmes 1988). The importance of scale has frequently been observed within macro-community ecology, however, there has only recently been an interest in understanding the influence of scale on microbial community structure and function (Nemergut *et al.* 2013). The current lack of understanding is likely

due to the differences in biologically relevant scales between host organisms and microbial taxa and is likely confounded by sampling efforts. For example, the actual bacterial diversity within a soil sample is likely underestimated using metabarcoding and sequencing due to the homogenization of unique microhabitats composing distinct bacterial communities (Nemergut *et al.* 2011). These cross-scale interactions have been acknowledged by ecologists and are considered with the application of metacommunity theory.

Metacommunity theory was developed to recognize that patterns observed within local communities can be influenced by interactions at the much larger regional (metacommunity) level (Leibold *et al.* 2004). A metacommunity is frequently defined as a group of habitat patches that are linked by dispersal and interactions of species between these patches (Leibold *et al.* 2004; Costello *et al.* 2012). The rates of dispersal, and nature of these interactions, can influence the patterns that are observed within local and regional habitat patches (Miller *et al.* 2018). Therefore, in order to draw meaningful conclusions, it is important to observe patterns across scales. Leibold *et al.* (2004) described scalar interactions using terminology such as microsites, localities, and metacommunities, to describe fine to broad scale patterns within a system (Leibold *et al.* 2004). Within my study system, a microsite was considered as a patch of skin on a bat host. Individual skin patches are interconnected forming a host-associated microbial assemblage (locality). Depending on bat species life-history (e.g. close communal hibernation), host-associated microbial assemblages (localities) of individual bats may interact with one another, or with the hibernation roost and/or cave environment. The

summation of interactions describes a metacommunity and the unit of study for my dissertation work.

Current work has classified four simplified approaches to metacommunity theory including species-sorting, mass effects, neutral processes, and patch dynamics (Leibold *et al.* 2004). Environmental conditions dictate community composition during the process of species-sorting (Cottenie 2005; Leibold and Loeuille 2015). Mass effects are characterized by a strong influence of source-sink dynamics. If the rate of dispersal is high enough, some species can survive outside of their optimal environment, which contributes to variation in community composition (Cottenie 2005; Leibold and Loeuille 2015). Neutral theory indicates the assembly of local communities is the result of purely stochastic factors, often resulting in unpredictable patterns of community composition across space. Patch dynamics are characterized by interspecific interactions resulting in extinctions that can be countered by dispersal. Patterns of patch dynamics can manifest in communities that vary both spatially and environmentally (Leibold *et al.* 2004).

My dissertation research as outlined below utilizes metacommunity theory to understand interactions among bat-microbiome-fungal pathogen relationships (see Fig. 1 and Fig. 2 for conceptual diagram). My main objective is to understand how the host microbiome responds to an invasive pathogen. More specifically, I will determine if the host microbiome is resistant to the pathogen and/or responds to invasion with functional redundancy. I will determine how the presence of a pathogen influences metacommunity structure and attempt to predict the relationship between the pathogen, environment, and assemblage variation. I hypothesize that the host microbiome is not resistant to pathogen mediated disturbance, but will be functionally redundant post disturbance. More

specifically, I hypothesize that changes in taxonomic composition will correlate with the presence of *P. destructans*, and that positive bats will have a microbial assemblage that is enriched with antifungal bacterial taxa. Additionally, I hypothesize that the presence of *P. destructans* will correlate with a shift in metacommunity structure, as well as, a shift in the relationship between structuring variables and community structure. My dissertation work will add to our understanding of microbial metacommunity theory and expand our knowledge of microbiome change to an invasive fungal pathogen.

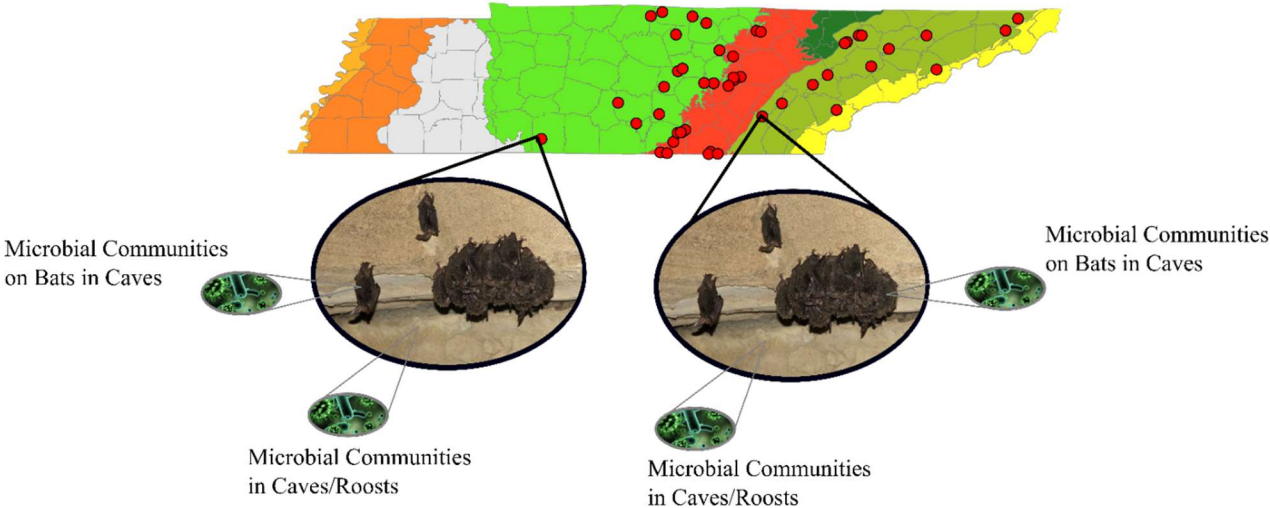


**Figure 1. Conceptual diagram of the spatial extent of sampling of bat skin, cave soil, and roost microbial assemblages.**

Bats were sampled in caves during the winter hibernation period. Caves were spread across Tennessee, with the majority of sampling occurring within three ecoregions (Interior Plateau in light green, South Western Appalachians in red, and Ridge and Valley in olive green). Photo credit: Daniel Istvanko.

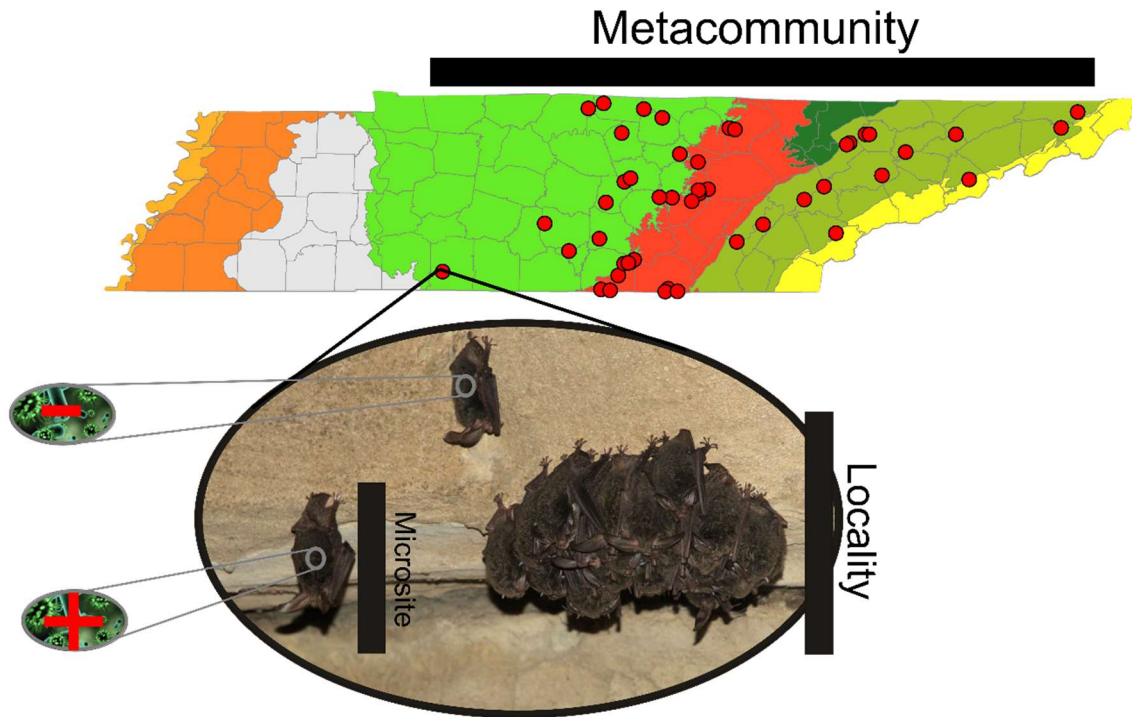


**Figure 2. Basic metacommunity structure of study.**

Caves (red dots) will be sampled across Tennessee during bat hibernation. Within each cave is a bat population (locality) whose cutaneous microbial assemblage (microsite) is sampled. Each locality is made up of interacting microsites. Bats within a cave will be divided into two categories, those with *P. destructans* present (+) and absent (-). Photo credit: Daniel Istvanko.

## References

- Allison SD, Martiny JBH. Resistance, resilience, and redundancy in microbial communities. *PNAS* 2008;**105**:11512–19.
- Avena CV, Parfrey LW, Leff JW *et al.* Deconstructing the bat skin microbiome: influences of the host and the environment. *Front Microbiol* 2016;**7**:1–14.
- Barton HA. Introduction to cave microbiology: A review for the non-specialist. *J Cave Karst Stud* 2006;**68**:43–54.
- Belden LK, Harris RN. Infectious diseases in wildlife: the community ecology context. *Front Ecol Environ* 2007 **5**;533–39.
- Blehert DS, Hicks AC, Behr M *et al.* Bat white-nose syndrome: An emerging fungal pathogen? *Science* 2009;**323**:227.
- Boyles JG, Cryan PM, McCracken GF *et al.* Economic importance of bats in agriculture. *Science* 2011;**332**:41–42.
- Carlsson NOL, Brönmark C, Hansson, LA. Invading herbivory: the golden apple snail alters ecosystem functioning in Asian wetlands. *Ecology* 2004;**85**:1575–80.
- Carrillo-Araujo M, Taş N, Alcántara-Hernández RJ *et al.* Phyllostomid bat microbiome composition is associated to host phylogeny and feeding strategies. *Front Microbiol* 2015;**6**:1–9.
- Cheng TL, Mayberry H, McGuire LP *et al.* Efficacy of a probiotic bacterium to treat bats affected by the disease white-nose syndrome. *J. Appl. Ecol.* 2016;**54**:701–08.
- Cho L, Blaser MJ. The human microbiome: at the interface of health and disease. *Nat Rev Genet* 2012;**13**:260–70.
- Cornelison CT, Gabriel KT, Barlament C *et al.* Inhibition of *Pseudogymnoascus destructans* growth from conidia and mycelial extension by bacterially produced volatile organic compounds. *Mycopathologia* 2014;**177**:1–10.
- Costello EK, Stagaman K, Dethlefsen L, Bohannan BJ *et al.* The application of ecological theory toward an understanding of the human microbiome. *Science* 2012;**336**:1255–62.
- Cottenie, K. Integrating environmental and spatial processes in ecological community dynamics. *Ecol Lett* 2005;**8**:1175–82.
- Crooks JA. Characterizing ecosystem-level consequences of biological invasions: the role of ecosystem engineers. *Oikos* 2002;**97**:153–66.
- Frick WF, Pollock JF, Hicks AC *et al.* An emerging disease causes regional population collapse of a common North American bat species. *Science* 2010;**329**:679–82.
- Friedman SK, Reich PB. Regional legacies of logging: departure from presettlement forest conditions in northern Minnesota. *Ecol Appl* 2005;**15**:726–44.
- Greenblum S, Turnbaugh PJ, Borenstein E. Metagenomic systems biology of the human gut microbiome reveals topological shifts associated with obesity and inflammatory bowel disease. *PNAS* 2011;**109**:594–99.
- Grice EA, Segre JA. The Skin microbiome. *Nat Rev Microbiol* 2011;**9**:244–53.
- Grisnik M, Bowers O, Moore AJ *et al.* The cutaneous bat microbiome has antifungal activity against the white nose pathogen. *FEMs Microbiol Ecol* 2020, DOI: 10.1093/femsec/fiz193.
- Harris RN, Brucker RM, Walke JB *et al.* Skin microbes on frogs prevent morbidity and mortality caused by a lethal skin fungus. *ISME J* 2009;**3**:818–24.

- Hill AJ, Leys JE, Bryan D *et al.* The potential of the snake cutaneous microbiome to inhibit *Ophidiomyces ophiodiicola*, the causative agent of snake fungal disease. *EcoHealth* 2017;**15**:109–20.
- Hoyt JR, Cheng TL, Langwig KE *et al.* Bacteria isolated from bats inhibit the growth of *Pseudogymnoascus destructans*, the causative agent of white-nose syndrome. *PLoS ONE* 2015, DOI:10:e0121329.
- Kourtev PS, Ehrenfeld JG, Häggblom M. Exotic plant species alter the microbial community structure and function in the soil. *Ecology* 2002;**83**:3152–66.
- Kunz TH, Braun de Torrez E, Bauer D *et al.* Ecosystem services provided by bats. *Ann NY Acad Sci* 2011;**1223**:1–38.
- Lauer A, Simon MA, Banning JL *et al.* Common cutaneous bacteria from the Eastern Red-Backed Salamander can inhibit pathogenic fungi. *Copeia* 2007;**2007**:630–40.
- Leibold MA, Holyoak M, Mouquet N *et al.* The metacommunity concept: a framework for multi-scale community ecology. *Ecol Lett* 2004, DOI:10.1111/j.1461-0248.2004.00608.x.
- Leibold MA, Loeuille N. Species sorting and patch dynamics in harlequin metacommunities affect the relative importance of environment and space. *Ecology* 2015;**96**:3227–33.
- Lemieux-Labonté V, Tromas N, Shapiro BJ *et al.* Environment and host species shape the skin microbiome of captive neotropical bats. *PeerJ* 2016, DOI: 10.7717/peerj.2430.
- Lemieux-Labonté V, Simard A, Willis CKR *et al.* Enrichment of beneficial bacteria in the skin microbiota of bats persisting with white-nose syndrome. *Microbiome* 2017;**5**:115–30.
- Leopardi S, Blake D, Suechmaille SJ. White-nose syndrome fungus introduced from Europe to North America. *Curr Biol* 2015;**25**:217–19.
- McNew GL. The nature, origin, and evolution of parasitism. In: Horsfall JG, Dimond AE (eds.). *Plant pathology: an advanced treatise*. New York: Academic Press, 1960,19–69.
- Miller ET, Svanbäck R, Bohannan BJ. Microbiomes as metacommunities: understanding host-associated microbes through metacommunity ecology. *Trends Ecol Evol* 2018;**33**:926–35.
- Morgan XC, Tickle TL, Sokol H *et al.* Dysfunction of the intestinal microbiome in inflammatory bowel disease and treatment. *Genome Biol* 2012;**13**:1–18.
- Nemergut DR, Costello EK, Hamady M *et al.* Global patterns in the biogeography of bacterial taxa. *Environ Microbiol* 2011;**13**:135–44.
- Nemergut DR, Schmidt SK, Fukami T *et al.* Patterns and processes of microbial community assembly. *Microbiol Mol Biol Rev* 2013;**77**:342–56.
- Parise M, Pascali V. Surface and subsurface environmental degradation in the karst of Apulia (southern Italy). *Environ Geol* 2003;**44**:247–56.
- Petren K, Case TJ. Habitat structure determines competition intensity and invasion success in gecko lizards. *Proc Natl Acad Sci* 1998;**95**:11739–44.
- Pimm SL. The complexity and stability of ecosystems. *Nature* 1984;**307**:321–26.

- Reeder DM, Frank CL, Turner GG *et al.* Frequent arousal from hibernation linked to severity of infection and mortality in bats with white-nose syndrome. *PLoS One* 2012, DOI:10.1371/journal.pone.0038920.
- Richardson DM, Pysek P, Rejmanek M *et al.* Naturalization and invasion of alien plants: concepts and definitions. *Divers Distrib* 2000;**6**:93–107.
- Rollins-Smith LA. The role of amphibian antimicrobial peptides in protection of amphibians from pathogens linked to global amphibian declines. *Biochemica et Biophysica Acta* 2009;**1788**:1593–99.
- Sanders NJ, Gotelli NJ, Heller NE *et al.* Community disassembly by an invasive species. *PNAS* 2003;**100**:2474–77.
- Savidge JA. Extinction of an island forest avifauna by an introduced snake. *Ecology* 1987;**68**:660–68.
- Scholthof KBG. The disease triangle: pathogens, the environment and society. *Nat Rev Microbiol* 2007;**5**:152–56.
- Shade A, Handelsman J. Beyond the Venn Diagram: the Hunt for a Core Microbiome. *Environ Microbiol* 2012;**14**:4–12.
- Sharpton TJ. An introduction to the analysis of shotgun metagenomic data. *Front Plant Sci* 2014;**5**:1–14.
- Sherry TW, Holmes RT. Habitat selection by breeding American Redstarts in response to a dominant competitor, the Least Flycatcher. *The Auk* 1988;**105**:350–64.
- Song SJ, Lauber C, Costello EK *et al.* Cohabiting family members share microbiota with one another and with their dog. *eLife* 2013;**2**:1–22.
- Sousa WP. The role of disturbance in natural communities. *Ann Rev Ecol Syst* 1984;**15**:353–91.
- Tung J, Barreiro LB, Burns MB *et al.* Social networks predict gut microbiome composition in wild baboons. *eLife* 2015, DOI:10.7554/eLife.05224.
- Vellend M. Conceptual synthesis in community ecology. *Q Rev Biol* 2010;**85**:183–206.
- White PS, Pickett STA. Natural disturbance and patch dynamics: an introduction. In: Pickett STA and White PS (eds.). *The ecology of natural disturbance and patch dynamics*. Orlando: Academic Press, 1985, 472.
- Whitenosesyndrome.org <https://www.whitenosesyndrome.org/static-spread-map/july-25-2019> Accessed 8/23/2019.
- Wiens JA. Spatial Scaling in Ecology. *Funct Eco* 1989;**3**:385–97.
- Zenni RD, Nuñez MA. The elephant in the room: the role of failed invasions in understanding invasion biology. *Oikos* 2013, DOI:10.1111/j.1600-0706.2012.00254.x.

**CHAPTER II: THE CUTANEOUS MICROBIOTA OF BATS HAS *IN VITRO*  
ANTIFUNGAL ACTIVITY AGAINST THE WHITE NOSE PATHOGEN**

Matthew Grisnik<sup>1</sup>, Olivia Bowers<sup>1</sup>, Andrew J. Moore<sup>2</sup>, Benjamin F. Jones<sup>2</sup>, Joshua R. Campbell<sup>3</sup>, and Donald M. Walker<sup>1</sup>

<sup>1</sup> Middle Tennessee State University, Toxicology and Disease Group, Biology Department, 1672 Greenland Drive, Murfreesboro, Tennessee 37132, USA.

<sup>2</sup> Tennessee Technological University, Department of Biological Sciences, 1100 N. Dixie Ave, Cookeville, Tennessee 38505, USA.

<sup>3</sup> Tennessee Wildlife Resources Agency, 5105 Edmondson Pike, Nashville, Tennessee 37211, USA.

Grisnik *et al.* The cutaneous microbiota of bats has *in vitro* antifungal activity against the white nose pathogen. FEMS Microbiology Ecology, 2020, 96, DOI: 10.1093/femsec/fiz193. By permission of Oxford University Press.

**Abstract**

Since its introduction into the USA, *Pseudogymnoascus destructans* (*Pd*), the fungal pathogen of white-nose syndrome, has killed millions of bats. Recently, bacteria capable of inhibiting the growth of *P. destructans* have been identified within bat microbial assemblages, leading to increased interest in elucidating bacterial assemblage-pathogen interactions. My objectives were to determine if bat cutaneous bacteria have antifungal activity against *P. destructans*, and correlate differences in the bat cutaneous microbiota with the presence/absence of *P. destructans*. I hypothesized that the cutaneous microbiota of bats is enriched with antifungal bacteria, and that the skin assemblage will

correlate with *P. destructans* status. To test this, I sampled bat microbiota, adjacent roost surfaces, and soil from *P. destructans* positive caves to infer possible overlap of antifungal taxa, I tested these bacteria for bioactivity *in vitro*, and lastly compared bacterial assemblages using both amplicon and shotgun high-throughput DNA sequencing. Results suggest that the presence of *P. destructans* has an inconsistent influence on the bat cutaneous microbial assemblage across sites. Operational taxonomic units (OTUs) that corresponded with cultured antifungal bacteria were present within all sample types but were significantly more abundant on bat skin relative to the environment. Additionally, the microbial assemblage of *P. destructans* negative bats was found to have more OTUs that corresponded to antifungal taxa than positive bats, suggesting an interaction between fungal pathogens and the cutaneous microbial assemblage.

## **Introduction**

Planet earth is currently entering its sixth major extinction event, with estimated rates of extinction 1000 – 10 000 times the accepted background rates (De Vos *et al.* 2014). Major causes of extinction include habitat degradation and destruction, pollution, climate change, as well as introduced pathogens (Gibbons *et al.* 2000; McCallum 2007). Introduced fungal pathogens are currently impacting a diverse range of taxa including amphibians, reptiles, and mammals (Fisher *et al.* 2012). For example, the fungal pathogens (*Batrachochytrium dendrobatidis* and *B. salamandrivorans*) that cause chytridiomycosis in amphibians are often cited as responsible for one of the greatest losses of biodiversity in recorded time (Gray *et al.* 2015). In addition, *Pseudogymnoascus*

*destructans* (*Pd*), the causative agent of white-nose syndrome (WNS), has caused bat populations to plummet in the US (Blehert *et al.* 2009).

Since its introduction to the United States in 2006, *P. destructans* has spread rapidly, killing millions of bats (Blehert *et al.* 2009). Clinical signs of white-nose syndrome present as cup-like erosions and ulcerations on the cutaneous layer of hibernating bats (Meteyer *et al.* 2009). Infection with *P. destructans* causes a hibernating bat to increase the frequency of arousal bouts, leading to the bat expending valuable energy reserves (Reeder *et al.* 2012). Within infected hibernacula, initial declines were reported as between 20 – 90% (Frick *et al.* 2010; Langwig *et al.* 2012). However, since then, some species have exhibited population stabilization in the years following an initial population crash (Dobony *et al.* 2011; Langwig *et al.* 2012; Frick *et al.* 2017).

Several North American bat species experienced population declines since the introduction of *P. destructans* (Langwig *et al.* 2012). These declines are not uniform across species and over time, with some bat species showing resistance to *P. destructans* infection (Langwig *et al.* 2017). Differences in persistence are hypothesized to be due to behavioral changes (Langwig *et al.* 2012), or alternatively, through genetic resistance and evolutionary rescue (Maslo and Fefferman 2015). *Perimyotis subflavus* (Tri-colored bats) initially experienced high levels of population decline, however, recent population stabilizations were observed (Langwig *et al.* 2012; Langwig *et al.* 2017). This is especially intriguing since *P. destructans* is still highly prevalent in many cave systems in the northeast which is an endemic area for *P. subflavus* (Frick *et al.* 2017).

A potential mechanism to explain innate immunity and disease tolerance in *P. subflavus* is a shift in the bat cutaneous microbial assemblage with selection for bacterial

taxa with protective antifungal capabilities (Lemieux-Labonté *et al.* 2017). The cutaneous layer of vertebrates hosts a diverse community of microbes interacting synergistically and potentially influencing disease dynamics (Belden and Harris 2007; Grice and Segre 2011). Recent studies have documented antifungal ‘probiotic’ bacterial species within the cutaneous microbiota of bats (Hoyt *et al.* 2015). Previous work has shown that the addition of antifungal bacteria to frog skin led to a reduction in morbidity due to chytridiomycosis, suggesting the role of this host-associated assemblage in skin defense (Harris *et al.* 2009). In addition, *M. lucifugus* (Little brown bats) persisting in *P. destructans* positive hibernacula have a microbiome with relatively more abundant antifungal bacterial species compared to bats from *P. destructans* naïve caves (Lemieux-Labonté *et al.* 2017). Selection and environmental filtering may serve as a mechanism for this cutaneous enrichment by *P. destructans* antagonists, and as a result might provide an innate immune response to fungal pathogenicity, although functional implications of the bat microbial assemblage composition are not fully understood.

Shotgun metagenomic sequencing allows for the elucidation of functional differences in microbial assemblages by comparing genomic DNA sequences within a sample to functional databases (Sharpton 2014). The presence of protein coding genes within a microbial assemblage serves as a proxy for the potential gene expression and thus function within that community (Greenblum *et al.* 2011). Recently, Louca *et al.* (2016) used shotgun metagenomic sequencing to show that host microbial assemblages can be taxonomically diverse, however, express functional redundancy. Metagenomic sequencing has infrequently been used to study wildlife host-microbiota-pathogen interactions but has shown utility to characterize differences in metabolic pathways

between individuals with/without inflammatory bowel disease (Morgan *et al.* 2012), which parallels this system.

The goal of this study was to elucidate patterns of community composition and function of the cutaneous microbial assemblage of *P. subflavus* in the presence of *P. destructans*. Additionally, I was interested in the overlap of microbes between the host and substrates within the host environment (i.e. roost and soil). My objectives were to 1) isolate cutaneous microbes with antifungal activity from the cutaneous microbial assemblage of bats, 2) use amplicon sequencing to characterize the microbial assemblages within the cave ecosystem including cave soil, bat roosts, and *P. destructans* positive/negative bats, to determine if antifungal activity is ubiquitous throughout the cave environment or correlates with *P. destructans* status, 3) determine if shotgun metagenomic sequencing is a viable method to understand shifts in cutaneous microbial assemblage function in the presence of a fungal pathogen. I hypothesized (1) that the cutaneous microbial assemblage of bats hosts taxa with antifungal activity against *P. destructans*. I also postulate (2) that bat skin is enriched with antifungal bacteria relative to the surrounding cave environment. Finally (3), I hypothesize that the taxonomic cutaneous assemblage of bats would correlate with *P. destructans* status (Lemieux-Labonté *et al.* 2017).

## **Methods**

### *Field work and sample collection*

To characterize the bat cutaneous microbial assemblage, I collected 83 cutaneous swabs from *P. subflavus* in conjunction with statewide surveys at 20 caves throughout East/Central Tennessee between December and April 2017. At each cave site two

cutaneous swabs (sterile Puritan polyester tipped swabs, Puritan) were collected from each bat. One swab was placed into a sterile dry tube for high-throughput sequencing (HTS) and the second was stored in a tube filled with sterile 15% glycerol and 2x R2B broth for isolation of bacteria into pure culture. Similar to Langwig *et al.* (2015), each swab was aseptically removed from the packaging and briefly dipped into a Falcon tube of sterile Millipore water. Ten swab strokes were taken from each bat including five strokes on the muzzle/ears and five from wings and fur while avoiding the mouth. To characterize the environmental pool of microbes, a corresponding roost sample and soil sample were collected adjacent to hibernating bats from each site. Roost swabs were collected by briefly dipping a swab into sterile Millipore water, then taking 10 strokes, 30 cm in length, of the cave wall at each of the main locations where bats were sampled. Soil samples were collected from beneath the roosting bats, being sure to avoid guano, by aseptically scooping soil into a sterile 15 mL Falcon tube. All samples were stored on ice in the field and transferred into a -20° C freezer until processing in the lab.

#### *Bacterial isolation, identification, and antifungal challenge assays*

Cutaneous swabs (n = 55 bat individuals) from frozen glycerol tubes were streak inoculated onto primary plates with R2A agar amended with 5% cycloheximide and incubated at 10 – 11° C. Morphologically distinct bacterial colonies were selected from primary plates, Gram stained, characterized using a light microscope, and isolated into pure culture. I chose 236 bacterial isolates that were morphologically unique and challenged them for antifungal activity against a two-week-old culture of *P. destructans* that was grown on Sabouraud dextrose agar (SDA) media at 10 – 11° C. To make a lawn

of *P. destructans* covering the surface of an agar plate, we harvested 2 cm<sup>2</sup> of *P. destructans* and further cut it into approximately 5 mm<sup>2</sup> pieces with a sterile scalpel before adding it into a 50 mL Falcon tube with 10 mL of sterile Millipore water and 10 small (2 mm) silica beads. The slurry was vortexed at 1800 RPM for 2 minutes to thoroughly homogenize the *P. destructans* mycelium/conidia. The concentration of fungal conidia and fragments/mL ('propagative units') was quantified using a hemocytometer and diluted to a standardized concentration of  $2.5 \times 10^6$  propagative units/mL. I inoculated 100  $\mu$ L of the homogenized slurry onto a 100 mm R2A petri plate and spread the liquid across the surface using a glass rod to make a fungal lawn. Each bacterial strain was point inoculated using a sterile swab onto independent plates in triplicate over top of the fungal lawn. After 14 days of growth, the diameter of the zone of inhibition was measured, and those that exhibited antifungal activity were sequenced using Sanger sequencing.

To DNA sequence, the 16S ribosomal RNA (rRNA) gene was amplified using primers 8F/1492R (Lane 1991) in 20  $\mu$ L reactions containing 10  $\mu$ L 2x Phire buffer, 1  $\mu$ L of 8F (10  $\mu$ M) primer, 1  $\mu$ L of 1492R (10  $\mu$ M) primer, 0.4  $\mu$ L polymerase, 6.6  $\mu$ L of PCR grade water, and 1  $\mu$ L of bacterial cell suspension. Thermocycling conditions included initial denaturation at 98°C for 5 min, followed by 35 cycles of 98°C for 5 s, 50°C for 5 s, 72°C for 30 s, and a final extension cycle of 72°C for 1 min. PCR products were purified using ExoSap-IT and sent to MCLAB Molecular Cloning Laboratories for Sanger sequencing. Sequences were edited in ChromasPro and compared to the Greengenes database (Greengenes Database Consortium, Second Genome, Inc.) for taxonomic identification purposes. The 16S sequences of antifungal strains were also

compared to the high-throughput sequencing data (described below) using a localized BLAST database developed in Bioedit (version 7.0.5.3; available at <http://jwbrown.mbio.ncsu.edu/BioEdit/bioedit.html>) to determine if antifungal bacteria isolated from the bat cutaneous microbiome were also found in the environment (soil or roost).

#### *Characterization of microbial assemblage structure and function*

DNA was extracted from 83 *P. subflavus* cutaneous swabs, 40 roost swabs, and 37 soil samples using the Qiagen DNeasy PowerSoil HTP 96 kit, following the manufacturer's protocol to a final elution volume of 100  $\mu$ L. DNA extraction, PCR setup, and post PCR processes were all conducted in separate AirClean System hoods using a dedicated set of pipettes that were routinely autoclaved and UV crosslinked in between experiments. DNA was concentrated four-fold to a volume of 25  $\mu$ L on a Thermo Scientific Savant SpeedVac. PCR amplification and high-throughput sequencing followed the Illumina 16S Metagenomic Sequencing Library Preparation protocol. More specifically, the V4 region of the 16S rRNA gene was PCR amplified using primers 806R/515F (Caporaso *et al.* 2011) in 25  $\mu$ L reactions containing 12.5  $\mu$ L MCLAB 2x Hi-Fi taq, 1  $\mu$ L of 806R (10  $\mu$ M), 1  $\mu$ L of 515F (10  $\mu$ M), 5.5  $\mu$ L PCR grade water, and 5  $\mu$ L concentrated DNA template. Thermocycling conditions included initial denaturation at 95°C for 2 mins, followed by 35 cycles of 98°C for 10 s, 55°C for 15 s, and 72°C for 5 s and a final extension cycle of 72°C for 5 min. Samples were size selected to remove primer/adaptor dimers using MAGBIO Highprep magnetic beads after the initial PCR, as well as after the index PCR step. After both the amplification and indexing reactions, PCR products were quantified on a Qubit fluorometer 3.0 per the manufacturer's protocol

and visualized for amplicon size (450 bp) on an Agilent 2100 Bioanalyzer according to the DNA 1000 protocol, and then normalized. After library quality control and quantitation, the library (4 picomolar concentration) was loaded on an Illumina MiSeq v2 flow cell and sequenced using a 500-cycle reagent kit (Paired-end 2×250 reads). Base calling was done on the Illumina MiSeq, demultiplexed, and converted to FastQ format for bioinformatic analyses.

Quantitative PCR (qPCR) was used to determine the presence/absence of *P. destructans* on cutaneous swabs. Reactions were performed in triplicate on a Roche LightCycler480 II following the qPCR assay described by Muller *et al.* (2013) to amplify the fungal intergenic spacer region (IGS) of rRNA. PCR reactions (10 µL volume) contained 5 µL 2x Primetime MasterMix, 0.4 µL forward primer (20 µM), 0.4 µL reverse primer (20 µM), 0.1 µL probe (20 µM), 3.1 µL PCR grade water, and 1 µL of DNA. Thermocycling conditions included a 3 min activation step at 95°C, followed by 50 cycles of 95°C for 3 s, and 60°C for 30 s. Each qPCR plate included both a positive control as well as a no template negative control run in triplicate. DNA extraction blanks were also tested with qPCR in order to determine if contamination occurred during the DNA isolation process. Criteria for a positive individual was exponential amplification in triplicate at or before C<sub>t</sub> 40 (Muller *et al.* 2013; Janicki *et al.* 2015). Samples that tested positive for one or two of the three replicates were re-analyzed. If they were still ambiguous after the second time (amplifying in one or two reactions) the sample was considered positive (Ellison *et al.* 2006). To determine the fungal load of *P. destructans* DNA present within each sample, a standard curve was created using a serial dilution of 1

$\times 10^{10} - 1$  amplicon copies of a synthetic gBlock (Integrated DNA technologies) fragment that matched the targeted region for qPCR in Muller *et al.* (2013). An equation was calculated to determine the number of copies per reaction by comparing the average  $C_t$  to the known gBlock amplicon copy number. The log copy number of the fungal IGS rRNA gene per qPCR reaction was calculated using the formula,  $y = -0.2936x + 11.439$ , with  $x$  being the average  $C_t$  value for each sample completed in triplicate.

Shotgun sequencing was used to characterize the functional profile of the bat cutaneous metagenome. The swab samples collected in this study yielded notoriously low quantities of DNA ( $\approx 1$  ng total yield) making library preparation for shotgun sequencing challenging. Therefore, after obtaining qPCR results, isolated DNA was pooled into *P. destructans* positive ( $n = 19$  pooled samples) and negative ( $n = 7$  pooled samples) categories to ensure sample input quantity was appropriate to proceed with library preparation based on the manufacturer's minimum suggested input quantity of 1 ng of total DNA. The pooled positive/negative samples were collected from the same set of six caves in an effort to control for site as contributing to variation in functional profiles. Unfortunately, due to low DNA yield from independent swabs we were unable to sequence biological replicates of samples in *P. destructans* positive/negative categories. PCR amplification and high-throughput sequencing followed the Illumina Nextera DNA Flex library preparation protocol. After library quality control and quantitation, the library was loaded onto an Illumina MiSeq v2 flow cell and sequenced using a 500-cycle reagent kit (Paired-end  $2 \times 250$  bp reads).

### *Bioinformatic analyses*

A total of 19 413 692 DNA sequence reads were obtained from amplicon sequencing (cutaneous, roost, and soil samples). Data were processed using mothur v1.40.2 (Schloss *et al.* 2009) by assembling paired-end reads into contigs. Sequences that contained homopolymers greater than eight nucleotides or contained any ambiguous base calls were removed. Unique sequences were then aligned to the SILVA v123 bacterial reference database (Quast *et al.* 2012). Sequences were curated to the V4 region, pre-clustered allowing for two nucleotide differences and chimeras removed using the vsearch function (Rognes *et al.* 2016). Sequences were classified into taxonomic lineages, and those that were identified as Archaea, Eukaryota, chloroplast, mitochondria, or unknown were removed (Kozich *et al.* 2013). Sequences were then clustered using *cluster.split* and operational taxonomic units (OTUs) were assigned at 97% similarity (Schloss and Westcott 2011). Rare OTUs appearing less than ten times and those found in the negative control DNA extraction blanks (n = 178 OTUs) were also removed from the dataset (Lindahl *et al.* 2013). A total of 3 504 518 sequence reads passed all filtering steps and were used in downstream analyses. A total of 29 samples (16 cutaneous swabs, 9 soil, 4 roost) did not pass the quality control and filtering steps due to poor sequencing depth coverage and were removed from the dataset (final dataset n = 67 bat cutaneous samples, n = 28 soil samples, n = 36 roost samples). I normalized the dataset by subsampling each library at 1300 sequence reads. All mothur commands are included in Appendix A for study reproducibility purposes.

DNA sequences from the shotgun metagenomics sequencing were analyzed using the Metagenomics Rapid Annotation (MG-RAST) pipeline version 4.0.3 (Meyer *et al.*

2008) (<http://metagenomics.theseed.org>). Sequences were filtered to include only bacterial DNA using the REFSEQ database at 60% similarity. The subsystems database (Aziz *et al.* 2008) was used to generate functional gene profiles with a minimum alignment length of 45 bp and  $E$  - value cutoff of  $E < 1 \times 10^{-5}$  (Randle-Boggis *et al.* 2016), and samples were normalized to allow for comparisons.

### *Statistical analyses*

To test if the bat cutaneous microbial assemblage differed from the environment, the bacterial OTU alpha diversity was calculated using the inverse Simpson index and data were normalized using a cubed root transformation (Morris *et al.* 2014). Alpha diversity was compared between the bat cutaneous microbial assemblage and the environmental samples (both roost and soil) using a linear mixed-effects model (LMM) with a random intercept of site and sample type as the sole fixed effect (package *lme4*, function *lmer*; Bates *et al.* 2014). The effect of sample type was determined by using a likelihood ratio test comparing nested models with and without sample type as a fixed effect.

In order to assess community level differences, beta diversity was calculated using the *vegdist* function in the *vegan* package to generate a Bray-Curtis dissimilarity matrix (Okansen *et al.* 2013). This matrix was further analyzed using the *metaMDS* function to generate a non-metric multidimensional scaling (nMDS) ordination and visualized using *ggplot2* (Wickham 2016). The *adonis* function was used to perform a permutational multivariate analysis of variance listing geographic site as ‘strata’, using 999 permutations on the Bray-Curtis dissimilarity matrix to determine if skin, soil, or the roost were explanatory variables for OTU assemblages. Since the bat skin differed (see

results) from the surrounding environment, I ran an indicator analysis (indicator values  $> 30$ ,  $\alpha < 0.05$ ) in *mothur* in order to determine OTUs that were indicative of each sample type (e.g. soil, roost, or bat skin), with the intention of determining which OTUs were indicative of the bat microbial assemblage for downstream analysis. I selected 11 OTUs that were explanatory of the bat skin microbial assemblage regardless of space (cave site). The *adonis* function was used to perform a permutational multivariate analysis of variance stratified by site, using 999 permutations on the Bray-Curtis dissimilarity matrix of the 11 indicator OTUs to test if the explanatory variables including cave site and *P. destructans* status (positive/negative) or interactions between these factors were predictive of skin microbial assemblages. The *betadisper* function was used to test for homogeneity of variances between *P. destructans* positive and negative bats. Alpha diversity was calculated using the inverse Simpson index, and then compared between *P. destructans* positive and negative bats using a linear mixed-model. *P. destructans* status was set as the fixed effect and geographic site as the random intercept, model fit was assessed using a likelihood ratio test to compare nested models with and without *P. destructans* status as a fixed effect. I performed a distance-based redundancy analysis (Db-RDA) using the *capscale* function in *vegan* to model fungal load of *P. destructans* (determined through qPCR) on Bray-Curtis dissimilarity values from the microbial community of *P. destructans* positive/negative bats. Fungal load and OTU relative abundances were normalized using a cube root transformation prior to the Db-RDA analysis.

To determine if bacteria with antifungal activity were found more frequently on bat skin, the roost, or in the soil, I compared the quantity of cultured antifungal bacteria found within each sample (richness). To assess if these antifungal bacteria were more abundant on bat skin or soil/roosts I created a local BLAST database by using the *get.oturep* command in *mothur* to extract a representative DNA sequence for each OTU in the high-throughput dataset. This allowed for me to compare 16S rRNA gene sequences from cultured antifungal bacteria to high-throughput data to determine if both richness and abundance (sequence read count) differed by sample type and/or *P. destructans* status. To determine if sample type (bat skin, the roost, or the soil) was enriched with antifungal bacterial taxa, I used two separate linear mixed-effects models in the package *lme4* to compare the richness or abundance of antifungal bacterial taxa with sample type as the fixed effect and site set as the random intercept. Model fit was assessed using a likelihood ratio test to compare nested models with and without sample type as a fixed effect for both sets of models. Abundance was log transformed to fit assumptions of normality. To determine if there was a higher richness or abundance of antifungal bacterial taxa based on *P. destructans* status, I again used two separate linear-mixed models, setting *P. destructans* status as the fixed effect and site as the random intercept. Model fit was assessed by using likelihood ratio tests of nested models, with and without *P. destructans* status, as a fixed effect for both sets of models. Abundance was log transformed to fit assumptions of normality. All statistical tests were performed with alpha ( $\alpha$ ) set at 0.05.

## Results

In total, 73 bat individuals (88%) tested positive in qPCR assays for the presence of *P. destructans* (Appendix B). All 20 caves had at least one *P. destructans* positive bat. All ten *P. destructans* negative bats were living amongst *P. destructans* positive individuals within eight of the 20 caves, only two of the negative bats were found in the same cave. Of the 236 bacterial isolates that I challenged against *P. destructans*, I found 18 with antifungal activity that were members of the bat cutaneous microbial assemblage (Table 1). BLAST results ( $> 97\%$  match,  $E < 1 \times 10^{-5}$ ) indicated that DNA sequences of all 18 antifungal isolates corresponded to OTUs from amplicon sequencing found in the bat cutaneous microbial assemblage or in the cave environment. The antifungal bacterial OTUs were classified as 16 bacterial genera occurring in three phyla (Table 1). Of the 18 antifungal bacterial species isolated from bat cutaneous swabs, 12 were found in all three sample types (cutaneous microbial assemblage, cave soil, and bat roost). One isolate occurred in the roost and the bat cutaneous microbial assemblage (CCB33.5, *Pseudomonas* sp.), and four antifungal isolates were found exclusively in the bat cutaneous microbial assemblage (CCB1.4 *Arthrobacter* sp., CCB52.1 *Bacillus* sp., CCB53.6 *Corynebacterium* sp., and CCB57.2 *Enterococcus* sp.) (Table 1). There was no difference between the models with and without sample type set as the fixed effect, suggesting OTUs that corresponded with cultured antifungal bacteria were present within all sample types (LMM,  $\chi^2(2) = 2.28$ ,  $p > 0.05$ , Fig. 3). When comparing antifungal OTU abundance, the model with sample type set as a fixed effect suggested that antifungal OTUs were more abundant in the bat cutaneous microbial assemblage (LMM,  $\chi^2(2) =$

28.09,  $p \leq 0.05$ , Fig. 4). The addition of *P. destructans* status significantly increased model fit explaining antifungal OTU richness (LMM,  $\chi^2(1) = 4.88$ ,  $p \leq 0.05$ , Fig. 5). However, *P. destructans* status did not influence model fit in describing antifungal bacterial abundance (LMM,  $\chi^2(1) = 0.05$ ,  $p > 0.05$ , Fig. 6), suggesting that antifungal bacteria were not more abundant on *P. destructans* positive relative to negative bats.



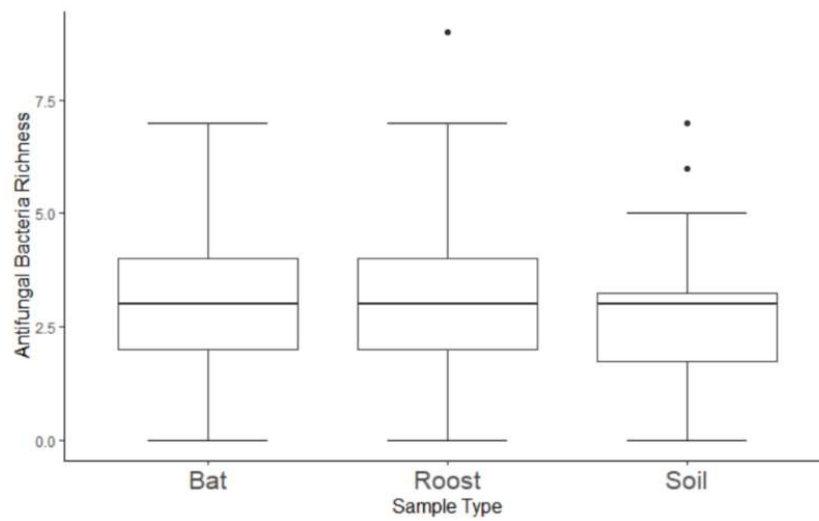


**Figure 3. Comparison of the number of culturable antifungal bacteria on bat skin, the roost, or in the soil.**

There was no significant difference between the presence of bacteria with anti- *P. destructans* activity between the three communities ( $p > 0.05$ ).

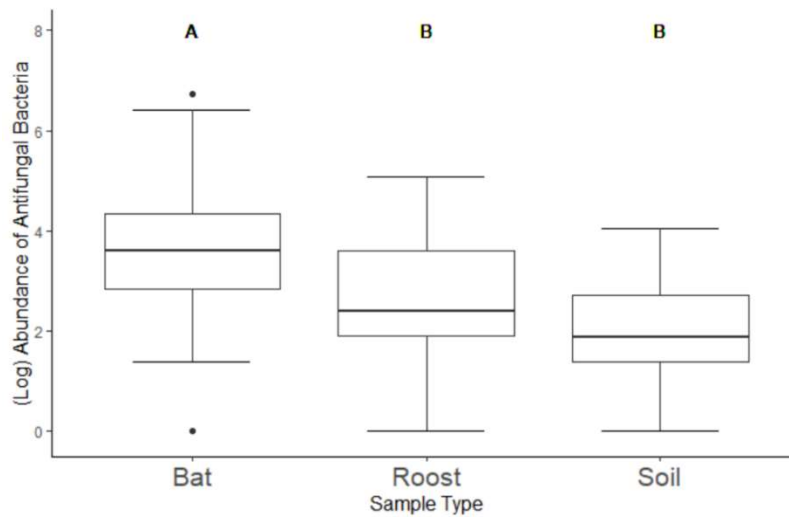


**Figure 4. Relative abundance of antifungal bacteria within each sample type.**

Bats have a microbial assemblage enriched with antifungal bacteria ( $p < 0.05$ ). Letters signify significant differences ( $p < 0.05$ ).

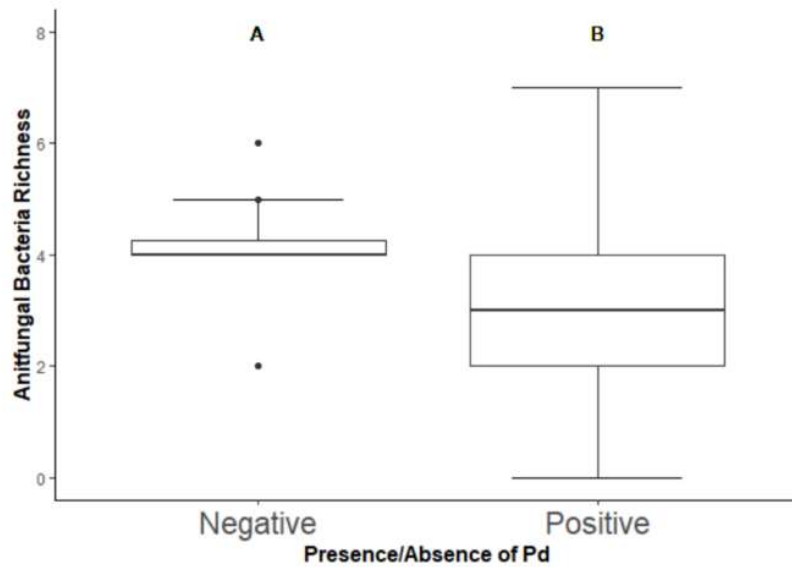


**Figure 5. Comparison of the number of culturable antifungal bacteria on bat skin based on *P. destructans* status.**

The number of antifungal bacteria found on bat skin is significantly different between *P. destructans* positive and *P. destructans* negative bats ( $p < 0.05$ ). Letters signify significant differences ( $p < 0.05$ ).

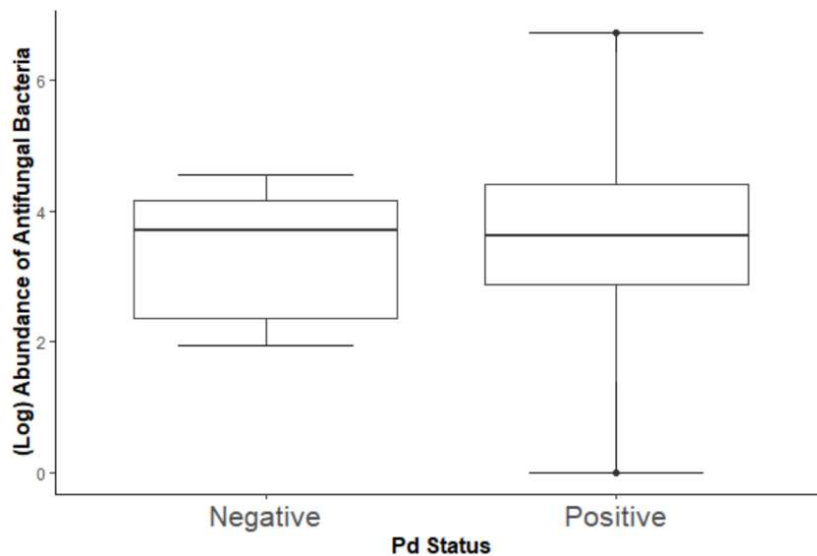


**Figure 6. Comparison of the abundance of culturable antifungal bacteria on bat skin based on *P. destructans* status**

The relative abundance of DNA sequence reads that correspond to bacteria that had anti-*P. destructans* activity *in vitro* in positive/negative bats does not differ by *P. destructans* status ( $p > 0.05$ ).

High-throughput sequencing analysis revealed that the bat cutaneous microbial assemblage contained 4784 OTUs, the roost site 2482 OTUs, and the soil environment 5589 OTUs. The average bat cutaneous microbial assemblage was significantly distinct from both the roost and the soil average microbial assemblages (PERMANOVA,  $F_{2, 130} = 4.68$ ,  $p \leq 0.05$ ,  $R^2 = 6.8\%$ , Fig. 7, Table 2). Similarly, sample type influenced alpha diversity (LMM,  $\chi^2(2) = 28.97$ ,  $p \leq 0.05$ ), with bat skin having the lowest diversity relative to the environment. I found that the effect of *P. destructans* status on the microbial assemblage was variable among cave sites (PERMANOVA,  $F_{5, 66} = 1.58$ ,  $p \leq 0.05$ ,  $R^2 = 9.8\%$ , Table 3). There was no difference in alpha diversity between *P. destructans* positive and negative bats (LMM,  $\chi^2(1) = 0.0484$ ,  $p > 0.05$ ). There was also no difference between the dispersion of variances between positive and negative bats (*betadisper*,  $F_{1, 65} = 0.158$ ,  $p > 0.05$ ). Additionally, the DB-RDA (*capscale*) analysis revealed six OTUs that correlated with an increase in *P. destructans* copy number, two of which had antifungal activity *in vitro* (Fig. 8).

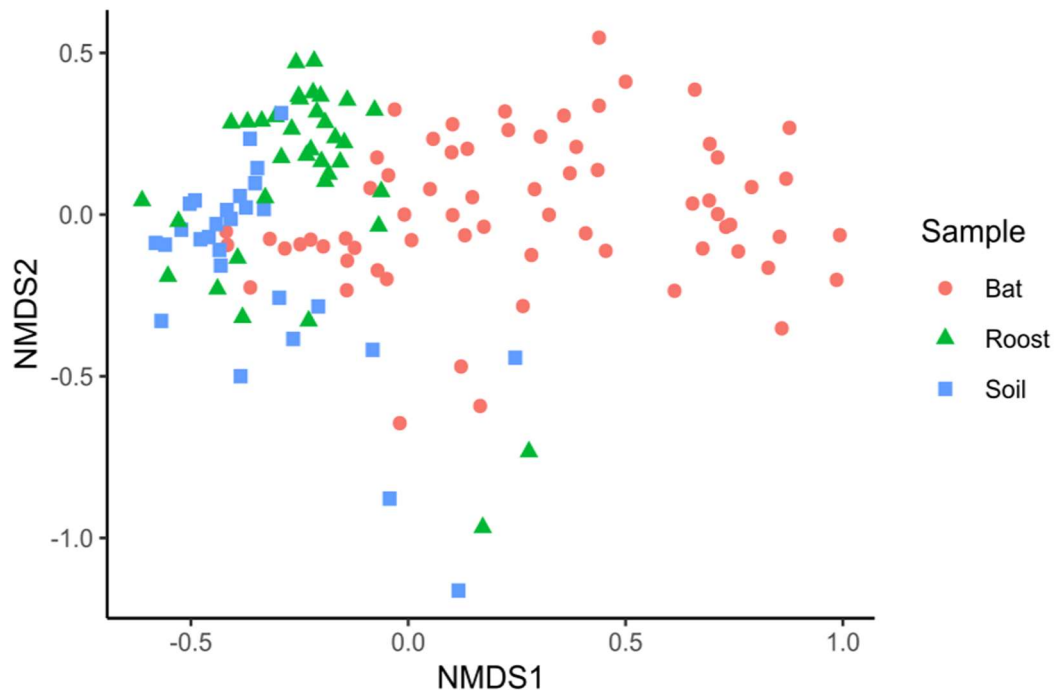


**Figure 7. Non-metric multidimensional scaling ordination showing beta diversity patterns of the bat cutaneous microbiota compared to the cave roost and cave soil microbial assemblages.**

The average bat cutaneous microbial assemblage is distinct from the roost and soil microbial assemblage ( $F_{2, 130} = 4.6823$ ,  $p \leq 0.05$ ,  $R^2 = 6.8\%$ ).

**Table 2. Analysis of average assemblage similarity across sample type.**

Adonis test on all OTUs within the bat cutaneous microbial assemblage, roost, and cave soil samples to determine differences in sample type. There is a significant difference between sample types ( $p < 0.05$ ).

	<b>Df</b>	<b>Sums of Squares</b>	<b>Mean Squares</b>	<b>F test</b>	<b>R<sup>2</sup></b>	<b>Pr (&gt;F)</b>
<b>Sample type</b>	2	3.81	1.90	4.68	0.07	0.001
<b>Residuals</b>	128	52.01	0.41		0.93	
<b>Total</b>	130	55.81			1	

**Table 3. Analysis of average assemblage similarity across *P. destructans* status.**

Adonis test on 11 indicator OTUs descriptive of variation in the bat skin microbial assemblage regardless of site or *P. destructans* (Pd) status. There is a significant difference between cave sites ( $p < 0.05$ ) and a significant interaction between cave site and *P. destructans* status ( $p < 0.05$ ).

	<b>Df</b>	<b>Sums of Squares</b>	<b>Mean Squares</b>	<b>F test</b>	<b>R<sup>2</sup></b>	<b>Pr(&gt;F)</b>
<b>pd</b>	1	0.48	0.48	1.82	0.02	0.058
<b>site</b>	19	7.95	0.42	1.59	0.37	0.001
<b>pd:site</b>	5	2.08	0.42	1.58	0.10	0.005
<b>Residuals</b>	41	10.77	0.26		0.51	
<b>Total</b>	66	21.28			1	

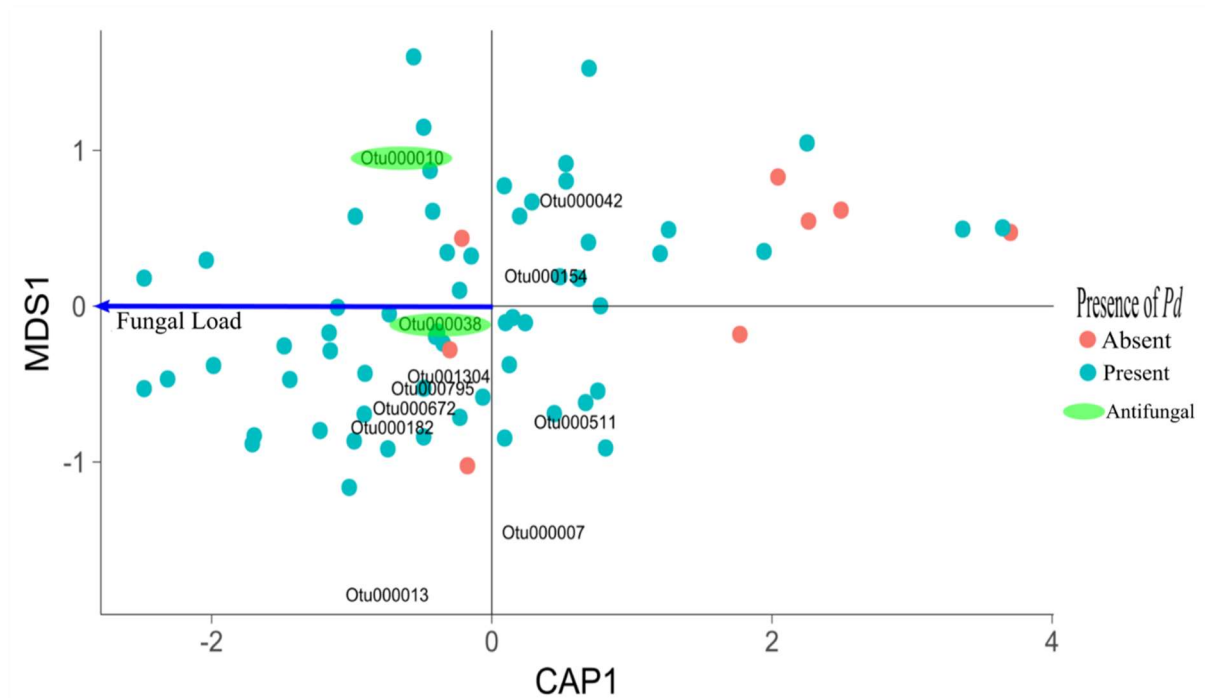


**Figure 8. Capscale analysis modeling *P. destructans* fungal load on Bray-Curtis dissimilarity values from the microbial assemblage of *P. destructans* positive and *P. destructans* negative bats.**

Colored circles represent the microbiota of *P. destructans* positive (blue) and *P. destructans* negative (red) bats. Light green ovals around OTU labels indicate a bacterial isolate that was found *in vitro* to inhibit the growth of *P. destructans*. The blue vector indicates the direction of increasing *P. destructans* fungal load from qPCR results and the relationship with bat cutaneous microbial assemblages, *P. destructans* load, and indicator OTUs.

The metagenomic profiling of functional genes provided a proof-of-concept that host-microbiome-pathogen interactions can be elucidated for wildlife pathogens using shotgun sequencing. Reads (3 193 964) from *P. destructans* negative bats averaged 183 base pairs in length. Of the reads that passed quality control, 39 027 (2%) were ribosomal RNA genes, 406 670 (21.05%) sequences contained predicted proteins with known function, and 1 486 296 (76.9%) sequences were predicted proteins with unknown function. Reads from *P. destructans* positive bats (2 864 036) averaged 205 base pairs in length. Of these reads that passed quality control, 27 444 (2%) were mapped to rRNA, 263 036 (15.09%) were predicted proteins with known function, and 1 452 225 (83.3%) were predicted proteins with unknown function. The most abundant functional gene classes for both negative and positive bats were clustering based subsystems (negative n = 13% of reads with predicted function, positive n = 14%), genes involved in carbohydrate metabolism (negative n = 11% of reads with predicted function, positive n = 12%), and genes involved with amino acid and derivatives metabolism (negative n = 9% of reads with predicted function, positive n = 9%). Tentative genes involved in disease resistance included those with production of secondary metabolites (negative bats n = 0.3% of reads with predicted function, positive n = 0.5%), and virulence, disease, and defense (negative bats n = 2.8% of reads with predicted function, and positive bats n = 3%; Fig. 9).

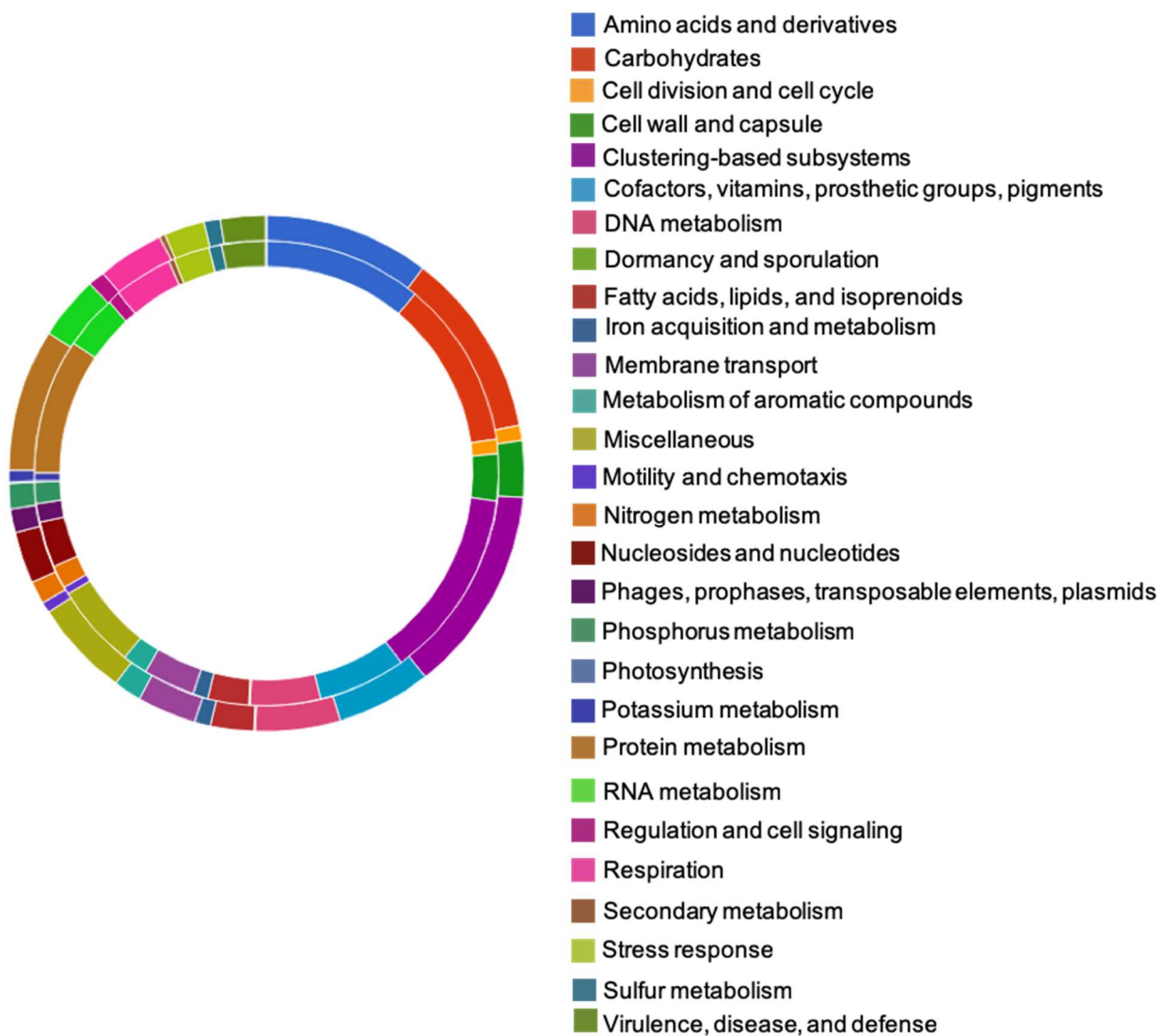


**Figure 9. Comparison of functional gene categories between *P. destructans* positive (inside circle) and *P. destructans* negative (outside circle) bats.**

Overall, it appears that bat cutaneous microbial assemblages exhibit functional redundancy regardless of *P. destructans* status.

## Discussion

This study elucidated the interaction between the host microbial assemblage, a wildlife pathogen, and environmental microbial communities. I determined that the bat microbial assemblage contains antifungal taxa, and is enriched with antifungal bacterial taxa when compared to the cave environment, supporting my first two hypotheses. Additionally, I found bats that are *P. destructans* negative have a microbial assemblage that has more antifungal bacterial taxa compared to positive bats supporting my third hypothesis. More specific to my objectives, I found that the effect of *P. destructans* on the bat cutaneous microbial assemblage varied spatially (between cave sites), further supporting the idea that the maintenance of the cutaneous microbial assemblage is driven by a complex interaction between the host and environment. Previous studies have shown that patterns in host microbial community structure were correlated with phylogenetic (Carrillo-Araujo *et al.* 2015) and environmental patterns (Avena *et al.* 2016; Lemieux-Labonté *et al.* 2016), interspecies interactions (Song *et al.* 2013), and social behaviors (Tung *et al.* 2015) suggesting that the drivers of microbiome community assembly are diverse and complicated to elucidate. Lemieux-Labonté *et al.* (2017) determined that the little brown bat (*M. lucifugus*) microbial assemblage differed between *P. destructans* positive cave sites compared to *P. destructans* naïve sites. They concluded that this difference could be confounded by geographical distances between cave sites (~1900 km apart). I also found significant differences in microbial assemblage composition between bats at different geographic sites, one possible explanation for this pattern is that microbial dispersal may be an explanatory factor for differences in skin microbial assemblages of different bats with/without *P. destructans*.

I found that bacterial isolates with anti- *P. destructans* activity are ubiquitous throughout the cave environment and on bat skin. This result might suggest potential source-sink dynamics between the environment and host skin. Cave environments are known to host microbial species capable of producing bioactive compounds (Ghosh *et al.* 2016). Antifungal taxa being found throughout the caves that I sampled, suggests that the environment may serve as a source for anti- *P. destructans* bacteria that can colonize bat skin. Alternatively, this pattern could be explained by bats shedding these bacterial cells into the surrounding environment with the soil acting as a sink. Determining the directionality of this source-sink relationship would require more carefully controlled experiments. When the relative abundance of each antifungal bacterium was quantified, the bat assemblage had a higher abundance of antifungal producing bacteria relative to the surrounding environment. In addition, total bat assemblages have a lower alpha diversity than the surrounding environment, which suggests that the bat skin may act as a selective medium for a particular community of bacteria. Similarly, previous work has shown that salamander skin acts as a selective medium for anti-*Batrachochytrium dendrobatidis* taxa, relative to the environment (Loudon *et al.* 2016).

I found that *P. destructans* status did not influence the overall alpha diversity of the bat cutaneous microbial assemblage. Ange-Stark *et al.* (2019) found similar patterns of unaltered bacterial assemblage alpha diversity for *P. subflavus* in *P. destructans* positive/negative bats. However, at a finer scale, I found that bats that were *P. destructans* negative had a microbial assemblage that had more antifungal taxa present. This result supports the hypothesis that antifungal taxa may play a role in host protection from invading fungal pathogens. Previous work by Lemieux-Labonté *et al.* (2017) also

showed enrichment of antifungal bacteria on little brown bats exposed to *P. destructans* when compared to individuals in *P. destructans* naïve caves. However, neither study is able to determine if antifungal bacteria enrichment is a cause or effect of *P. destructans* status. Future studies should work to address this by tracking the fate of *P. destructans* negative bats within this system, as well as, tracking the antifungal taxa present within each assemblage. Alternatively, when taking a more quantitative approach, I found two antifungal isolates correlated with increasing *P. destructans* fungal load (CCB44.6 and CCB311.5; Fig. 8). One of the isolates (CCB 311.5) was determined to be a species of *Rhodococcus*, a genus previously identified with anti-*P. destructans* activity (Cornelison *et al.* 2014). Taken together these results suggest that the host microbial community may influence or be influenced by fungal pathogen invasion, however the interactions between fungus and individual antifungal bacterial taxa is complex.

This study, like others (Loudon *et al.* 2016; Lemieux-Labonté *et al.* 2017) focused exclusively on culturable bacteria with antifungal activity and is therefore biased by microbes able to grow on synthetic media. Additionally, *in vitro* assays included co-culture of one bacterium with *P. destructans*, when in reality, antifungal bacteria are part of a much larger community. Designating a bacterial species as an antifungal member of the microbiome is likely an oversimplification of microbial function within the community. Cryptic antibiotics were discovered in co-culture of bacteria as a potential result of bacterial interactions (Onaka *et al.* 2011), further indicating the need to understand the bacterial assemblage as a whole rather than the simplistic interactions described here. Additional work within this system will allow for a more thorough

understanding about how ecological patterns translate into functional processes in complex host-microbe-pathogen systems.

Recent work has found taxonomic diversity but functional redundancy in microbial systems (Louca *et al.* 2016) and suggested that microbial communities should be classified by function rather than using OTU data. Bacterial assemblages have been suggested to form stochastically from within a pool of functionally similar but taxonomically distinct organisms (Burke *et al.* 2011). Here, I attempted to determine if bat skin bacterial communities are functionally redundant, and if the presence of a fungal pathogen could alter microbial community function. Functional profiles seemed to have minor differences (Fig. 9), however, overall it appears that there is considerable functional redundancy between bats with/without *P. destructans*. While there appears to be functional redundancy in taxonomically diverse assemblages across geographic space, it is difficult to discern for the population of bats sampled here given the small sample size. The limiting factor for biological replication in this study was low DNA yield. Whole genome amplification using multiple displacement amplification (MDA; Oh *et al.* 2014) is a viable option to improve DNA yield for metagenomic library preparation. However, Direito *et al.* (2014) has shown that MDA is biased against some DNA fragments, potentially limiting its utility. Additionally, all metagenomic studies are limited by the databases used to make functional predictions. In this study, like others (Louca *et al.* 2016, Rebollar *et al.* 2018), I was only able to predict  $\approx 20\%$  of functional genes. Producing more data is the only way to explore these relationships and allow for continued development of reference databases. This study served as a proof of concept to establish that functional genes can be profiled for wildlife-pathogen-microbiome

communities and will allow for future work to better elucidate functional differences between *P. destructans* positive/negative bats.

This study aimed to elucidate differences in the host bacterial community assemblages between *P. destructans* positive and negative bats. I determined a differential effect of *P. destructans* on bat microbial assemblages across space. I found that antifungal taxa were ubiquitous throughout the cave environment, but enriched in the bat cutaneous microbial assemblage, suggesting a potential source-sink relationship of environmental microbial communities and the host microbiome. Additionally, I found that *P. destructans* negative bats had a microbial assemblage with more antifungal bacterial taxa compared to *P. destructans* positive bat assemblages, supporting the hypothesis that the bat cutaneous microbial assemblage may play a role in disease defense.

### **Acknowledgements**

I would like to thank Daniel Istvanko, Cory Holiday, Chris Simpson, Chris Ogle, and Dustin Thames for assistance during field work, Megan Wharton for assistance during lab work, Joshua Grinath for statistical help, and Sarah E Bergemann for helpful comments. This work was approved by IACUC TTU-16-17-003 and USFWS 2009-038. Funding and support for this research project was provided by Tennessee Wildlife Resources Agency as a State Wildlife Grant to DMW. All raw sequence data were submitted to GenBank SRA under the accession number PRJNA565423 and PRJNA565431.

## References

- Avena CV, Parfrey LW, Leff JW *et al.* Deconstructing the bat skin microbiome: influences of the host and the environment. *Front Microbiol* 2016;**7**:1–14.
- Ange-Stark MA, Cheng TL, Hoyt JR *et al.* White-nose syndrome restructures bat skin microbiomes. *bioRxiv* 2019, DOI:10.1101/614842.
- Aziz RK, Bartels D, Best AA *et al.* The RAST server: Rapid annotations using subsystems technology. *BMC Genom* 2008;**9**:75-89.
- Bates D, Maechler M, Bolker B *et al.* Package lme4. R package version 1.1–7. <https://cran.r-project.org/web/packages/lme4/index.html>.
- Belden LK, Harris RN. Infectious diseases in wildlife: the community ecology context. *Front Ecol Environ* 2007;**5**:533–39.
- Blehert DS, Hicks AC, Behr M *et al.* Bat white-nose syndrome: An emerging fungal pathogen? *Science* 2009;**323**:227.
- Burke C, Steinberg P, Rusch D. Bacterial community assembly based on functional genes rather than species. *PNAS* 2011;**108**:14288–93.
- Caporaso JG, Lauber CL, Walters WA *et al.* Global patterns of 16S rRNA diversity at a depth of millions of sequences per sample. *PNAS* 2011;**108**:4516–22.
- Carrillo-Araujo M, Taş N, Alcántara-Hernández RJ *et al.* Phyllostomid bat microbiome composition is associated to host phylogeny and feeding strategies. *Front Microbiol* 2015;**6**:1–9.
- Cornelison CT, Keel MK, Gabriel KT *et al.* A preliminary report on the contact-independent antagonism of *Pseudogymnoascus destructans* by *Rhodococcus rhodochrous* strain DAP96253. *BMC Microbiol* 2014;**14**:1–7.
- De Vos JM, Joppa LN, Gittleman JL *et al.* Estimating the normal background rate of species extinction. *Conserv Biol* 2014;**29**:452–62.
- Direito SOL, Zaura E, Little M *et al.* Systematic evaluation of bias in microbial community profiles induced by whole genome amplification. *Environ Microbiol* 2014;**16**:643–57.
- Dobony CA, Hicks AC, Langwig KE *et al.* Little brown myotis persist despite exposure to white-nose syndrome. *J Fish Wildl Manag* 2011;**2**:190–95.
- Ellison SL, English CA, Burns MJ *et al.* Routes to improving the reliability of low-level DNA analysis using real-time PCR. *BMC Biotechnol* 2006;**6**:33.
- Fisher MC, Henk DA, Briggs CJ *et al.* Emerging fungal threats to animal, plant, and ecosystem health. *Nature* 2012;**484**:186–94.
- Frick WF, Pollock JF, Hicks AC *et al.* An emerging disease causes regional population collapse of a common North American bat species. *Science* 2010;**329**:679–82.
- Frick WF, Cheng TL, Langwig KE *et al.* Pathogen dynamics during invasion and establishment of white-nose syndrome explain mechanisms of host persistence. *Ecology* 2017;**98**:624–31.
- Ghosh S, Kuisiense N, Cheeptham N. The cave microbiome as a source for drug discovery: reality or pipe dream? *Biochem Pharmacol* 2016;**134**:18–34.
- Gibbons JW, Scott DE, Ryan TJ *et al.* The global decline of reptiles, de ja vu amphibians. *Bioscience* 2000;**50**:653–66.

- Gray MJ, Lewis JP, Nanjappa P *et al.* Batrachochytrium salamandrivorans: the North American response and a call for action. *PLoS Pathog* 2015, DOI:10.1371/journal.ppat.1005251.
- Greenblum S, Turnbaugh PJ, Borenstein E. Metagenomic systems biology of the human gut microbiome reveals topological shifts associated with obesity and inflammatory bowel disease. *PNAS* 2011;**109**:594–99.
- Grice EA, Segre JA. The skin microbiome. *Nat Rev Microbiol* 2011;**9**:244–253.
- Harris RN, Brucker RM, Walke JB *et al.* Skin microbes on frogs prevent morbidity and mortality caused by a lethal skin fungus. *ISME J* 2009;**3**:818–24.
- Hoyt JR, Cheng TL, Langwig KE *et al.* Bacteria isolated from bats inhibit the growth of *Pseudogymnoascus destructans*, the causative agent of white-nose syndrome. *PLoS One* 2015, DOI:10:e0121329.
- Janicki AF, Frick WF, Kilpatrick AM *et al.* Efficacy of Visual Surveys for White-Nose Syndrome at Bat Hibernacula. *PLoS One* 2015, DOI:10.1371/journal.pone.0133390.
- Kozich JJ, Westcott SL, Baxter NT *et al.* Development of a dual-index sequencing strategy and curation pipeline for analyzing amplicon sequence data on the MiSeq Illumina sequencing platform. *Appl Environ Microbiol* 2013;**79**:5112–20.
- Lane, DJ. 16S/23S rRNA sequencing. In: Stackebrandt E, Goodfellow M (eds.). *Nucleic acid techniques in bacterial systematics*. New York: John Wiley and Sons, 1991, 115–75.
- Langwig KE, Frick WF, Bried JT *et al.* Sociality, density-dependence and microclimates determine the persistence of populations suffering from a novel fungal disease, white-nose syndrome. *Ecol Lett* 2012;**15**:1050–57.
- Langwig KE, Frick WF, Reynolds R *et al.* Host and pathogen ecology drive the season dynamics of a fungal disease, white-nose syndrome. *Proc Royal Soc B* 2015, DOI:10.1098/rspb.2014.2335.
- Langwig KE, Hoyt JR, Parise KL *et al.* Resistance in persisting bat populations after white-nose syndrome invasion. *Philos Trans Royal Soc B* 2017;**372**:1–9.
- Lemieux-Labonté V, Tromas N, Shapiro BJ *et al.* Environment and host species shape the skin microbiome of captive neotropical bats. *PeerJ* 2016, DOI: 10.7717/peerj.2430.
- Lemieux-Labonté V, Simard A, Willis CKR *et al.* Enrichment of beneficial bacteria in the skin microbiota of bats persisting with white-nose syndrome. *Microbiome* 2017;**5**:115–30.
- Lindahl BD, Nilsson RH, Tedersoo L *et al.* Fungal community analysis by high-throughput sequencing of amplified markers - a user's guide. *New Phytol* 2013;**199**:288–99.
- Louca S, Jacques SMS, Pires APF *et al.* High taxonomic variability despite stable functional structures across microbial communities. *Nat Ecol Evol* 2016, DOI: 10.1038/s41559-016-0015.
- Loudon AH, Venkataraman A, Treuren WV *et al.* Vertebrate hosts as islands: dynamics of selection, immigration, loss, persistence, and potential function of bacteria on salamander skin. *Front Microbiol* 2016, DOI:10.3389/fmicb.2016.00333.

- Maslo B, Fefferman NH. A case study of bats and white-nose syndrome demonstrating how to model population viability with evolutionary effects. *Conserv Biol* 2015;**29**:1176–85.
- McCallum ML. Amphibian Decline or Extinction? Current Declines Dwarf Background Extinction Rate. *J Herpetol* 2007;**41**:483–91.
- Meteyer CU, Buckles EL, Blehert DS *et al*. Histopathologic criteria to confirm white-nose syndrome in bats. *J Vet Diagn Investig* 2009;**21**:411–14.
- Meyer F, Paarmann D, D’Souza M *et al*. The metagenomics RAST server—a public resource for the automated phylogenetic and functional analysis of metagenomes. *BMC Bioinform* 2008, DOI:10.1186/1471-2105-9-386.
- Morgan XC, Tickle TL, Sokol H *et al*. Dysfunction of the intestinal microbiome in inflammatory bowel disease and treatment. *Genome Biol* 2012, DOI:10.1186/gb-2012-13-9-r79.
- Morris EK, Caruso T, Buscot F *et al*. Choosing and using diversity indices: insights for ecological applications from the German Biodiversity Exploratories. *Ecol Evol* 2014;**4**:3514–24.
- Muller LK, Lorch JM, Linder DL *et al*. Bat white-nose syndrome: a real-time TaqMan polymerase chain reaction test targeting the intergenic spacer region of *Geomyces destructans*. *Mycologia* 2013;**105**:253–59.
- Oh J, Byrd AL, Deming C *et al*. Biogeography and individuality shape function in the human skin metagenome. *Nature* 2014;**514**:59–64.
- Oksanen J, Blanchet FG, Friendly M *et al*. Vegan: Community Ecology Package. R package version 2.5-2 2018. <https://CRAN.R-project.org/package=vegan> (05 Sept. 2019, date last accessed).
- Onaka H, Mori Y, Igarashi Y *et al*. Mycolic acid containing bacteria induce natural-product biosynthesis in *Streptomyces* species. *Appl Environ Microbiol* 2011;**77**:400–06.
- Quast C, Pruesse E, Yilmaz P *et al*. The SILVA ribosomal RNA gene database project: improved data processing and web-based tools. *Nuc Acids Res* 2012, DOI:10.1093/nar/gks/1219.
- Randle-Boggis RJ, Helgason T, Sapp M *et al*. Evaluating techniques for metagenome annotation using simulated sequence data. *FEMS Microbiol Ecol* 2016, DOI:10.1093/femsec/fiw095.
- Rebollar EA, Gutiérrez-Preciado A, Noecker C *et al*. The skin microbiome of the neotropical frog *Craugastor fitzingeri*: inferring potential bacterial-host-pathogen interactions from metagenomic data. *Front Microbiol*. 2018; DOI:10.3389/fmicb.2018.00466.
- Reeder DM, Frank LC, Turner GG *et al*. Frequent arousal from hibernation linked to severity of infection and mortality in bats with white-nose syndrome. *PLoS One* 2012, DOI:10.1371/journal.pone.0038920.
- Rognes T, Flouri T, Nichols B *et al*. VSEARCH: a versatile open source tool for metagenomics. *PeerJ* 2016, DOI:10.7717/peerj.2584.
- Schloss PD, Westcott SL, Ryabin T *et al*. Introducing mothur: open-source, platform-independent, community-supported software for describing and comparing microbial communities. *Appl Environ Microbiol* 2009;**75**:7537–41.

- Schloss PD, Westcott SL. Assessing and improving methods used in operational taxonomic unit-based approaches for 16S rRNA gene sequence analysis. *Appl Environ Microbiol* 2011;**77**:3219–26.
- Sharpton TJ. An introduction to the analysis of shotgun metagenomic data. *Front Plant Sci* 2014;**5**:1–14.
- Song SJ, Lauber C, Costello EK *et al.* Cohabiting family members share microbiota with one another and with their dog. *eLife* 2013, DOI:10.7554/eLife.00458.
- Tung J, Barreiro LB, Burns MB *et al.* Social networks predict gut microbiome composition in wild baboons. *eLife* 2015, DOI:10.7554/eLife.05224.001.
- Wickham H. *ggplot2: Elegant Graphics for Data Analysis*. New York: Springer-Verlag, 2016.

## CHAPTER III: HOST MICROBIAL ASSEMBLAGE FUNCTIONAL REDUNDANCY TO FUNGAL PATHOGENICITY

Matthew Grisnik<sup>1</sup>, Joshua B Grinath<sup>2</sup>, John P. Munafo Jr<sup>3</sup>, Donald M Walker<sup>1</sup>

<sup>1</sup> Middle Tennessee State University, Department of Biology, Murfreesboro, Tennessee 37132, USA

<sup>2</sup> Idaho State University, Department of Biological Sciences, Pocatello, Idaho 83209, USA

<sup>3</sup> University of Tennessee Knoxville, Department of Food Science, Knoxville, Tennessee 37996, USA

### **Abstract**

Understanding how host associated microbial assemblages respond to pathogen invasion has implications for host health. Until recently, most work has focused on understanding the taxonomic composition of these assemblages. However, recent work has suggested that microbial assemblage taxonomic composition is decoupled from its function, with assemblages being taxonomically varied but functionally constrained. Therefore, there is increased need for understanding host associated microbial assemblage function. My objective was to understand how the host cutaneous microbial assemblage responds to fungal pathogen invasion within a functional context. I hypothesized that there will be no difference in the functional assemblages between *P. destructans* positive and negative bats, and that this pattern will be driven by the functional redundancy of bacterial taxa. I hypothesize that the bat cutaneous microbial assemblage will have functions for the production of antifungal metabolites. To test this, I used a combination of shotgun metagenomic and amplicon sequencing to characterize

the bat cutaneous microbial assemblage in the presence/absence of *P. destructans*.

Results show that while there is a shift in taxonomic assemblage composition between *P. destructans* positive and negative bats, there is no difference between functions.

Additionally, results show that at a broad scale there is likely functional redundancy across bacterial taxa, however at a finer scale, there is variation in functional capabilities.

## **Introduction**

Understanding the processes that drive community assembly is central to microbial ecology (Nemergut *et al.* 2013). It is important to elucidate factors that influence the host associated microbial assemblage as this community is hypothesized to influence host health (Belden and Harris 2007; Grice and Segre 2011). Host microbial assemblages can be described by their functional and/or taxonomic composition. Recent work has shown that a wide range of factors can influence the taxonomic composition of host cutaneous microbial assemblages such as host evolutionary history (Carrillo-Araujo *et al.* 2015), environmental patterns (Avena *et al.* 2016; Lemieux-Labonté *et al.* 2016), host behavior (Song *et al.* 2013; Tung *et al.* 2015), and presence of disease (Cho and Blaser 2012; Lemieux-Labonté *et al.* 2017). While a considerable amount of work has gone into understanding factors that influence microbial taxonomic assemblages, those that influence assemblage function are less well understood.

Functions present within the host associated microbial assemblage have been suggested to play a role in host development (Braendle *et al.* 2003), nutrient acquisition (Gill *et al.* 2006), and host fitness (Dharampal *et al.* 2020). The relationship between host associated microbial assemblage function and host health suggests that understanding functional rather than taxonomic assemblages may be a more informative measure in

microbiome science (Allison and Martiny 2008; Louca *et al.* 2018; Escalas *et al.* 2019). Additionally, recent work has suggested that microbial community taxonomic composition can be decoupled from its function, with communities being taxonomically variable, but functionally redundant (Green *et al.* 2008; Burke *et al.* 2011; Louca *et al.* 2016). Two mechanisms have been proposed to explain this pattern including microbial niches may be filled by a lottery type mechanism, with selection for functionally redundant bacteria, of which the taxonomic identity is largely determined through stochastic processes (Burke *et al.* 2011). Alternatively, individual taxa may vary in functional capabilities, however, as an assemblage they have similar function (Allison and Martiny 2008). Microbial communities may be assembled through species sorting mechanisms (environmental selection) across functional groups, but with neutral processes dictating which taxa fill the functional role (Van der Gucht *et al.* 2007). For this to be the case, individual bacterial taxa likely have a wide range of functional capabilities (Louca *et al.* 2018). Additionally, metabolic functions show a lack of phylogenetic signal (Aguilar *et al.* 2004), further supporting the idea that multiple taxa can play similar roles within an assemblage.

Host associated cutaneous microbial assemblages play a role in host defense (Grice and Segre 2011; Rebollar *et al.* 2018; Grisnik *et al.* 2020) due to their ability to produce antifungal compounds (Flórez *et al.* 2015). Previous work has shown that individual bats that are exposed to, but not invaded by *P. destructans*, have microbial assemblages enriched in antifungal bacterial taxa (Lemieux-Labonté *et al.* 2017; Grisnik *et al.* 2020). However, it is likely that using taxonomic data to infer function is an oversimplification of these complex communities. Until recently, microbial community

function has been limited to interpretation within a phylogenetic context (Langille *et al.* 2013), however, the development of metagenomic sequencing has allowed for the inference of community metabolic profiles (Sharpton 2014). Functional pathways including membrane transport, biosynthesis of secondary metabolites, and metabolism of terpenoid and polyketides are important in host defense from fungal pathogens (Rebollar *et al.* 2018). These pathways are hypothesized to play an essential role in bacterial communication within a microbiome, as well as, bacterial response to external stimuli such as pathogen invasion (Flórez *et al.* 2015; Rebollar *et al.* 2018). Understanding the differential abundance of important functional pathways may provide insight into microbial assemblage response to fungal pathogen invasion.

Fungal pathogens have impacted multiple animal phyla and are considered a predominant threat to worldwide biodiversity (Fisher *et al.* 2012). The fungal pathogen *Pseudogymnoascus destructans* was introduced into the United States in 2006 and has contributed to the decline of multiple species of bats and threatens several more with extinction (Langwig *et al.* 2012; Langwig *et al.* 2015). Bat declines were not consistently observed across species or sites, suggesting that some bats are able to persist in the presence of *P. destructans* (Dobony *et al.* 2011; Langwig *et al.* 2012; Frick *et al.* 2017). One species that has recently shown signs of persistence despite a *P. destructans* rich environment, is the Tri-colored bat (*Perimyotis subflavus*; Langwig *et al.* 2017). A variety of mechanisms including behavioral changes (Langwig *et al.* 2012), genetic resistance and evolutionary rescue (Maslo and Fefferman 2015), acquired resistance, and/or antifungal properties of the host cutaneous microbial assemblage are hypothesized to explain Tri-colored bat resistance to *P. destructans* (Lemieux-Labonté *et al.* 2017).

The objective of this study was to use a combination of shotgun metagenomic and amplicon sequencing to understand how the host cutaneous microbial assemblage responds to fungal pathogen invasion within a functional context. Specifically, I aimed to 1) determine if host microbial assemblages exhibit functional redundancy in the presence of a fungal pathogen, 2) understand how microbial assemblage function relates to disease status, and 3) determine the presence of genes responsible for antifungal metabolite production in the bat cutaneous microbiome. If functional redundancy is observed, it would suggest that species sorting mechanisms drive functional community assembly in the face of pathogen mediated disturbance. More specifically I hypothesize that there will be no difference in functional assemblages between *P. destructans* positive and negative bats. I hypothesize these patterns to be driven by functional redundancy of bacterial taxa. Additionally, I hypothesize that the bat cutaneous microbial assemblage will have functions associated with the production of antifungal metabolites, suggesting the role of the microbiome in host defense from pathogens.

## **Methods**

### *Field Work/Sample Collection*

Cutaneous swabs from 252 *P. subflavus* individuals were collected from caves throughout Tennessee during the 2017 to 2019 statewide surveys (January-April). Specifically, when a bat was located, a sterile swab (Puritan polyester tipped swabs, Puritan VWR cat # 10805165) was briefly dipped into a Falcon tube of sterile Millipore water and five swab strokes of each bat muzzle/ear and five from wings/fur were taken. These samples were temporarily stored on ice in the field and moved to storage at -80°C until processing.

### *Quantitative PCR Assays*

Quantitative PCR (qPCR) was performed to determine the presence of *P. destructans* within each sample. Each sample was tested in triplicate on a Bio-Rad C1000 Thermal cycler following the qPCR assay described in Muller *et al.* (2013). Briefly each PCR reaction was 10  $\mu$ L total volume and contained 5  $\mu$ L 2x Primetime MasterMix, 0.4  $\mu$ L forward primer (20  $\mu$ M), 0.4  $\mu$ L reverse primer (20  $\mu$ M), 0.1  $\mu$ L probe (20  $\mu$ M), 3.1  $\mu$ L PCR grade water, and 1  $\mu$ L of DNA. Thermocycling conditions consisted of a 3 min activation step at 95°C, followed by 50 cycles of 95°C for 3 s, and 60°C for 30 s. Additionally each qPCR plate contained a positive and a no template negative control run in triplicate. DNA extraction blanks were also analyzed using qPCR to rule out contamination during the DNA extraction process. A positive sample was defined as exponential amplification in triplicate at or before  $C_t$  40 (Muller *et al.* 2013; Janicki *et al.* 2015). Ambiguous samples (those that amplified in one or two of the 3 replicates) were re-analyzed, if one or more reactions amplified the sample was then considered positive (Ellison *et al.* 2006). While false positive and negative designations are always a possibility, Shuey *et al.* (2014) determined that as low as 8 fg of *P. destructans* can be detected with this assay.

### *Characterization of Microbial Assemblage Structure and Function*

Swabs from 187 *P. subflavus* individuals were selected for DNA extraction based on *P. destructans* status. DNA was extracted using the Qiagen DNeasy PowerSoil HTP 96 kit following the manufacture's protocol. Final elution (~ 100  $\mu$ L) was concentrated four-fold to a final volume of ~25  $\mu$ L using an Eppendorf Vacufuge plus. To reduce contamination, each step (DNA extraction, PCR setup, and post PCR processes) were

conducted in separate PCR cabinets. Additionally, each cabinet had an assigned set of pipettes that were routinely sterilized by autoclaving. Lastly in order to reduce potential bias caused by well to well contamination each sample was randomly distributed across DNA extraction and PCR plates (Minich *et al.* 2019).

### *Shotgun Metagenomic Sequencing*

A total of 54 *P. subflavus* individuals from 17 caves were selected for shotgun metagenomic sequencing based on their *P. destructans* status (n = 27 negative and n = 27 positive individuals). Due to low DNA yield from individual swabs, samples were combined based on *P. destructans* status into six pooled libraries (three *P. destructans* positive and three *P. destructans* negative pools) with a final quantity of DNA greater than 1 ng in each pool. Each pooled sample consisted of nine individual bat samples. Samples were prepared following the Illumina Nextera DNA Flex library preparation protocol and loaded onto an Illumina NextSeq flow cell and sequenced (paired-end 2 × 150 bp reads).

### *Amplicon Sequencing*

Swabs from 159 *P. subflavus* (n = 28 negative, n = 131 positive individuals) were selected from 45 caves for 16S metabarcoding and amplicon sequencing. Samples were prepared following a slightly modified version of the Illumina 16S Metagenomic Sequencing Library Preparation protocol. The V4 region of 16S rRNA marker was targeted using the primers 806R/515F (Caporaso *et al.* 2011). PCR reactions consisted of 12.5 µL MCLAB I-5 Hi-Fi Taq mastermix, 1 µL of 806R (10 µM), 1 µL of 515F (10 µM), 5.5 µL PCR grade water, and 5 µL DNA template for a total volume of 25 µL. PCR was performed with an initial denaturation at 95°C for 2 mins, followed by 35 cycles of

98°C for 10 s, 55°C for 15 s, and 72°C for 5 s, with a final extension cycle of 72°C for 5 min. After amplicon PCR and indexing steps MAGBIO High-prep magnetic beads were used to remove primer/adaptor dimers. Each sample was quantified using a Promega Quantus Fluorometer, normalized, pooled at 4 picomolar concentration, and loaded onto an Illumina MiSeq v2 flow cell. Sequencing was performed using a 500-cycle reagent kit (paired-end, 2 × 250 bp reads).

### *Amplicon Bioinformatics*

Processing of amplicon sequencing reads was done using mothur v 1.42.1 (Schloss *et al.* 2009). Contigs were assembled from paired-end reads and I removed any sequences containing homopolymers greater than eight nucleotides or ambiguous base calls. Unique sequences were identified and aligned to the SILVA v123 bacterial reference database (Quast *et al.* 2012). Sequences were then trimmed to the V4 region and *pre-clustered* allowing for two nucleotide differences. Chimeras were removed using the *vsearch* function in mothur (Rognes *et al.* 2016), and sequences were classified into taxonomic lineages. Non-target reads, those that were identified as Archaea, Eukarya, chloroplasts, mitochondria, and unknowns were removed. Sequences were clustered into operational taxonomic units (OTUs) at 97% similarity using the *cluster.split* command in mothur (Schloss and Westcott 2011). Rare OTUs ( $n < 5$ ) were removed from the dataset as well as those that were found within the DNA extraction blank controls ( $n = 1669$  OTUs). A total of 5 701 307 sequences passed all quality control filtering steps. Data were then normalized by subsampling each library at 1200 sequence reads. Subsampling was chosen as the normalization method as previous work has shown that it is the most effective way to account for variation in final library size post sequencing (Weiss *et al.*

2017). OTUs were selected as the focal taxonomic level of study, as previous work has suggested that there is a lack of a difference in broadscale ecological patterns observed when comparing OTUs and ASVs (Glassman and Martiny 2018). All mothur commands are included in Appendix C.

### *Shotgun Metagenomic Sequencing and Bioinformatics*

DNA sequences from shotgun metagenomics sequencing were analyzed following the MetaWRAP pipeline (Uritskiy *et al.* 2018). More specifically, the MetaWRAP read\_qc module was used to trim adapters from sequencing reads and remove human and bat-based contamination. To remove bat-based contamination I used the genome for *Eptesicus fuscus* which is the closest relative to *P. subflavus* with a genome sequence in the NCBI database. The metaWRAP assembly module (using MegaHIT option; Li *et al.* 2015) was then used to assemble reads. Reads were binned into draft genomes on a per sample basis using three binning module algorithms; CONCOCT (Alneberg *et al.* 2014), Maxbin (Wu *et al.* 2016), and metaBIN (Sharma *et al.* 2012), and then consolidated into a single draft genome bin using the Bin\_refinement module with refinement parameters set to the default (70% completion, 5% contamination). I used Salmon (Quant\_bins module) to quantify bins (Patro *et al.* 2017), which calculates weighted contig abundance by multiplying the contig read depth by contig length, and then standardizes to the total abundance. PROKKA (Seemann 2014) was used for functional gene prediction of metagenome bins. I then used the output from Salmon to determine bins that were differentially abundant on *P. destructans* positive and negative samples, as well as, bins that were found only in one disease category. In total nine metagenome bins were selected for further analysis. I then used BlastKoala (Kanehisa *et al.* 2016) to classify

metabolic functions using the KEGG database at both the pathway and at the KEGG ortholog (KO) level for each of the nine metagenome bins. Gene functional identity is determined based on an evaluation of sequence similarity scores and best hit relations (Kanehisa *et al.* 2013). Additionally, in order to take phylogenetic relationship of the bacterial metagenomes into account, I created a species tree within KBase (Arkin *et al.* 2018). The species tree was created using 49 universal genes defined by Clusters of Orthologous groups (COGS; Tausov *et al.* 2000). The nine bat cutaneous bacterial metagenomes were combined with closely related publicly available genomes to form a multiple sequence alignment (MSA) and were then curated using Gblocks (Castresana 2000). The curated MSA was then used to build a phylogenetic tree, inferred with FastTree2 (Price *et al.* 2010). Both KEGG pathways and KEGG orthologs were mapped back to the species tree to assess potential functional phylogenetic signal or redundancy.

### *Statistical Analyses*

To address questions of functional redundancy, I used a multi-teared approach outlined by the subheadings below. For purposes of data curation, I removed the bottom 5% of OTUs based on abundance (OTUs that were observed less than two times), as previous work has suggested that rare taxa can influence assemblage analyses (Presley *et al.* 2010). Since I was interested in determining if there are differences in the presence of functions, I transformed the abundance data to presence/absence.

*Assessment of Functional Redundancy* - I performed an indicator analysis to identify OTUs that are indicative of *P. destructans* presence or absence within a sample using the *multipatt* function in R package *indicspecies* (De Cáceres *et al.* 2020).

Assemblages were then averaged by site within disease category (*P. destructans* presence

or absence) to remove the nestedness of the dataset, which resulted in one to two “averaged assemblages” for each site, including one for *P. destructans* positive and one for *P. destructans* negative bats. I used a generalized linear model (GLM) to compare the abundance of indicator OTUs for *P. destructans* negative samples between *P. destructans* positive and *P. destructans* negative averaged samples.

I then used Tax4Fun2 (Wemheuer *et al.* 2020) to make functional predictions based on the 16S rRNA amplicon data. I ran Tax4Fun2 twice, once on the full dataset (*P. destructans* negative, n = 28; *P. destructans* positive, n = 131), and once on just the indicator OTUs of *P. destructans* negative samples. This allowed for me to predict the functions (KEGG orthologs) associated with the OTUs that are indicative of *P. destructans* negative samples and determine if they are found within *P. destructans* positive assemblages. Tax4Fun2 makes functional predictions using previously sequenced and annotated bacterial genomes. Since many microbial taxa do not have a representative genome sequence, Tax4Fun2 provides a metric, the fraction of taxonomic units unused (FTU), to assess how well represented the data is by the functional database. I used a GLM to compare the FTU values between site averaged *P. destructans* positive and *P. destructans* negative samples to ensure that there was no difference in how well particular disease state assemblages were represented.

Functional gene annotations were presence/absence transformed and the least abundant 5% of functions were removed (abundance of less than  $1.5 \times 10^{-5}$ ). Functional assemblages were averaged by site within a disease category to remove nestedness of the data. I then ran a GLM to compare the richness of the KEGG orthologs associated with *P.*

*destructans* negative indicator OTUs between *P. destructans* positive and *P. destructans* negative samples averaged by site.

*Assessment of Community Level Function* - To determine if the presence of *P. destructans* correlated with a change in taxonomic or putative functional assemblage structure I generated three distance matrices for total beta diversity (SOR), turnover (SIM), and nestedness (SNE) components of Sørensen diversity on the averaged assemblage data (package *betapart*; Baselga and Orme 2012) for both OTU (16S rRNA data) and Tax4Fun2 (predicted functions) data. I then compared beta diversity measured as multivariate dispersion (*betadisper* function, package *vegan*; Oksanen *et al.* 2013) across *P. destructans* status. I then used permutational multivariate analysis of variance (PERMANOVA) with 999 permutations (function *adonis*; package *vegan*) on SOR, SIM, and SNE metrics to assess the influence of *P. destructans* status on average assemblage structure.

*Assessment of Metagenomic Assembled Genomes* - In order to determine functional differences, comparisons were made using nine metagenome bins that were differentially abundant between *P. destructans* disease categories (Fig. 10). I selected and assessed 22 major functional pathways with a focus on three pathways of hypothesized interest including the abundance of genes within the biosynthesis of secondary metabolites, membrane transport, and metabolism of terpenoids and polyketides pathways. These markers were chosen to assess bacterial-fungal interactions of the microbiome.

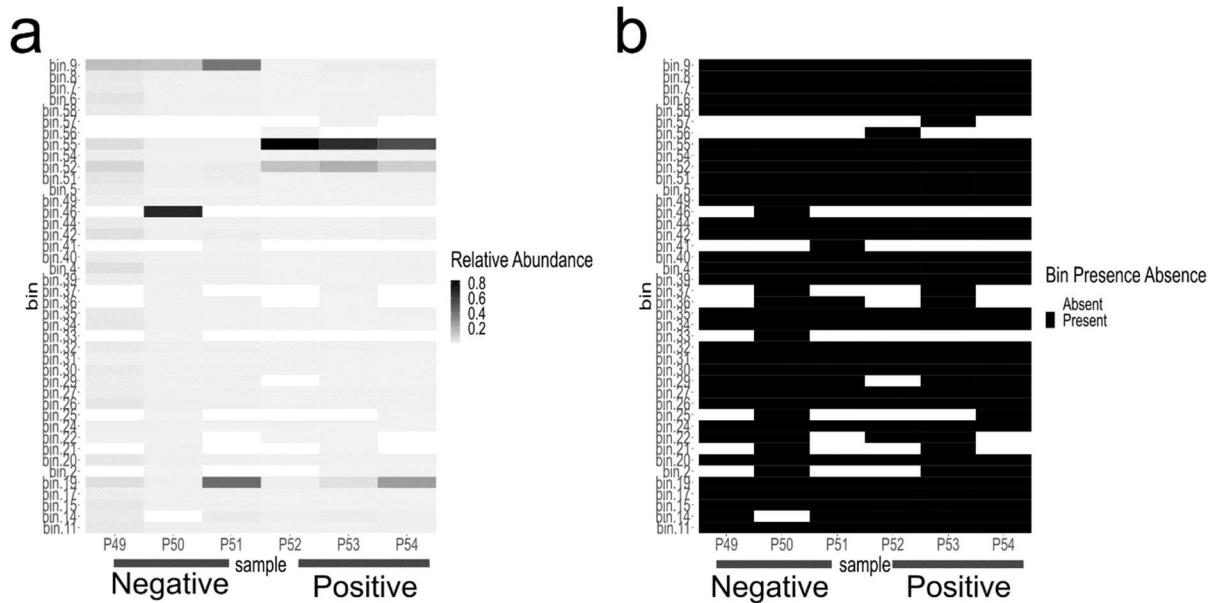


**Figure 10. Heatmap comparing the abundance and presence/absence of bins across *P. destructans* status.**

Heatmaps comparing Abundance (A) and the presence/absence of bins (B) between *P. destructans* negative (P49, P50, P51) and *P. destructans* positive (P52, P53, P54) samples. Bins 56 and 57 are found only on *Pd* positive samples while Bins 41, 46, and 33 are only found on *Pd* negative. Bins 19, 52, and 55 are more abundant on positive samples, while Bins 46 and 9 are more abundant on negative.

## Results

*Functional Redundancy* - High-throughput sequencing resulted in a total of 7498 OTUs. Indicator analysis run on the 16S rRNA data revealed 147 OTUs that were indicative of samples without *P. destructans* and four OTUs that were indicative of samples with *P. destructans*. OTUs indicative of *P. destructans* negative bats were more abundant within *P. destructans* negative assemblages relative to *P. destructans* positive assemblages when averaged by site (GLM;  $z = -17.01$ ,  $p < 0.05$ , Fig. 11A).

The percentage of OTUs used by Tax4Fun2 in the predictions of KEGG orthologs was on average 28% of OTUs (average FTU = 0.72, min = 0.35, max = 0.86). FTU values were not significantly different between *P. destructans* positive and *P. destructans* negative samples (GLM;  $z = -0.36$ ,  $p > 0.05$ ). Tax4Fun2 identified 6357 KEGG orthologs (KOs) associated with the OTUs that were indicative of *P. destructans* negative samples. These KOs were significantly more abundant on *P. destructans* positive samples than on *P. destructans* negative samples when averaged by site (GLM;  $z = 4.59$ ,  $p \leq 0.05$ ; Fig. 11B).

*Community Level Functional Redundancy* - Taxonomic beta diversity, measured as multivariate dispersion, was not significantly different between *P. destructans* positive and negative bats (betadisper; SOR:  $F_{1,54} = 0.1$ ,  $p > 0.05$ ; SIM:  $F_{1,54} = 1.7$ ,  $p > 0.05$ ; SNE:  $F_{1,54} = 3.7$ ,  $p > 0.05$ ). However, PERMANOVA revealed that average taxonomic assemblage structure differed between *P. destructans* positive and negative bats averaged by site for both total and turnover (PERMANOVA; SOR:  $F_{1,54} = 1.3$ ,  $p < 0.05$ ; SIM:  $F_{1,54} = 1.4$ ,  $p < 0.05$ , Fig 11C), but not the nestedness component of beta diversity (PERMANOVA; SNE:  $F_{1,54} = 1.0$ ,  $p > 0.05$ ). There was no significant difference in multivariate dispersion of putative functions determined by Tax4Fun2 (betadisper; SOR:  $F_{1,54} = 1.2$ ,  $p > 0.05$ ; SIM:  $F_{1,54} = 1.4$ ,  $p > 0.05$ ; SNE:  $F_{1,54} = 0.04$ ,  $p > 0.05$ ) between *P. destructans* positive and negative bats averaged by site. Additionally, there was no significant difference in average structure of putative microbiome function between *P. destructans* positive and negative bats averaged by site (PERMANOVA; SOR:  $F_{1,54} = 2.3$ ,  $p > 0.05$ ; SIM:  $F_{1,54} = 1.5$ ,  $p > 0.05$ ; SNE:  $F_{1,54} = 3.1$ ,  $p > 0.05$ , Fig 11D).

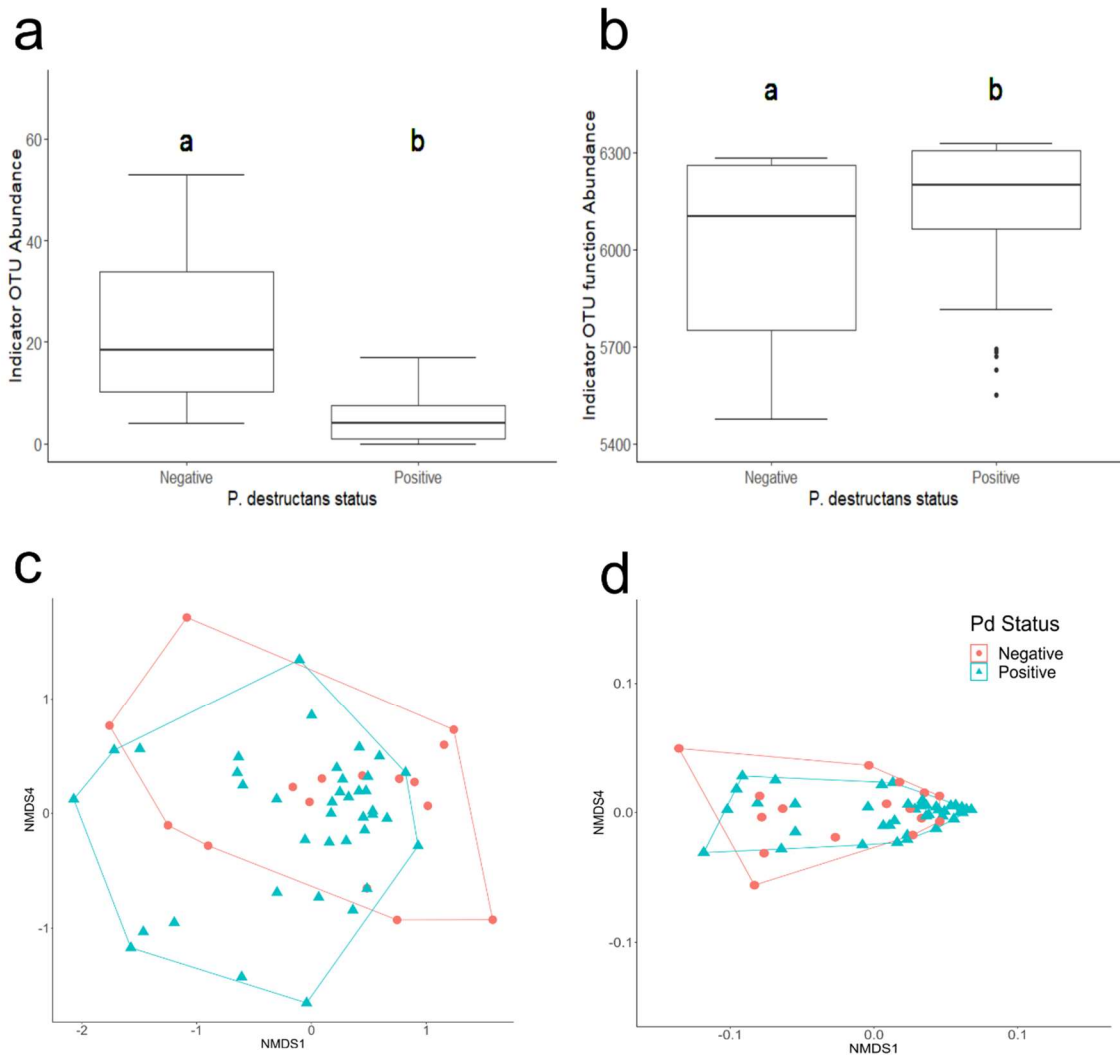


**Figure 11. Comparison of *P. destructans* negative indicator taxa (A) and punitive function (B) across *P. destructans* status. Non-metric multidimensional scaling ordination for taxonomic assemblage structure (C), and functional assemblage (D) across *P. destructans* positive and negative bats.**

A). Abundance of taxa indicative of *P. destructans* negative samples compared between *P. destructans* positive and *P. destructans* negative bats averaged by site. B). Abundance of KEGG Orthologs associated with the OTUs indicative of *P. destructans* negative samples compared between *P. destructans* positive and negative bats averaged by site. There is a significant effect of *P. destructans* ( $p < 0.05$ ) on average taxonomic assemblage structure (C), however, there is no significant effect of *P. destructans* ( $p < 0.05$ ) on average functional assemblage structure (D).

*Metagenomic Assembled Metagenomes* - The nine metagenomes that were selected for more in-depth analysis included bin number 56 (*Flavobacteriaceae*), and bin 57 (*Sphingopyxis*) were only found on *P. destructans* positive samples, whereas, bins 33 (*Antricoccus*), 41 (*Staphylococcus*), and 46 (*Parvularculaceae*) were only found on *P. destructans* negative bats. Bins 19 (*Ralstonia*), 52 (*Rhodococcus*), and 55 (*Micrococcaceae*) were more abundant on *P. destructans* positive samples, whereas, bins 46 (*Parvularculaceae*) and 9 (*Euzebyaceae*) were more abundant on *P. destructans* negative bats (Fig. 10). Using BlastKoala, I was able to annotate between 33.4% and 62.3% of reads from nine metagenome bins. I found that at the broadest scale (KEGG functional pathways) the metagenomes appeared functionally redundant, with some minor variation (Fig. 12). The pathways with the highest relative abundance within each metagenome were carbohydrate metabolism (mean = 17.5%, SD = 0.04), amino acid metabolism (mean = 15.7%, SD = 0.01), metabolism of cofactors and vitamins (mean = 8.7%, SD = 0.007), and energy metabolism (mean = 8.2%, SD = 0.01).

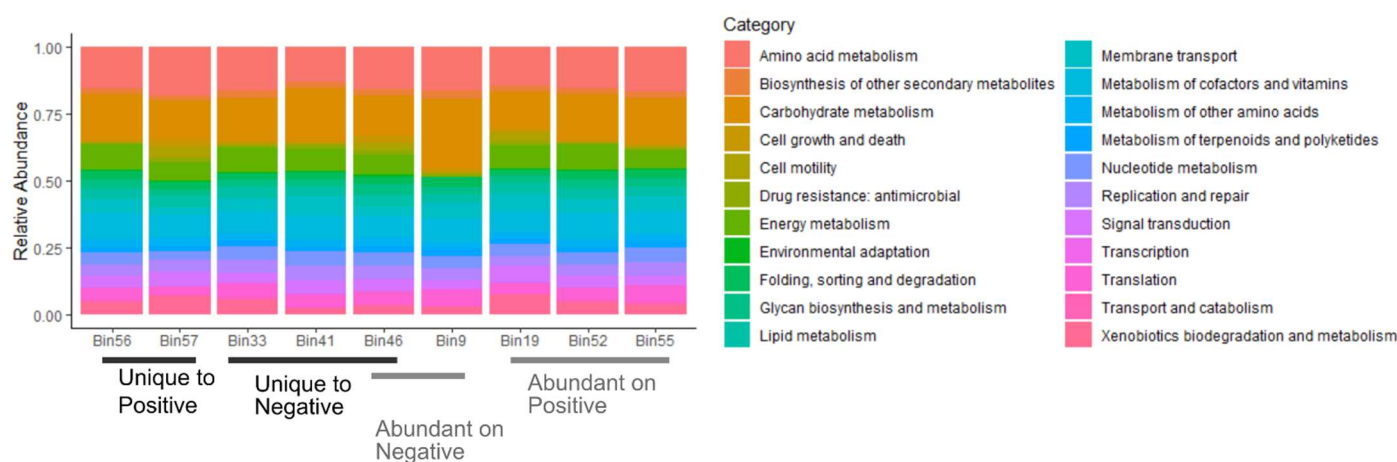


**Figure 12. Broadscale functional redundancy across functional pathways.** Stacked bar chart of KEGG identified functional pathways for the 9 selected Bins. In general, there appears to be functional redundancy across differentially abundant Bins.

Variation was observed within the KEGG pathway for the biosynthesis of secondary metabolites based on *P. destructans* status (Fig. 13A). Metagenomes of bacteria in *P. destructans* positive samples had genes that play a role in carbapenem biosynthesis. Metagenomes of bacteria living on *P. destructans* negative bats had genes involved in biosynthesis of various secondary metabolites (specifically cycloserine, staphyloferrin A and B, roseoflavin, dapdiamides, grixazone, ethynylserine, and aerobactin). Metagenomes that are more abundant on *P. destructans* negative samples had genes involved with the staurosporine biosynthesis pathway (Fig. 13B). Metagenomes of bacteria on *P. destructans* positive bats had genes responsible for penicillin and cephalosporin biosynthesis.

KEGG pathways for membrane transport showed some minor differences when comparing metagenomes by disease state. For metagenomes found only in *P. destructans* positive samples, genes associated with a phosphotransferase system are missing from bin 56 (Fig. 13C). This gene is also missing from bin 52, a representative metagenome differentially abundant, on *P. destructans* positive bats (Fig. 13D).

Within a phylogenetic context I found that broadscale functions exhibit functional redundancy across four distinct bacterial phyla (Fig. 14). For example, genes involved in amino acid metabolism were highly conserved across all nine metagenomes, with only minor variation in abundance. At a finer scale (within pathways; Fig. 15), there is more variation. For example, genes associated with amino acid biosynthesis are fairly conserved across all metagenomes, however, genes associated with cellular processes vary across both closely and distantly related bacterial phyla (Fig. 15).

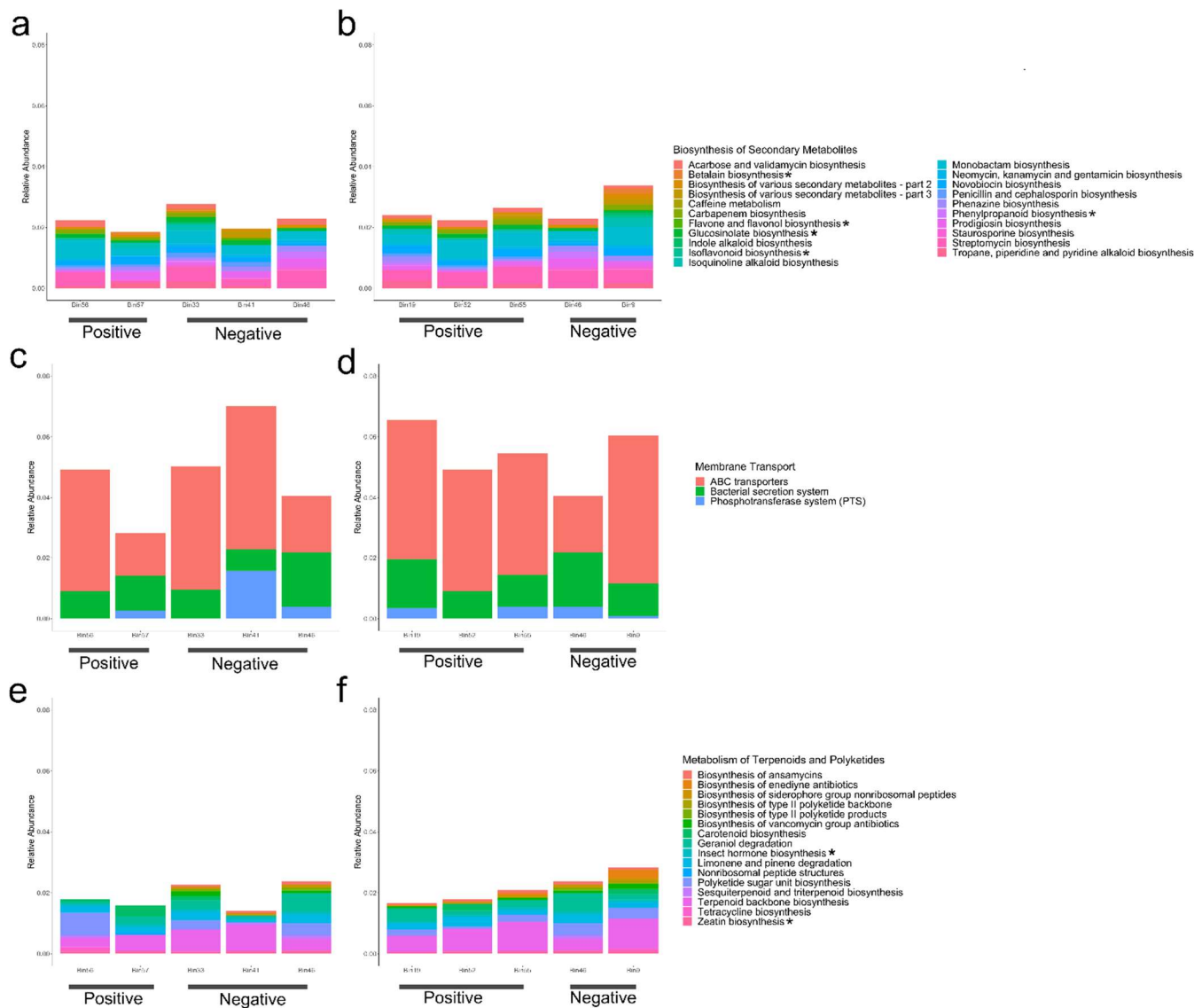


### Figure 13. Fine scale functional variability across functional orthologs.

Stacked bar chart of gene relative abundance within hypothesized KEGG pathways of interest. Charts A, C, and E represent bins that are unique to one *P. destructans* status (bins 56 and 57 *P. destructans* positive, and bins 33, 41, and 46 *P. destructans* negative). Charts B, D, and F are bins that are associated with differential abundance between *P. destructans* status (bins 19, 52, and 55 are more abundant on *P. destructans* positive whereas bins 46 and 9 are more abundant on *P. destructans* negative). Charts A and B represent genes within the biosynthesis of secondary metabolites KEGG pathway. Charts C and D represent genes within membrane transport pathway. Charts E and F represent genes within the metabolism of terpenoids and polyketides pathway. While most genes are represented in assemblages regardless of *P. destructans* status, there are some differences in relative abundance. \* indicates questionable functions based on comparisons to nonbacterial databases.

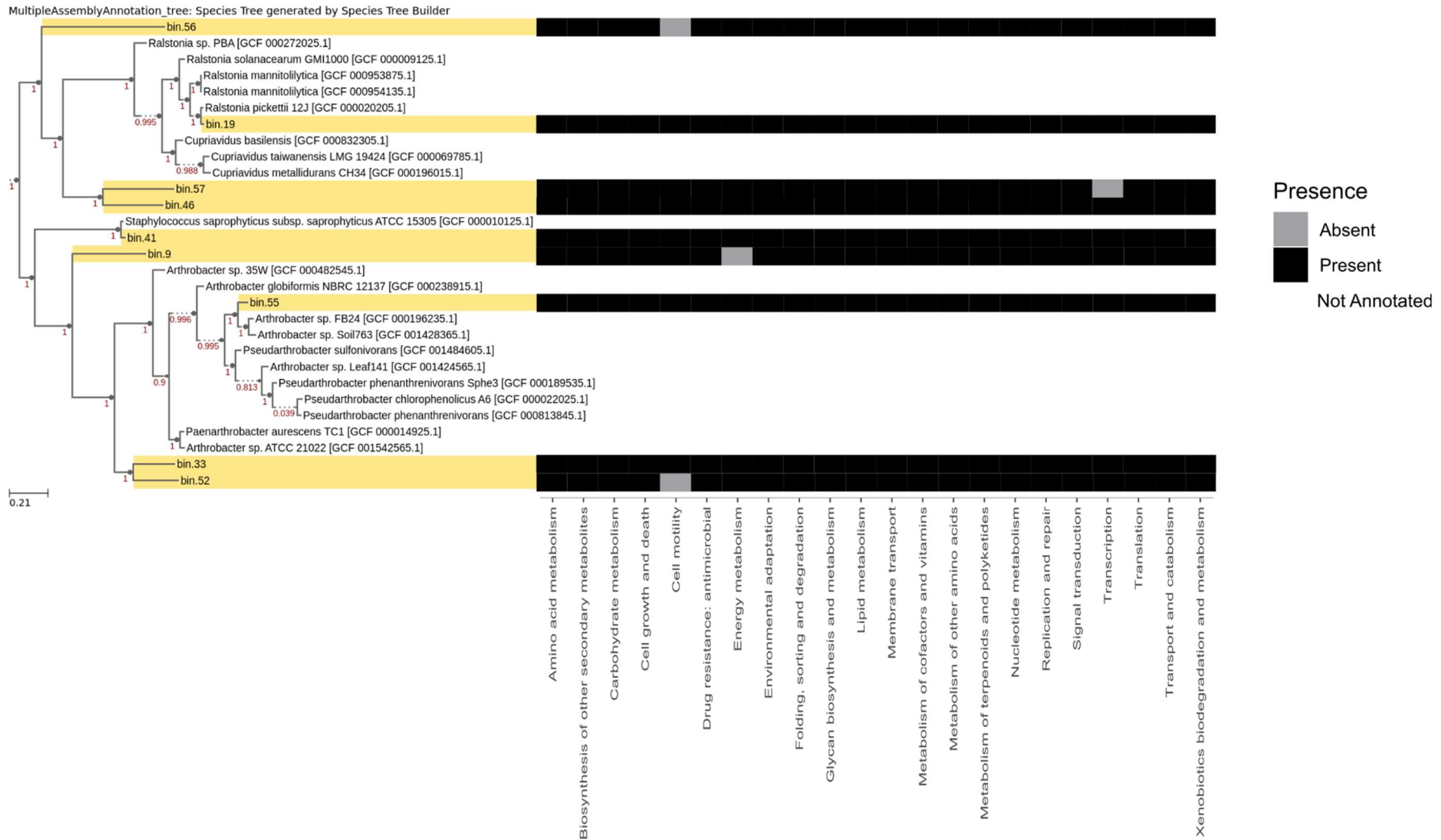


**Figure 14. Broadscale functional redundancy regardless of bacterial taxonomy.**

Bacterial phylogeny showing conserved functions as determined by KEGG pathways across the nine selected metagenomes. Overall, there is broadscale functional redundancy regardless of bacterial taxonomy. Branches highlighted in yellow are the nine focal metagenomes.

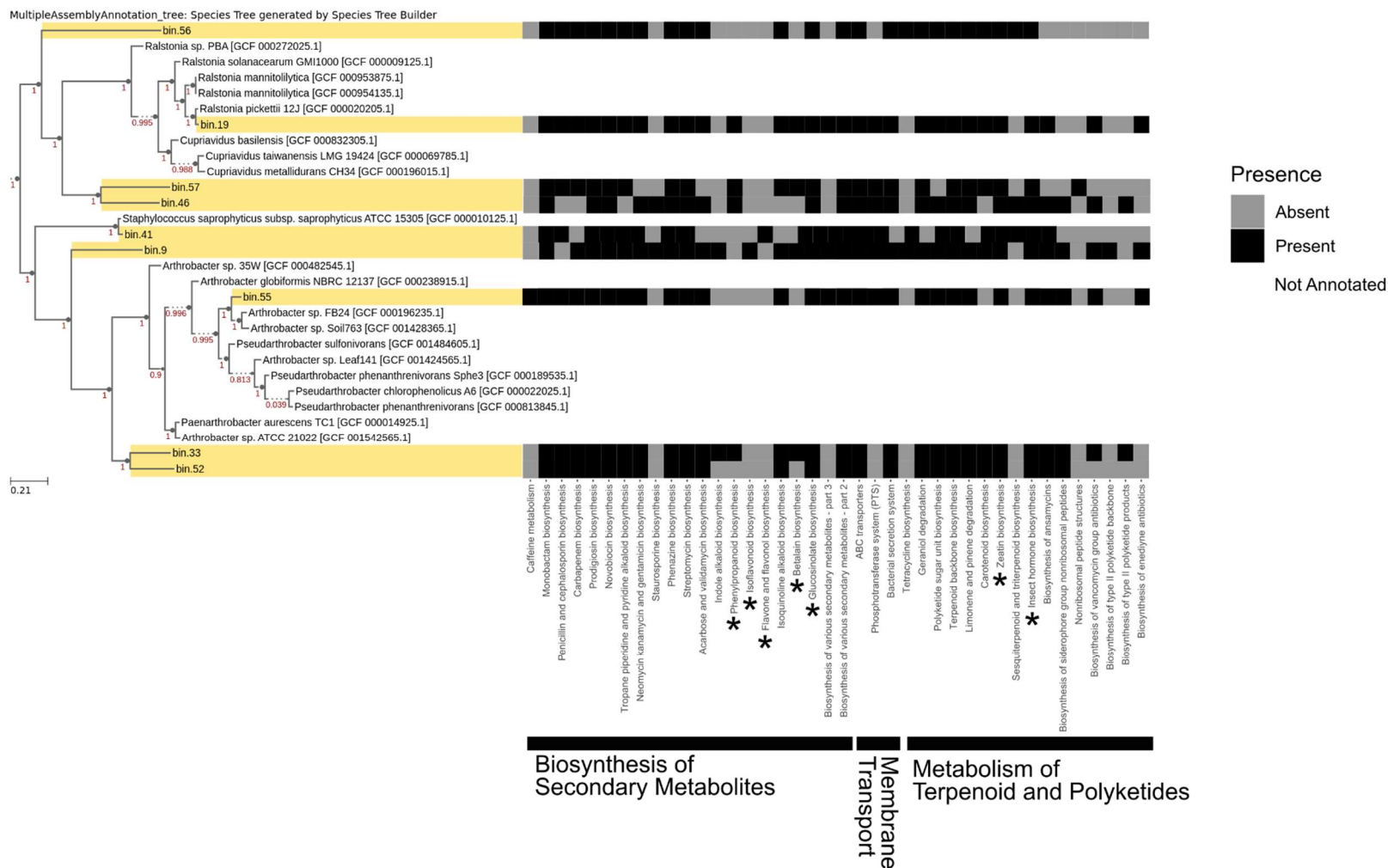


**Figure 15. Fine scale functional variation within a phylogenetic context.**

Bacterial phylogeny showing functional variation within the KEGG orthologs within three select pathways (Biosynthesis of secondary metabolites, membrane transport, and metabolism of terpenoid and polyketides). Branches highlighted in yellow are the nine focal metagenomes. Overall, there is variation in the presence of functional genes between individual taxa as well as variation between phyla. \* indicates questionable functions based on comparisons to nonbacterial databases.

## Discussion

This study aimed to understand how the taxonomic and functional component of the bat cutaneous microbial assemblage responds to pathogen invasion. Overall, I found that the presence of *P. destructans* correlates with a shift in assemblage taxonomic composition, however, this shift was not observed in overall metagenome function of skin assemblages. Results from Tax4Fun2 indicated a lack of overall difference in putative function of assemblages by *P. destructans* status. The lack of difference is likely caused by multiple bacterial taxa having similar functional pathways. However, when detailed observations were made, differences were noted within several pathways important for understanding bacterial-fungal interactions. More specifically, host associated bacterial metagenomes have genes present for the production of antifungal compounds, suggesting the potential role of these organisms in host defense from fungal pathogens. Overall, these results suggest that the host cutaneous microbial assemblage is likely assembled through species sorting mechanisms across functional groups, allowing the taxonomic composition to vary stochastically (Van der Gucht *et al.* 2007), and functional assemblages to be broadly redundant.

At the community level, I observed a shift in taxonomic composition but conserved putative function across *P. destructans* status. This low resistance to *P. destructans* mediated change within the taxonomic assemblage has been observed in other studies and was hypothesized to be driven by environmental selection (species-sorting) for taxa with antifungal properties (Lemieux-Labonté 2017; Grisnik *et al.* 2020). However, when the putative functional community was observed, broad scale differences were absent, suggesting functional redundancy within the system. While this does not

directly support the claim that taxa are selected based on the presence of antifungal functions, it does support the hypothesis that microbial communities are likely maintained based on function rather than taxonomy (Burke *et al.* 2011). Alternatively, a lack of an observed functional shift could be the result of functional resilience, with changes in assemblage function decreasing in magnitude over time. Results of the indicator analysis revealed that taxa indicative of *P. destructans* negative bats are less abundant on *P. destructans* positive bats, but their functions are taxonomically ubiquitous, supporting the notion that different bacteria share similar functions (Burke *et al.* 2011). The notion that bacteria share functions regardless of taxonomic identity is further supported by the phylogenetic trees (Figs. 14 and 15) that show a lack of taxonomically conserved functions across the nine analyzed metagenomes that were representative of four different bacterial phyla. Taxonomic shifts of indicator taxa on *P. destructans* positive bats correlated with changes in putative function. This partially contradicts metagenome results, however, it is important to note that Tax4Fun2 was only able to use ~28% of OTUs per sample to determine putative assemblage function. This number, while low, is on par with studies of host associated microbial assemblage functions utilizing shotgun metagenomic methods (Louca *et al.* 2016; Rebollar *et al.* 2018; Grisnik *et al.* 2020). Only a fraction of bacterial taxa associated with bat skin are represented in reference databases and highlights the need for continued development of genomic, microbial resources and reference databases.

Within the shotgun metagenomic data I found that at the broadest scale (KEGG functional pathways), bacterial metagenomes appear functionally redundant (Fig. 12 and 14). This was expected, as these pathways represent ubiquitous and essential cell

functions, likely represented across most bacterial phyla (i.e., amino acid metabolism). The conserved nature of these functions is observed within the phylogenetic tree, where these broadscale functions are seen across all nine metagenomes, regardless of relatedness. Similar to this study, Rebollar *et al.* (2018) also found amino acid metabolism, carbohydrate metabolism, and metabolism of cofactors and vitamins to be the most abundant pathways within frog skin microbial assemblages. Additionally, other studies have found functional pathways such as respiration to represent functional assemblages, despite differences in taxonomic assemblage structure (Girvan *et al.* 2005; Langenheder *et al.* 2005). Past research has shown that at this level, functional assemblages can change based on environmental interactions. For example, Morris *et al.* (2020) showed that functional pathway abundance in nectar microbial assemblages depended on interactions with pollinators, or alternatively pollen-exploiting insects. In this study, carbohydrate metabolism and amino acid and derivatives metabolism were differentially abundant, suggesting that while these pathways may be important as core pathways for bacterial survival, the abundance may be system dependent.

At a finer scale, I investigated the KEGG orthologs present within three pathways hypothesized to be important in host defense. I observed intergenomic variation, for example, the genes for the phosphotransferase system (PTS; membrane transport pathway) are missing within the metagenomes of two bacterial taxa found on the skin of *P. destructans* positive bats (Fig. 13C-D). The phosphotransferase system is involved with bacterial uptake of a variety of carbohydrates (Deutscher *et al.* 2006) some of which are likely present on bat skin (Nassar *et al.* 2008). Previous work on mouse distal gut microbial assemblages found an enrichment of PTS genes within mice fed a “western

diet” high in fats (saturated and unsaturated) and carbohydrates used as human food additives (Turnbaugh *et al.* 2008). This suggests that shifts in the presence of these genes may be an indicator of the trophic structure of the assemblage and might suggest differences in the availability of these carbohydrates as an energy source within the bat cutaneous microbial assemblage. The lack of taxonomic signature of PTS genes further supports the hypothesis that multiple bacterial taxa have similar functions. The differential presence of these genes suggests that while individual taxa may differ in their energy source, there is assemblage level redundancy since metagenomes from both disease states have PTS genes. Genes coding for secondary metabolite antibiotic compounds are found in all draft genomes regardless of *P. destructans* status and bacterial taxonomy. These antibiotics include monobactam, novobiocin, and streptomycin. Previous work has suggested the role of antibiotics in competition within microbial assemblages (Chao and Levin 1981). However, more recently the role of antibacterial compounds has been called into question, and instead studies have suggested their role in interspecies bacterial communication (Goh *et al.* 2002; Yim *et al.* 2007). Regardless of their role within the assemblage, the ubiquitous presence of genes for the production of antibacterial compounds suggests their importance, as well as, overall redundancy within the system. In general, intergenomic variation in functions suggests that if assemblages are formed via species sorting on functions, the selection is at the assemblage level, allowing for moderate variation in functional capabilities between individual bacterial taxa.

Several orthologs coding for secondary metabolites support the notion that skin bacterial assemblages of bats play a role in protecting the host from pathogens (Lemieux-

Labonté 2017; Grisnik *et al.* 2020). For example, the antifungal compound staurosporine (Li *et al.* 2014) is produced by a variety of actinomycetes (Park *et al.* 2006) and was found in metagenomes of *P. destructans* negative bats (Fig. 13B). This is suggestive of the role of microbially produced staurosporine in the protection of bat hosts, however, a controlled experiment would be necessary to confirm this conclusion. The secondary metabolite validamycin A has the potential to play a role in slowing the spread of fungal pathogens, and is widely used to control rice sheath blight (Robson *et al.* 1988).

Validamycin A is inhibitory, but not lethal to fungi, as it has the ability to slow the rate of hyphal extension (Trinci 1984). Validamycin is often cited as being produced by species of *Streptomyces* (Guirao-Abad *et al.* 2013) and has been shown to halt the growth of a variety of basidiomycetes, but with limited effects on ascomycete fungi (Robson *et al.* 1988; Guirao-Abad *et al.* 2013). Interestingly previous work has shown that cultured *Streptomyces* sp. have the ability to inhibit the growth of *P. destructans* on a petri plate (Grisnik *et al.* 2020). Orthologs for the production of Validamycin were present within all metagenomes, regardless of the *P. destructans* status, suggesting that the bacterial taxa surveyed in this analysis were redundant in regard to this function.

Overall, shotgun metagenomic data revealed patterns of functional redundancy within broad functional categories, but variation within select orthologs coding for specific pathways. I, like others (Rebollar *et al.* 2018), suggest the continued development of shotgun metagenomics as a method to better understand functional diversity within host associated microbial assemblages. However, I stress that within this study, samples were pooled due to low concentrations of DNA, likely resulting in an underestimate of functional variation between individual bat hosts. Lastly, it is important

to acknowledge the limitations of shotgun metagenomic sequencing, specifically, there is no way to determine if genes are transcriptionally active under a set of ecological and host-based conditions. Additionally, it is important to note that function is based on best fit to annotated functional genes, potentially resulting in incorrect annotation. Future work should aim to overcome these limitations by using methods such as metatranscriptomics or qPCR to determine how functions are being expressed rather than functional capability as well as continued development of functional reference databases.

This study aimed to elucidate the interaction between microbial assemblage structure and function in the presence of a fungal pathogen, with implications for host health. Overall, I found that taxonomy and function are decoupled, with multiple bacterial taxa having similar functions at a broad level, thus suggesting functional redundancy. At finer scales, variation was observed between bacterial taxa functional capabilities and/or ecological roles. This suggests that if assemblages are formed via species sorting of functions, the level of selection is likely at that of the assemblage, allowing individual taxa to vary somewhat in functional capabilities, but maintaining overall function.

## References

- Allison SD, Martiny JBH. Resistance, resilience, and redundancy in microbial communities. *PNAS* 2008;**105**:11512–19.
- Alneberg J, Bjarnason BS, de Bruijn I *et al*. Binning metagenomic contigs by coverage and composition. *Nat Methods* 2014;**11**:1144–46.
- Aguilar D, Aviles FX, Querol E *et al*. Analysis of phenetic trees based on metabolic capabilities across the three domains of life. *J Mol Biol* 2004;**340**:491–512.
- Arkin AP, Cottingham RW, Henry CS *et al*. KBase: the United States department of energy systems biology knowledgebase. *Nat Biotechnol* 2018;**36**:566–69.
- Avena CV, Parfrey LW, Leff JW *et al*. Deconstructing the bat skin microbiome: influences of the host and the environment. *Front Microbiol* 2016;**7**:1–14.
- Baselga A, Orme CDL. betapart: an R package for the study of beta diversity. *Methods Ecol Evol* 2012;**3**:808–12.
- Belden LK, Harris RN. Infectious diseases in wildlife: the community ecology context. *Front Ecol Environ* 2007;**5**:533–39.
- Braendle C, Miura T, Bickel R *et al*. Developmental origin and evolution of bacteriocytes in the aphid–*Buchnera* symbiosis. *PLoS Biol* 2003;**1**:70–76.
- Burke C, Steinberg P, Rusch D. Bacterial community assembly based on functional genes rather than species. *PNAS* 2011;**108**:14288–93.
- Caporaso JG, Lauber CL, Walters WA *et al*. Global patterns of 16S rRNA diversity at a depth of millions of sequences per sample. *PNAS* 2011;**108**:4516–22.
- Carrillo-Araujo M, Taş N, Alcántara-Hernández RJ *et al*. Phyllostomid bat microbiome composition is associated to host phylogeny and feeding strategies. *Front Microbiol* 2015;**6**:1–9.
- Castresana J. Selection of conserved blocks from multiple alignments for their use in phylogenetic analysis. *Mol Biol Evol* 2000;**17**:540–552.
- Chao L, Levin BR. Structured habitats and the evolution of anticompetitor toxins in bacteria. *PNAS* 1981;**78**:6324–28.
- Cho L, Blaser MJ. The human microbiome: at the interface of health and disease. *Nat Rev Genet* 2012;**13**:260–70.
- De Caceres M, Jansen F, De Caceres MM. ‘indicspecies’. R package version 1.7.9. 2020. <https://CRAN.R-project.org/package=indicspecies> (03 March 2021, date last accessed).
- Deutscher J, Francke C, Postma PW. How phosphotransferase system-related protein phosphorylation regulates carbohydrate metabolism in bacteria. *Microbiol Mol Biol Rev* 2006;**70**:939–1031.
- Dharampal PS, Hetherington MC, Steffan SA. Microbes make the meal: oligolectic bees require microbes within their host pollen to thrive. *Ecol Entomol* 2020;**45**:1418–27.
- Dobony CA, Hicks AC, Langwig KE *et al*. Little brown myotis persist despite exposure to white-nose syndrome. *J Fish Wildl Manag* 2011;**2**:190–5.
- Ellison SL, English CA, Burns MJ *et al*. Routes to improving the reliability of low-level DNA analysis using real-time PCR. *BMC Biotechnol* 2006;**6**:33.
- Escalas A, Hale L, Voordeckers JW *et al*. Microbial functional diversity: From concepts to applications. *Ecol Evol* 2019;**9**:12000–16.

- Fisher MC, Henk DA, Briggs CJ *et al.* Emerging fungal threats to animal, plant, and ecosystem health. *Nature* 2012;**484**:186–94.
- Flórez LV, Biedermann PHW, Engl T *et al.* Defensive symbioses of animals with prokaryotic and eukaryotic microorganisms. *Nat Prod Rep* 2015;**32**:904–36.
- Frick WF, Cheng TL, Langwig KE *et al.* Pathogen dynamics during invasion and establishment of white-nose syndrome explain mechanisms of host persistence. *Ecology* 2017;**98**:624–31.
- Gill SR, Pop M, DeBoy RT *et al.* Metagenomic analysis of the human distal gut microbiome. *Science* 2006;**312**:1355–59.
- Girvan MS, Campbell CD, Killham K *et al.* Bacterial diversity promotes community stability and functional resilience after perturbation. *Environ Microbiol* 2005;**7**:301–13.
- Glassman SI, Martiny JB. Broudscale ecological patterns are robust to use of exact sequence variants versus operational taxonomic units. *mSphere* 2018, DOI:10.1128/mSphere.00148–18.
- Goh EB, Yim G, Tsui W *et al.* Transcriptional modulation of bacterial gene expression by subinhibitory concentrations of antibiotics. *PNAS* 2002;**99**:17025–30.
- Green JL, Bohannan BJM, Whitaker RJ. Microbial biogeography: from taxonomy to traits. *Science* 2008;**320**:1039–43.
- Grice EA, Segre JA. The skin microbiome. *Nat Rev Microbiol* 2011;**9**:244–53.
- Grisnik M, Bowers O, Moore AJ *et al.* The cutaneous microbiota of bats has in vitro antifungal activity against the white nose pathogen. *FEMS Microbiol Ecol* 2020, DOI:10.1093/femsec/fiz193.
- Guirao-Abad JP, Sánchez-Fresneda R, Valentín E *et al.* Analysis of validamycin as a potential antifungal compound against *Candida albicans*. *Int Microbiol* 2013;**16**:217–25.
- Janicki AF, Frick WF, Kilpatrick AM *et al.* Efficacy of visual surveys for white-nose syndrome at bat hibernacula. *PLoS One* 2015, DOI:10.1371/journal.pone.013390.
- Kanehisa M, Goto S, Sato Y *et al.* Data, information, knowledge and principle: back to metabolism in KEGG. *Nucleic Acids Res* 2013;**42**:199–205.
- Kanehisa M, Sato Y, Morishima K. BlastKOALA and GhostKOALA: KEGG tools for functional characterization of genome and metagenome sequences. *J Mol Biol* 2016;**428**:726–31.
- Langenheder S, Lindström ES, Tranvik LJ. Weak coupling between community composition and functioning of aquatic bacteria. *Limnol Oceanogr* 2005;**50**:957–67.
- Langille MG, Zaneveld J, Caporaso JG *et al.* Predictive functional profiling of microbial communities using 16s rRNA marker gene sequences. *Nat Biotechnol* 2013;**31**:814–21.
- Langwig KE, Frick WF, Bried JT *et al.* Sociality, density-dependence and microclimates determine the persistence of populations suffering from a novel fungal disease, white-nose syndrome. *Ecol Lett* 2012;**15**:1050–57.
- Langwig KE, Frick WF, Reynolds R *et al.* Host and pathogen ecology drive the season dynamics of a fungal disease, white-nose syndrome. *Proc Royal Soc B* 2015, DOI:10.1098/rspb.2014.2335.

- Langwig KE, Hoyt JR, Parise KL *et al.* Resistance in persisting bat populations after white-nose syndrome invasion. *Philos Trans Royal Soc B* 2017;**372**:1–9.
- Lemieux-Labonté V, Tromas N, Shapiro BJ *et al.* Environment and host species shape the skin microbiome of captive neotropical bats. *PeerJ* 2016, DOI:10.7717/peerj.2430.
- Lemieux-Labonté V, Simard A, Willis CKR *et al.* Enrichment of beneficial bacteria in the skin microbiota of bats persisting with white-nose syndrome. *Microbiome* 2017; **5**:115–30.
- Li D, Liu CM, Luo R *et al.* MEGAHIT: an ultra-fast single-node solution for large and complex metagenomics assembly via succinct de Bruijn graph. *Bioinformatics* 2015; **31**:1674–1676.
- Li X, Huang P, Wang Q *et al.* Staurosporine from the endophytic *Streptomyces* sp. strain CNS-42 acts as a potential biocontrol agent and growth elicitor in cucumber. *Antonie Van Leeuwenhoek* 2014;**106**:515–25.
- Louca S, Jacques SMS, Pires APF *et al.* High taxonomic variability despite stable functional structures across microbial communities. *Nat Ecol Evol* 2016, DOI: 10.1038/s41559-016-0015.
- Louca S, Polz MF, Mazel F *et al.* Function and functional redundancy in microbial systems. *Nat Ecol Evol* 2018, DOI:10.1038/s41559-018-0519–1.
- Maslo B, Fefferman NH. A case study of bats and white-nose syndrome demonstrating how to model population viability with evolutionary effects. *Conserv Biol* 2015;**29**:1176–85.
- Minich JJ, Sanders JG, Amir A *et al.* Quantifying and understanding well-to-well contamination in microbiome research. *MSystems* 2019, DOI: 10.1128/mSystems.00186–19.
- Morris MM, Frixione NJ, Burkert AC *et al.* Microbial abundance, composition, and function in nectar are shaped by flower visitor identity. *FEMS Microbiol Ecol* 2020, DOI:10.1093/femsec/fiaa003.
- Muller LK, Lorch JM, Linder DL *et al.* Bat white-nose syndrome: a real-time TaqMan polymerase chain reaction test targeting the intergenic spacer region of *Geomyces destructans*. *Mycologia* 2013;**105**:253–59.
- Nassar JM, Salazar MV, Quintero A *et al.* Seasonal sebaceous patch in the nectar-feeding bats *Leptonycteris curasoae* and *L. yerbabuenae* (Phyllostomidae: Glossophaginae): phenological, histological, and preliminary chemical characterization. *Zoology* 2008;**111**:363–376.
- Nemergut DR, Schmidt SK, Fukami T *et al.* Patterns and processes of microbial community assembly. *Microbiol Mol Biol Rev* 2013;**77**:342–56.
- Oksanen J, Blanchet FG, Guillaume B *et al.* 2013. Vegan: Community Ecology Package. R package version 2.5-2 2018. <https://CRAN.R-project.org/package=vegan> (03 March 2021, date last accessed).
- Park HJ, Lee JY, Hwang IS *et al.* Isolation and antifungal and antioomycete activities of staurosporine from *Streptomyces roseoflavus* strain LS-A24. *J Agric Food Chem* 2006;**54**:3041–46.
- Patro R, Duggal G, Love MI *et al.* Salmon provides fast and bias-aware quantification of transcript expression. *Nat Methods* 2017;**14**:417–26.

- Presley SJ, Higgins CL, Willig MR. A comprehensive framework for the evaluation of metacommunity structure. *Oikos* 2010;**119**:908–17.
- Price MN, Dehal PS, Arkin AP. FastTree 2—approximately maximum-likelihood trees for large alignments. *PloS one* 2010, DOI: 10.1371/journal.pone.0009490.
- Quast C, Pruesse E, Yilmaz P *et al.* The SILVA ribosomal RNA gene database project: improved data processing and web-based tools. *Nuc Acids Res* 2012, DOI:10.1093/nar/gks/1219.
- Rebollar EA, Gutiérrez-Preciado A, Noecker C *et al.* The skin microbiome of the neotropical frog *Craugastor fitzingeri*: inferring potential bacterial-host-pathogen interactions from metagenomic data. *Front Microbiol* 2018, DOI:10.3389/fmicb.2018.00466.
- Robson GD, Kuhn PJ, Trinci AP. Effects of validamycin A on the morphology, growth and sporulation of *Rhizoctonia cerealis*, *Fusarium culmorum* and other fungi. *Microbiology* 1988;**134**:3187–94.
- Rognes T, Flouri T, Nichols B *et al.* VSEARCH: a versatile open source tool for metagenomics. *PeerJ* 2016, DOI:10.1371/journal.pone.0038920.
- Schloss PD, Westcott SL, Ryabin T *et al.* Introducing mothur: open-source, platform-independent, community supported software for describing and comparing microbial communities. *Appl Environ Microbiol* 2009;**75**:7537–41.
- Schloss PD, Westcott SL. Assessing and improving methods used in operational taxonomic unit-based approaches for 16S rRNA gene sequence analysis. *Appl Environ Microbiol* 2011;**77**:3219–26.
- Seemann T. Prokka: a rapid prokaryotic genome annotation. *Bioinformatics* 2014;**30**:2068–69.
- Sharma VK, Kumar N, Prakash T *et al.* Fast and accurate taxonomic assignments of metagenomic sequences using MetaBin. *PloS one* 2012, DOI: 10.1371/journal.pone.0034030.
- Sharpton TJ. An introduction to the analysis of shotgun metagenomic data. *Front Plant Sci* 2014;**5**:1–14.
- Shuey MM, Drees KP, Lindner DL *et al.* Highly sensitive quantitative PCR for the detection and differentiation of *Pseudogymnoascus destructans* and other *Pseudogymnoascus* species. *Appl Environ Microbiol* 2014;**80**:1726–31.
- Song SJ, Lauber C, Costello EK *et al.* Cohabiting family members share microbiota with one another and with their dog. *eLife* 2013;**2**:1–22.
- Tatusov RL, Galperin MY, Natale DA *et al.* The COG database: a tool for genome-scale analysis of protein functions and evolution. *Nucleic Acids Res* 2000;**28**:33–36.
- Trinci APJ. Antifungal agents which affect hyphal extension and hyphal branching. In: Trinci APJ, Ryley JF (eds). *Modes of Action of Antifungal Agents*. Cambridge: Cambridge University Press, 1984;113–124.
- Tung J, Barreiro LB, Burns MB *et al.* Social networks predict gut microbiome composition in wild baboons. *eLife* 2015, DOI:10.7554/eLife.05224.
- Turnbaugh PJ, Bäckhed F, Fulton L *et al.* Diet-induced obesity is linked to marked but reversible alterations in the mouse distal gut microbiome. *Cell Host Microbe* 2008;**3**:213–23.

- Uritskiy GV, DiRuggiero D, Taylor J. MetaWrap—a flexible pipeline for genome-resolved metagenomic data analysis. *Microbiome* 2018, DOI:10.1186/s40168-018-0541-1.
- Van der Gucht K, Cottenie K, Muylaert K *et al.* The power of species sorting: Local factors drive bacterial community composition over a wide range of spatial scales. *PNAS* 2007;**104**:20404–09.
- Weiss S, Xu ZZ, Peddada S *et al.* Normalization and microbial differential abundance strategies depend upon data characteristics. *Microbiome* 2017;**5**:1–18.
- Wemheuer F, Taylor JA, Daniel R *et al.* Tax4Fun2: prediction of habitat-specific functional profiles and functional redundancy based on 16S rRNA gene sequences. *Environ Microbiom* 2020;**15**:1–12.
- Wu YW, Simmons BA, Singer SW. MaxBin 2.0: an automated binning algorithm to recover genomes from multiple metagenomic datasets. *Bioinformatics* 2016;**32**:605–07.
- Yim G, Huimi Wang H, Davies Frs J. Antibiotics as signaling molecules. *Philos Trans R Soc B* 2007;**362**:1195–1200.

**Chapter IV: THE PRESENCE OF PSEUDOGYMNOASCUS DESTRUCTANS, A  
FUNGAL PATHOGEN OF BATS, CORRELATES WITH CHANGES IN  
MICROBIAL METACOMMUNITY STRUCTURE**

Matthew Grisnik<sup>1</sup>, Joshua B Grinath<sup>2</sup>, Donald M Walker<sup>1</sup>

<sup>1</sup>Middle Tennessee State University, Department of Biology, Murfreesboro, Tennessee  
37132, USA

<sup>2</sup>Idaho State University, Department of Biological Sciences, Pocatello, Idaho 83209,  
USA

Accepted with Major Revisions to Scientific Reports

**Abstract**

Metacommunity theory provides a framework for how community patterns arise from processes across scales, which is relevant for understanding patterns in host-associated microbial assemblages. Microbial metacommunities may have important roles in host health through interactions with pathogens; however, it is unclear how pathogens affect host microbial metacommunities. Here, I studied relationships between a fungal pathogen and a host-associated microbial metacommunity. I hypothesized that a fungal pathogen of bats, *Pseudogymnoascus destructans*, correlates with a shift in metacommunity structure and changes in relationships between community composition, and factors shaping these assemblages, such as ecoregion. I sampled bat cutaneous microbial assemblages in the presence/absence of *P. destructans* and analyzed microbial metacommunity composition and relationships with structuring variables. Absence of *P. destructans* correlated with a metacommunity characterized by a common core microbial group that was lacking in disease positive bats. Additionally, *P. destructans* presence

correlated with a change in the relationship between community structure and ecoregion. These results suggest that the fungal pathogen intensifies local processes influencing a microbial metacommunity and highlights the importance of cutaneous microbial assemblages in host-pathogen interactions.

## **Introduction**

Elucidating how patterns of community structure relate to underlying structuring variables and processes of community assembly is a primary goal of community ecologists. Patterns observed at one scale of observation can be directly influenced by processes occurring at another scale (Levin 1992). For example, rescue effects describe the process by which species can persist in unfavorable local environments through dispersal from regional source populations (Brown and Kodric-Brown 1977). Communities interacting between scales, including local and regional, form a spatial patchwork of taxa referred to as a metacommunity (Leibold *et al.* 2004).

Metacommunities are defined as groups of habitat patches, linked by species dispersal and interactions between taxa among these patches (Leibold *et al.* 2004; Costello *et al.* 2012). Both local and regional processes contribute to shaping metacommunity structure and the distribution of species across habitat patches (Costello *et al.* 2012). By using pattern-based assessments, one can analyze species distributions along environmental and spatial gradients to diagnose metacommunity structure (Leibold and Mikkelsen 2002; Presley *et al.* 2010).

Leibold and Mikkelsen (2002) developed a framework to identify metacommunity patterns, called the Elements of Metacommunity Structure (EMS), which uses three metrics to describe metacommunity structures: coherence, turnover, and

boundary clumping (Fig. 16). Coherence is measured as the number of embedded species absences from a site and describes the overall response of a community to an environmental or spatial gradient (Fig. 16A). Turnover is measured as the number of species replacements across samples. Boundary clumping describes clustering in species' range boundaries and is a metric that defines how cohesive species ranges are across sites (Leibold and Mikkelsen 2002). After determining the EMS, an idealized distributional pattern including hyperdispersed species loss, clumped species loss, evenly spaced, or Clementsian (Fig. 16B-E) can be used to describe metacommunity structure (Leibold and Mikkelsen 2002; Presley *et al.* 2010). Clementsian structure (Fig. 16E) describes communities of species that have similar responses to environmental differences, resulting in discrete community boundaries (Clements 1916; Leibold and Mikkelsen 2002; Presley *et al.* 2010). Specifically, Clementsian metacommunities have positive coherence, turnover, and clumping, meaning there are less absences (positive coherence) but more frequent species replacements (positive turnover) than expected by chance alone. Additionally, Clementsian metacommunities have clumped species boundaries defined by positive boundary clumping. For example, Clementsian succession occurs when communities of species replace each other over time, with little overlap in community composition. Evenly spaced metacommunities (Fig. 16D) are similar to Clementsian, in that they have positive coherence and turnover, but they have hyperdispersed species boundaries as opposed to clumped species loss. Evenly spaced metacommunities still exhibit turnover, with species replacing each other across sites, however there are no distinct communities characteristic of Clementsian metacommunities. Nested patterns consist of less diverse assemblages making up subsets

of more diverse communities (Patterson and Atmar 1986; Leibold and Mikkelson 2002; Presley *et al.* 2010). Nested community structures result from positive coherence, but negative turnover, where species do not replace each other but rather, are lost from sites. For example, nested sites are made up of subsets of species from a much larger species pool. Nested metacommunities that exhibit positive clumping have clumped species loss (Fig. 16C) where species are lost from sites in groups. Those with negative clumping have hyperdispersed loss (Fig. 16B) where individual species are lost from sites. While EMS analyses provide descriptions of metacommunity structure, they do not reveal the variables responsible for such processes.

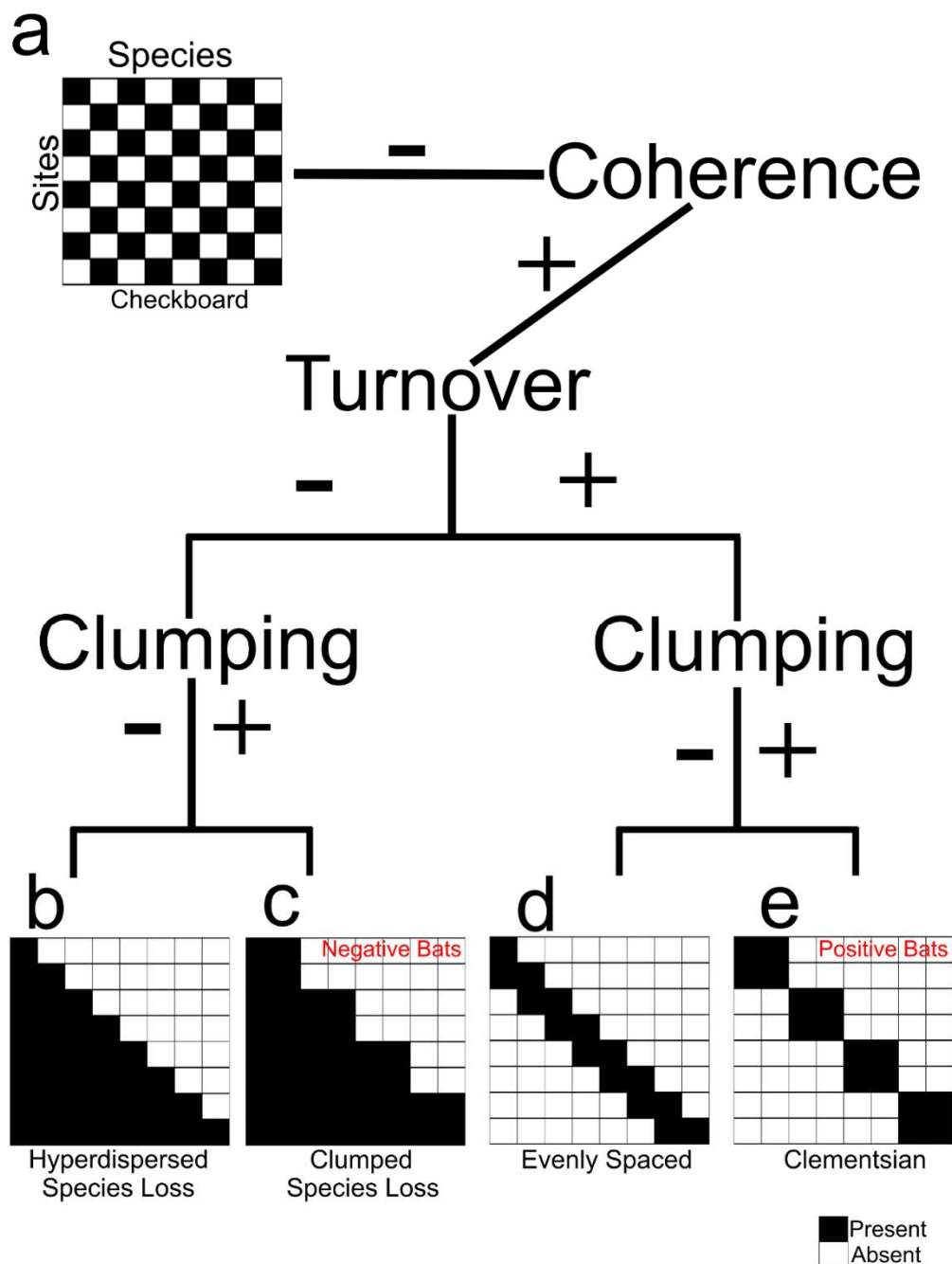


**Figure 16. The elements of metacommunity structure and their resulting patterns.** Plus signs (+) indicate a significantly positive relationship, whereas minus signs (-) indicate a negative relationship. A. metacommunity with checkerboard pattern. B. nested metacommunity with hyperdispersed species loss. C. nested metacommunity with clumped species loss. D. evenly spaced metacommunity. E. Clementsian metacommunity structure. (Modified from Presley *et al.* (2010) using the software Inkscape 1.0 [www.inkscape.org](http://www.inkscape.org)).

Complementary analyses are needed to elucidate the variables driving metacommunity structure. The influence of geographic distance on community structure is assessed using distance-decay models, which estimate the rate of species turnover along a gradient (Nekola and White 1999). Positive relationships between community dissimilarity and geographic distance may indicate that species' distributions are highly affected by dispersal limitation (Tornero *et al.* 2018), whereas, the lack of a relationship suggests that environmental filtering and species sorting may be more important for determining community structure (Heino 2013). Species sorting and environmental filtering emphasize the role of the local abiotic environment in determining what species can persist within an assemblage, resulting in assemblages correlating with local habitat factors, such as precipitation (Leibold *et al.* 2004). In addition, permutational multivariate methods are frequently implemented to understand the effects of environmental factors on community patterns. For instance, permutational models can distinguish differences in community composition and turnover across environmental variables, as well as the interactive effects of multiple environmental variables (Walker *et al.* 2019). Interactive effects are especially important to consider when new structuring variables, such as invasive species or anthropogenic perturbations, are introduced to a metacommunity, as they might change the role of established structuring factors.

While macroorganismal metacommunities have been studied in some detail (Presley *et al.* 2012; Heino *et al.* 2015; Tornero *et al.* 2018), minimal work has focused on characterization of host-associated microbial metacommunities (Hernández-Gómez *et al.* 2017; Brown *et al.* 2020; Wilber *et al.* 2020). Understanding variation in structure of host-associated microbial metacommunities may be especially important given the role of

host assemblages in pathogen defense (Belden and Harris 2007; Grice and Segre 2011). For instance, the pathogenic fungus *Pseudogymnoascus destructans*, the causative agent of white-nose syndrome, was introduced into the United States in 2006, and is responsible for massive bat population declines (Blehert *et al.* 2009; Frick *et al.* 2016). Recently, declines have been shown to be highly variable across space, bat species, and time (Langwig *et al.* 2017). Tri-colored bats (*Perimyotis subflavus*) have shown recent population stabilizations possibly due in part to the presence of antifungal bacteria composing the cutaneous microbial assemblage (Langwig *et al.* 2012; Langwig *et al.* 2017). Previous work has shown *P. subflavus* that are exposed to, but not invaded by *P. destructans*, have microbial assemblages enriched in antifungal bacterial taxa (Grisnik *et al.* 2020). Determining the structure and drivers of bat cutaneous microbial metacommunities in relation to this fungal pathogen may improve our understanding of microbial metacommunity response to fungal invasion, as well as our understanding of assemblages that are resistant to fungal invasion.

The objectives of this study were to understand how the presence of a fungal pathogen correlates with the composition of a host-associated cutaneous microbial metacommunity and its structuring factors. I investigated the relationship between *P. destructans* and the cutaneous microbial metacommunity of *P. subflavus* across 48 sites in Tennessee, USA. I hypothesized that the presence of *P. destructans* would be correlated with a shift in 1) metacommunity structure and 2) relationships between structuring variables and community composition. I tested the first hypothesis using EMS, further informed by indicator operational taxonomic unit (OTU) and fungal pathogen load analyses. I tested the second hypothesis with distance-decay and

permutational models to understand how spatial and environmental variables structure the bat cutaneous microbial assemblage in the presence/absence of a fungal pathogen.

## **Methods**

### *Sample collection*

Swabs from 369 individuals of adult *P. subflavus* were collected during statewide surveys between December 2016 and March 2019 across 57 cave sites in Tennessee. After bioinformatics processing and quality control, 249 *P. subflavus* from 48 sites were statistically analyzed (see methods below). Each bat had its cutaneous microbial assemblage sampled following the protocol outlined in Grisnik *et al.* (2020). Briefly I took five swab (sterile Puritan polyester tipped swabs, Puritan, Guilford Maine) strokes of each bat muzzle/ear and five from wings/fur while avoiding the mouth using one sterile swab per bat individual. Due to the conservation status of *P. subflavus*, when possible, bats were left hanging attached to their roost and swabbed without disturbing torpor. All samples were stored on ice in the field and permanently at -20° C until processing. This study was approved by the Tennessee Technological University Institutional Animal Care and Use Committee (TTU-16-17-003) and USFWS (2009-038). All methods were carried out following relevant guidelines and regulations. I isolated DNA from 369 bats using the Qiagen DNeasy PowerSoil HTP 96 kit following the manufacturer's protocol. Each plate of 96 samples contained a single DNA extraction blank (n = 8 total blanks) to filter out kit-based contamination during bioinformatics processing and quantitative PCR reactions (see below). When setting up each DNA extraction plate and subsequent library preparation, the location of samples on each 96 well plate was randomized, in order to reduce biased effects of well-to-well

contamination (Minich *et al.* 2019). Extracted DNA was then used for molecular characterization of the microbial community, as well as, qPCR for the detection of *P. destructans*.

#### *Characterization of microbial community*

Each step of library preparation (DNA isolation, PCR setup, and post PCR processes) was separated into specific PCR cabinet hoods with designated pipettes to minimize environmental and/or cross-contamination. Pipettes were autoclaved, and UV crosslinked periodically throughout library preparation. Once isolated, DNA was concentrated, using an Eppendorf Vacufuge plus, to a final volume of ~25  $\mu\text{L}$ . After concentration, PCR amplification and high-throughput sequencing was performed following a modified version of the Illumina 16S Metagenomic Sequencing Library Preparation protocol. Specifically, I targeted the V4 region of 16S rRNA marker using primers 806R/515F (Caporaso *et al.* 2011). Each PCR reaction contained 12.5  $\mu\text{L}$  MCLAB I-5 Hi-Fi taq mastermix, 1  $\mu\text{L}$  of 806R (10  $\mu\text{M}$ ), 1  $\mu\text{L}$  of 515F (10  $\mu\text{M}$ ), 5.5  $\mu\text{L}$  PCR grade water, and 5  $\mu\text{L}$  DNA template. PCR amplification was performed with an initial denaturation at 95°C for 2 min, followed by 35 cycles of 98°C for 10 s, 55°C for 15 s, and 72°C for 5 s, with a final extension cycle of 72°C for 5 mins. MAGBIO High-prep magnetic beads were used to remove primer/adaptor dimers after amplicon PCR and indexing steps. Samples were quantified with a Promega Quantus Fluorometer then normalized, pooled at a 4 picomolar concentration, and loaded onto an Illumina MiSeq v2 flow cell. Sequencing was performed in eight separate runs each using a 500-cycle reagent kit (paired-end, 2  $\times$  250 bp reads).

### *Quantitative PCR*

To determine the presence or absence of *P. destructans* within a sample I followed the protocol outlined by Muller *et al.* (2013) to amplify the fungal intergenic spacer region (IGS). Each reaction was run in triplicate on an Agilent AriaMx Real-Time PCR system, and contained 5  $\mu$ L 2x Primetime MasterMix, 0.4  $\mu$ L forward primer (20  $\mu$ M), 0.4  $\mu$ L reverse primer (20  $\mu$ M), 0.1  $\mu$ L probe (20  $\mu$ M), 3.1  $\mu$ L PCR grade water, and 1  $\mu$ L sample DNA for a total of 10  $\mu$ L per reaction. Thermocycling conditions included a 3-min activation step at 95°C, then 50 cycles of 95°C for 3 s and 60°C for 30 s. Each plate included both a known concentration of synthetically made *P. destructans* DNA (gBlocks; Integrated DNA Technologies) to serve as a positive control and a no template negative control (run in triplicate) to account for within plate contamination. A positive sample was indicated by exponential amplification in triplicate with a  $C_t$  value of less than 40 (Muller *et al.* 2013; Janicki *et al.* 2015). If samples did not test positive in triplicate, they were re-tested, and were considered positive if there was amplification in at least one of the three subsequent reactions (Ellison *et al.* 2006). In order to quantify *P. destructans* fungal load, qPCR reactions of a serial dilution of synthetic DNA was used to generate the standard curve equation  $y = -0.2936x + 11.439$ , with  $x$  being the average  $C_t$  value for each sample run in triplicate, and  $y$  being the log DNA copy number.

### *Bioinformatic analysis*

Amplicon sequencing reads were processed using mothur v1.42.1 (Schloss *et al.* 2009). A total of 48 442 995 raw data sequence reads were obtained from eight sequencing runs. Paired-end reads were assembled into contigs, and sequences containing homopolymers greater than eight nucleotides or any ambiguous base calls were removed.

I identified unique sequences and aligned them to the SILVA v123 bacterial reference database (Quast *et al.* 2012). After alignment, sequences were trimmed to the V4 region and *pre-clustered* allowing for two-nucleotide differences between clusters. Chimera removal was then done using the *vsearch* function in mothur (Rognes *et al.* 2016). Sequences were classified into taxonomic lineages and reads identified as Archaea, Eukaryota, chloroplast, mitochondria, and unknown were removed. The *cluster.split* command in mothur was used to cluster sequences into operational taxonomic units at 97% similarity (Schloss and Westcott 2011). OTUs that appeared less than five times were considered rare and were removed from the dataset. Additionally, OTUs that were found within the DNA extraction blanks were also removed (n = 1669 OTUs). OTUs were selected as the focal taxonomic level rather than ASVs, as previous work has shown that there is negligible difference in ecological patterns observed when OTU or ASV data are analyzed (Glassman and Martiny 2018). In total 5 701 307 sequences (11.7%) passed all quality control steps. I compared final library sizes across all samples and found that they were significantly different (Kruskal-Wallis:  $\chi^2 [2] = 83.98, p < 0.05$ ). Therefore, the data were normalized by subsampling each library at 1200 sequence reads (Weiss *et al.* 2017). Data were subsampled as previous work has shown that it is an effective way to account for variation in library size (Weiss *et al.* 2017). The final OTU  $\times$  sample matrix included 268 samples of *P. subflavus*. Since I was interested in observing variation between *P. destructans* positive and negative bats over geographic distance I standardized the data so that geographic distances between sample sites were equal for *P. destructans* positive and negative *P. subflavus*. This resulted in a total of 249 *P. subflavus*

(40 *P. destructans* negative and 209 positive) used for the statistical analysis described below. All mothur commands are included in Appendix C for reproducibility purposes.

### *Statistical analyses*

Previous work has shown that rare OTUs can skew the results of elements of metacommunity structure (EMS) analysis (Presley *et al.* 2010). Prior to conducting analyses, all OTUs that summed to less than two were removed resulting in 12 603 OTUs in the complete OTU  $\times$  sample matrix. All analyses were conducted in R 3.4.2 (R Core Team 2020) using  $\alpha = 0.05$  unless multiple comparisons were made, and thus Bonferroni adjusted.

I used the *metacom* package (version 1.5.3) in R (Dallas 2014) to determine if the presence of *P. destructans* correlated with changes in metacommunity structure of cutaneous microbial assemblages as outlined in Leibold and Mikkelsen (2002) and Presley *et al.* (2010) following the Elements of Metacommunity Structure (EMS) framework. I evaluated three EMS metrics (coherence, turnover, and boundary clumping) using a site-by-species presence/absence matrix to determine metacommunity structure. *Coherence* was assessed as the number of embedded species absences, or the number of gaps/interruptions in species distributions, within an ordinated community matrix (Fig. 16). The number of observed absences was compared to an expected number of absences determined through the formulation of a null distribution created from simulated matrices with 1000 iterations. Negative coherence describes a pattern of significantly more observed embedded absences than predicted by the null model, and a metacommunity perceived with a “checkerboard” appearance (Fig. 16A). A random metacommunity is

identified when there is a non-significant difference between observed and expected embedded absences. Significantly less embedded absences indicate positive coherence, which is suggestive of species responding to a structuring gradient. The latter pattern requires further analysis of *turnover* and *boundary clumping* for more specific designation of metacommunity structure. *Turnover*, was assessed to describe the number of times a species is replaced by another between two sites. As with coherence, the number of turnover events observed is compared to the number of expected events using a null model prediction. If there are significantly more replacements than expected by chance, this represents positive turnover and signals a Clementsian (Fig. 16E) or evenly spaced (Fig. 16D) metacommunity structure. If there are significantly less replacements than expected, this represents negative turnover and signals a nested metacommunity structure. *Boundary clumping* was evaluated using Morisita's index to describe how distinct blocks of species are clumped along a range boundary. A Morisita's index significantly greater than one, indicates clumped species loss (positive turnover: Fig. 16E; negative turnover: Fig. 16C), whereas, an index value significantly fewer than one indicates evenly spaced, i.e. hyperdispersed, species loss (positive turnover: Fig. 16D; negative turnover: Fig. 16B). To assess significance for each EMS metric I used the default fixed-proportional null model ("r1"), 1000 permutations, and allowed for null matrices to have empty rows and columns (Dallas 2014). EMS analysis was performed using the *metacommunity* function (Dallas 2014) and analyses for *P. destructans* positive and negative samples were run separately.

In order to further describe how *P. destructans* status correlated with changes in community structure I performed an indicator analysis using the *multipatt* function in R

package *indicspecies* (version 1.7.9; De Caceres *et al.* 2020). I used a generalized linear mixed-effects model (GLMM) with the *glmer* function (package *lme4*; Bates *et al.* 2020) assuming a Poisson error structure, with site set as the random effect to account for nested data, to compare the abundance of significant indicator taxa of *P. destructans* negative bats across all samples. Additionally, I compared the amount of *P. destructans* present (number of copies using qPCR) to the abundance of indicator taxa using a GLMM assuming a Poisson error structure, with site set as the random effect. To determine if fungal load influenced community dissimilarity, I converted fungal copy number to a distance matrix representing differences between samples using the *dist* function with Euclidean distances. This allowed for us to determine if bats having more similar fungal loads have more similar microbial assemblages. The resulting distance matrix was compared to total beta diversity (Sørensen dissimilarity: SOR), the turnover (Simpson dissimilarity: SIM), and nested (nestedness: SNE) components of total beta diversity (package *betapart*; Baselga and Orme 2012). To address the nested structure of the data, a dummy variable was created to describe the pairwise site level comparisons by grouping the samples by geographic distances into a categorical “site contrast” variable. Due to issues resulting in singular fit of mixed models, I then averaged both fungal load and beta diversity (SOR, SIM, and SNE) by the “site contrast” variable resulting in an average dissimilarity between two samples, thus removing the nested structure of the data. I then used a GLM (function *glm*) to compare average fungal load difference to average beta diversity metrics. The GLM was run assuming a binomial distribution with log transformed fungal load dissimilarity set as a fixed effect.

To assess how the presence of *P. destructans* correlated with differences in the rate of turnover and patterns of distance-decay, I compared total beta diversity (SOR), the turnover (SIM), and nestedness (SNE) components of Sørensen diversity across geographic distances. Pairwise geographic distances between samples were computed as the Euclidian distance between sample points using the *dist* function in the package *vegan* (Oksanen *et al.* 2019) Similar to the analysis comparing assemblage dissimilarity to fungal load difference, beta diversity (SOR, SIM, and SNE) was averaged by site contrast, in order to remove the nested structure of the dataset, and to accommodate issues of singular fit in the mixed models. The relationship between average community dissimilarity and average geographic distance (distance-decay relationship) was determined using a generalized linear model (GLM). GLM was performed assuming a binomial distribution using the *glm* function with geographic distance, *P. destructans* status, and the interaction between these variables being set as fixed effects and a Bonferroni adjusted p-value of 0.016. The analysis was conducted using type II sum of squares with the *Anova* function in the package *car* (Fox *et al.* 2016) to account for unequal sample sizes across groups.

To elucidate how environmental variables influenced beta diversity across *P. destructans* status I compared variation in beta diversity, measured as multivariate dispersion (function *betadisper*, package *vegan*), across *P. destructans* status, ecoregion (specifically ecoregion level 3, as delineated by the Environmental Protection Agency), and *P. destructans* × ecoregion interaction. Ecoregion was selected as the environmental variable as it represents a composite variable encompassing multiple fine scale environmental factors. A Tukey's post hoc test was then used to determine pairwise

differences between the groups of the interactive effect. I used permutational multivariate analysis of variance (PERMANOVA) stratified by site with 999 permutations using the *adonis* function (package *vegan*) on SOR, SIM, and SNE dissimilarity metrics to assess the influence of ecoregion on average assemblage similarity. Explanatory variables included ecoregion, *P. destructans* status, the *P. destructans* x ecoregion interaction, as well as year and site as covariates accounting for data structure. The PERMANOVA assumption of homogeneity of variance was violated, however previous work (Anderson and Walsh 2013) has shown that PERMANOVA is robust to violations of this assumption when the variable with the greater sample size has a larger variance, as seen with these data.

## Results

Of the 249 individuals of *P. subflavus* studied, quantitative PCR (qPCR) results indicated that there were 40 negative and 209 *P. destructans* positive bat individuals collected from 48 sites across three ecoregions (Interior, Ridge and Valley, and the South West Appalachians; Fig. 17A). All sites were determined to have at least one *P. destructans* positive bat. Post processing of high-throughput sequence data resulted in a mean read depth of 194 550 sequences per sample (14 899 – 2 968 637 reads) and a total of 11 071 OTUs for *P. destructans* positive and 3370 OTUs for *P. destructans* negative bats.

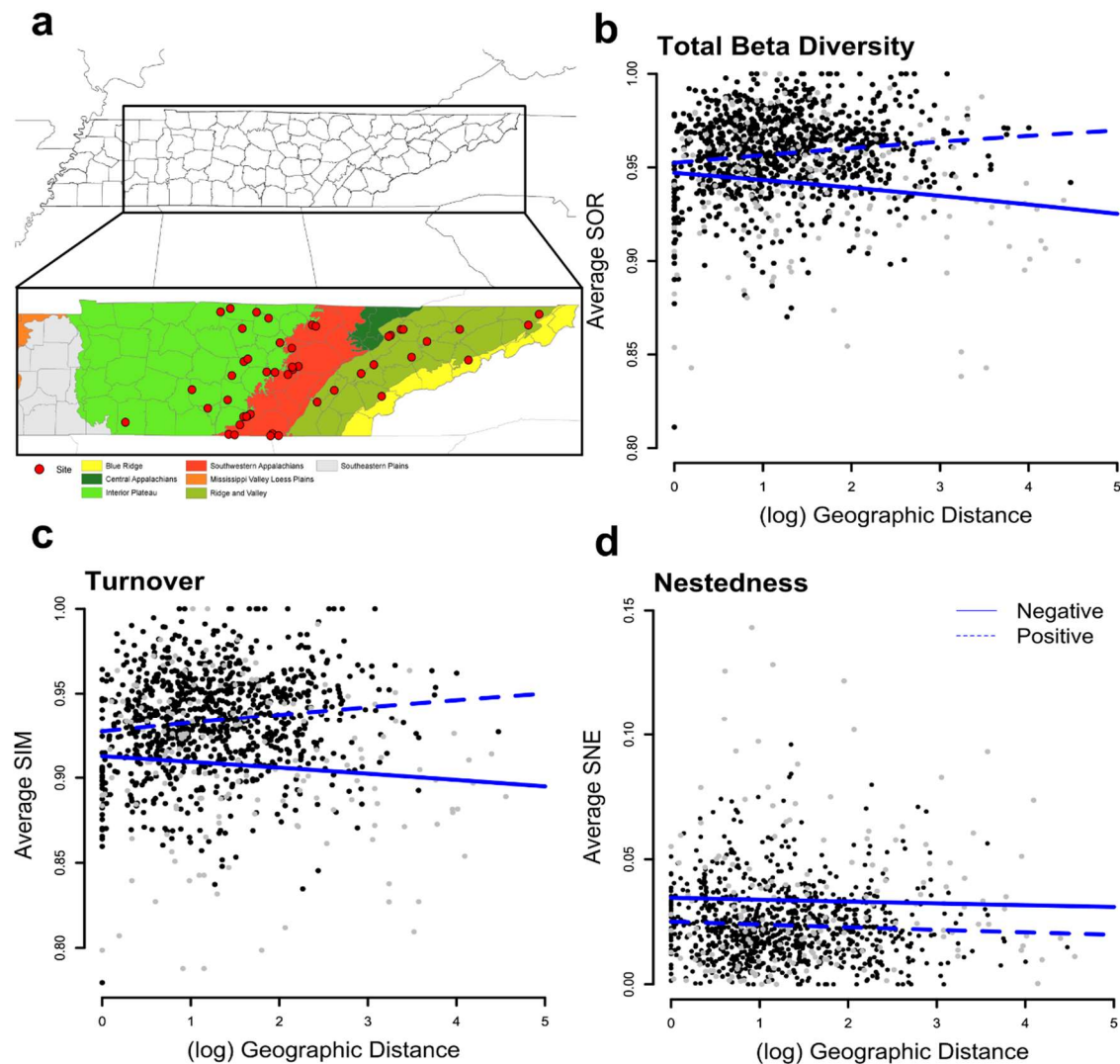


**Figure 17. Distance decay analysis.**

A. Map of the study system, red dots indicate sample sites. Samples were collected across three Tennessee ecoregions (Interior Plateau in light green, South West Appalachians in red, and Ridge and Valley in olive green). Map produced using ArcGis 10.7.1.

(<https://desktop.arcgis.com/en/arcmap/>) Copyright 1995-2018 Esri. All rights reserved.

Published in the United States of America. Distance-decay relationships, comparing geographic distances between sites and B. total beta diversity, C. turnover, D. nestedness, for *P. destructans* positive (dashed line and black dots) and *P. destructans* negative (solid line and grey dots) bats averaged by site. There is no significant relationship between geographic distance and community dissimilarity (SOR: GLM;  $z = 0.79$ ,  $p > 0.05$ ; SIM: GLM;  $z = 0.86$ ,  $p > 0.05$ ; SNE: GLM;  $z = 0.96$ ,  $p > 0.05$ ) or decay rates between disease states ( $p > 0.05$ ) for any metric (SOR; ANOVA;  $p > 0.05$ , SIM; ANOVA;  $p > 0.05$ , SNE; ANOVA;  $p > 0.05$ ).

*Metacommunity structure*

Metacommunities for both *P. destructans* positive and negative bats showed positive coherence, with significantly ( $p \leq 0.05$ ) less embedded absences than expected based on null models (positive = 1 142 539 embedded absences,  $1\,376\,131.98 \pm 1943.23$  expected; negative = 46 167 embedded absences,  $52\,651 \pm 186.4$  expected; Fig. 18, Table 4). The *P. destructans* positive metacommunity was characterized by significant positive turnover ( $p \leq 0.05$ ,  $2.48e+10$  replacements; simulated mean  $2.26e+10 \pm 2.25e+08$ ), while the *P. destructans* negative metacommunity had significant negative turnover ( $p \leq 0.05$ , 42 579 240 replacements;  $47\,012\,450 \pm 1\,005\,206$  expected replacements). Both *P. destructans* positive and negative metacommunities had significant clumping of species range boundaries (positive bats; Morisita's index = 1.44,  $p \leq 0.05$ ; negative bats; Morisita's index = 1.39,  $p \leq 0.05$ ). Together, these results indicate that the *P. destructans* positive metacommunity can be described as having a Clementsian structure (Fig. 16E), whereas, the *P. destructans* negative metacommunity had a nested structure with clumped species losses (Fig. 16C; Presley *et al.* 2010).

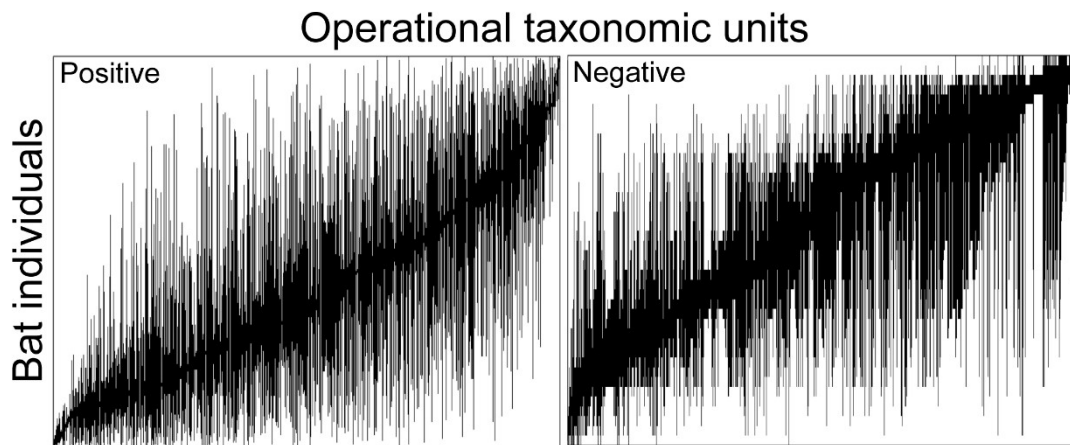


**Figure 18. Visual representation of microbial metacommunities across *P. destructans* status.**

Site by species incidence matrix for OTUs on *P. destructans* positive/negative bats describing the actual metacommunity patterns. EMS analysis suggests a Clementsian structure for *P. destructans* positive and a nested structure for *P. destructans* negative bat microbial metacommunities.

**Table 4. Results for the EMS analysis of bats across *P. destructans* status.** Results suggest Clementsian metacommunity structure for *P. destructans* positive bats, and a nested metacommunity structure for *P. destructans* negative bats (Presley *et al.* 2010).

<i>P. destructans</i> positive bats		
	<b>Coherence</b>	<b>p-value</b>
Absences	1 142 539	$\leq 0.0001$
Simulated mean	1 376 131.9 ( $\pm 1,943.2$ )	
<b>Turnover</b>		
Turnover	2.48 e +10	$\leq 0.0001$
Simulated mean	2.26 e +10 ( $\pm 2.25$ e +8)	
<b>Boundary</b>		
Index	1.44	$\leq 0.0001$
<i>P. destructans</i> negative bats		
	<b>Coherence</b>	<b>p-value</b>
Absences	46 167	$\leq 0.0001$
Simulated mean	52 651 ( $\pm 186.4$ )	
<b>Turnover</b>		
Turnover	42 579 240	$\leq 0.0001$
Simulated mean	47 012 450 ( $\pm 1 005 206$ )	
<b>Boundary</b>		
Index	1.39	$\leq 0.0001$

A total of 14 OTUs were identified as indicator taxa for *P. destructans* positive and 363 OTUs for negative bats. The group of indicator OTUs for the *P. destructans* negative bats represents the common taxa occurring across the individual microbial communities that contributed to the nestedness in metacommunity structure. OTUs indicative of *P. destructans* negative bats were significantly more abundant on *P. destructans* negative, relative to *P. destructans* positive bats (GLMM;  $z = -62.84$ ,  $p \leq 0.05$ ; Fig. 19A.). Additionally, there was a significant negative relationship between log

transformed fungal load and indicator taxa abundance (GLMM;  $z = -10.78$ ,  $p \leq 0.05$ ; Fig. 19B), with increased fungal load predictive of fewer indicator taxa. However, similar patterns were not found when analyzing the relationship between *P. destructans* load and the nested component (SNE) of averaged community dissimilarities (GLM;  $z = -0.10$ ,  $p > 0.05$ ; Fig. 19C). Between site average community dissimilarity (SOR and SIM) was not related to the between site average difference in log transformed fungal load (GLM; SOR;  $z = 0.237$ ,  $p > 0.05$ ; SIM;  $z = 0.798$ ,  $p > 0.05$ ).

#### *Relationship between community structure and structuring variables*

All three measures of beta diversity lacked a distance-decay relationship (SOR: GLM;  $z = 0.79$ ,  $p > 0.05$ ; SIM: GLM;  $z = 0.86$ ,  $p > 0.05$ ; SNE: GLM;  $z = 0.96$ ,  $p > 0.05$ ; Fig. 17). There was no difference in the rate of decay between positive and negative bats for total beta diversity (SOR; ANOVA;  $p > 0.05$ , Fig. 17B), the turnover component of beta diversity (SIM; ANOVA;  $p > 0.05$ ; Fig. 17C), or nestedness (SNE; ANOVA;  $p > 0.05$  Fig. 17D). Multivariate dispersion was statistically different between *P. destructans* positive and negative bats for total beta diversity (SOR: betadisper;  $F_{1, 247} = 5.89$ ,  $p \leq 0.05$ ). Interestingly, analyses of multivariate dispersion indicated that there was a significant interactive effect between *P. destructans* status and ecoregion for both total beta diversity and turnover (betadisper; SOR:  $F_{5, 243} = 15.232$ ,  $p \leq 0.05$ ; SIM:  $F_{5, 243} = 8.646$ ,  $p \leq 0.05$ , Fig. 20A-B, Fig. 21). Post-hoc analysis of the interaction term for total beta diversity showed that dispersion was not different across ecoregions for *P. destructans* positive bats but varied for *P. destructans* negative bats (Fig. 20A). In general, dispersion was large in *P. destructans* positive bats, with negative bats within the Interior Plateau having significantly less dispersion (Fig. 20A), largely driven by a

difference in the turnover component (Fig. 20B). PERMANOVA revealed that average community composition (multivariate centroids) differed between *P. destructans* status and ecoregion when analyzing both total dissimilarities and the turnover component, but not nestedness, and that these effects were independent of each other (Fig. 21, Table 5).

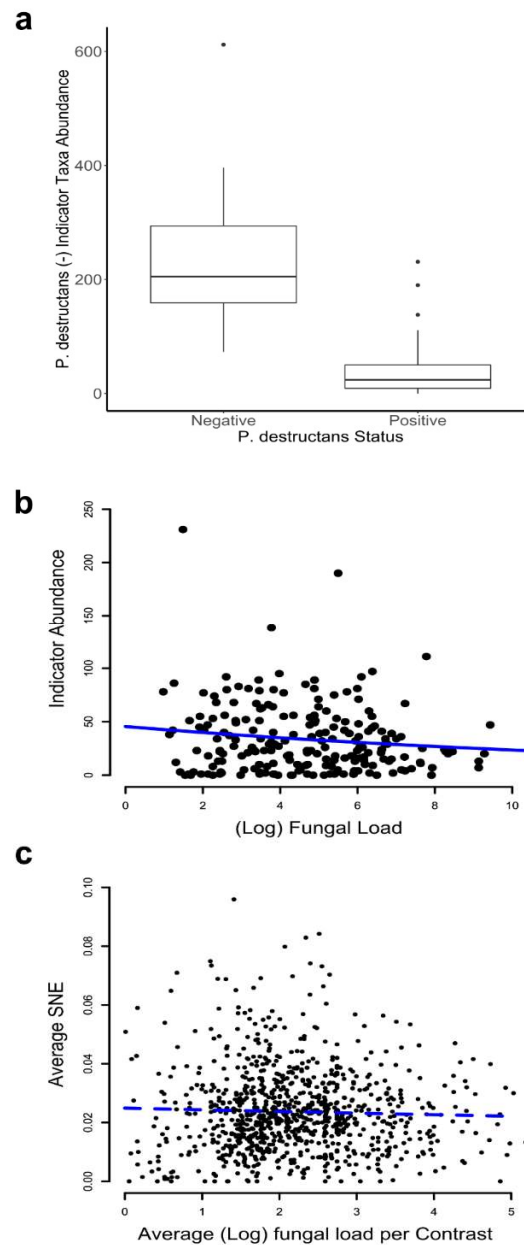


**Figure 19. Nestedness analysis.**

A. Comparison of the abundance of *P. destructans* negative indicator taxa between *P. destructans* positive/negative samples. Indicator taxa are significantly more abundant within *P. destructans* negative samples (GLMM;  $z = -62.84$ ,  $p \leq 0.05$ ). B. Comparison of the abundance of *P. destructans* negative indicator taxa by fungal load. There is a significantly negative relationship between indicator taxa abundance and amount of *P. destructans* present (GLMM;  $z = -10.78$ ,  $p \leq 0.05$ ). C. Comparison of the (log) difference in average fungal load and average nestedness (SNE) of bats averaged by site. There is no significant relationship between similarity in fungal load and nestedness (GLM;  $z = -0.10$ ,  $p > 0.05$ ).

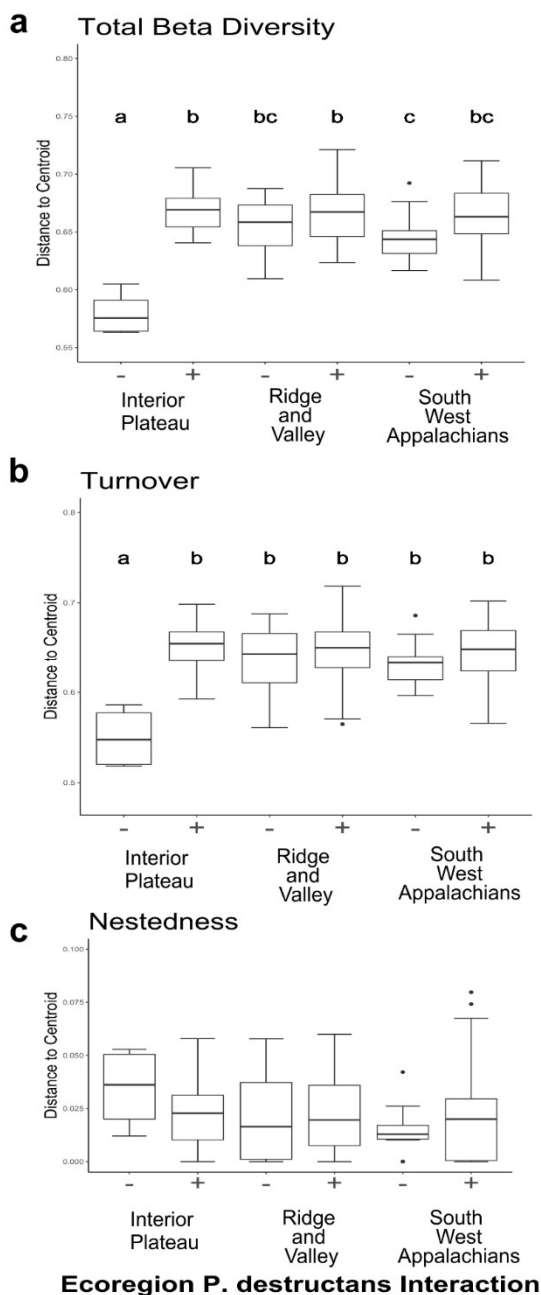


**Figure 20. Comparison of beta diversity measured as multivariate dispersion across the interaction of ecoregion and *P. destructans* status.**

Betadisper analysis comparing beta diversity measured as multivariate dispersion across the interaction of ecoregion and *P. destructans* status, for A. total beta diversity (SOR), B. turnover (SIM), and C. nestedness (SNE). Different lowercase letters indicate a significant difference ( $p \leq 0.05$ ) between groups, lowercase letters are missing from panel C due to lack of significant differences between groups. There is a significant interaction between *P. destructans* status and ecoregion for both total beta diversity as well as turnover (SOR:  $F_{5,243} = 15.232$ ,  $p \leq 0.05$ ; SIM:  $F_{5,243} = 8.646$ ,  $p \leq 0.05$ ).

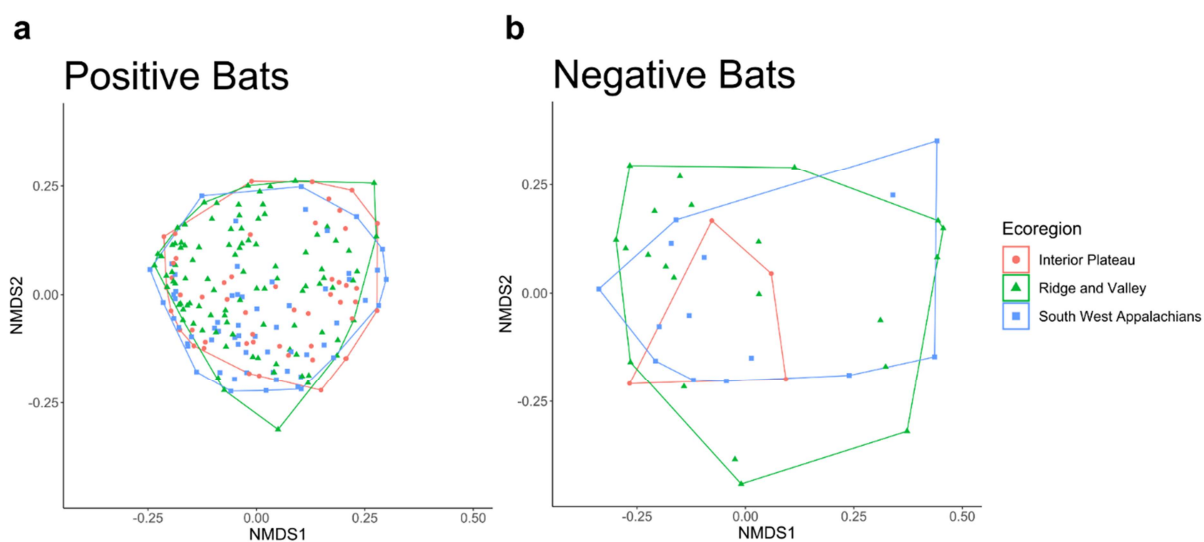


**Figure 21. Non-metric multidimensional scaling ordination for *P. destructans* positive and negative bats.**

Non-metric multidimensional scaling ordination for A. *P. destructans* positive and B. *P. destructans* negative bats across ecoregions (A. stress 0.17; B. stress 0.14). There is a significant effect of *P. destructans*, year and ecoregion ( $p < 0.05$ ), however, there is no significant interaction between *P. destructans* status and ecoregion. There is significant variation in dispersion across ecoregions for *P. destructans* negative bats (B).

**Table 5. Analysis of average assemblage similarity across *P. destructans* status and Ecoregion.**

PERMANOVA results for total beta diversity (SOR), the turnover component of beta diversity (SIM), and the nested component of beta diversity (SNE). There is a significant difference between *P. destructans* status, Ecoregion, and year for both SOR and SIM ( $p < 0.05$ ).

<b>Total Beta Diversity</b>	Df	Sums of squares	Mean squares	F test	R <sup>2</sup>	p-value
<i>P. destructans</i> status	1	0.746	0.746	1.7403	0.006	0.018*
Ecoregion	2	1.427	0.713	1.664	0.012	0.011*
year	1	0.795	0.794	1.8541	0.007	0.001***
site	45	24.357	0.541	1.2626	0.216	0.771
<i>P. destructans</i> status:Ecoregion	2	0.905	0.452	1.055	0.008	0.107
Residuals	197	84.454	0.428		0.749	
Total	248	112.683			1	
<b>Turnover</b>	Df	Sums of squares	Mean squares	F test	R <sup>2</sup>	p-value
<i>P. destructans</i> status	1	0.862	0.861	2.139	0.008	0.003**
Ecoregion	2	1.591	0.795	1.975	0.014	0.033*
year	1	0.605	0.605	1.502	0.005	0.012*
site	45	23.712	0.526	1.308	0.221	0.72
<i>P. destructans</i> status:Ecoregion	2	0.876	0.437	1.087	0.008	0.22
Residuals	197	79.344	0.402		0.741	
Total	248	106.99			1	
<b>Nestedness</b>	Df	Sums of squares	Mean squares	F test	R <sup>2</sup>	p-value
<i>P. destructans</i> status	1	-0.007	-0.007	-7.92	-0.045	1
Ecoregion	2	-0.01	-0.005	-5.955	-0.067	0.347
year	1	0.009	0.009	11.111	0.063	0.105
site	45	-0.01	-0.0002	-0.269	-0.069	0.737
<i>P. destructans</i> status:Ecoregion	2	-0.0003	-0.0001	-0.22	-0.002	0.745
Residuals	197	0.174	0.0008		1.121	
Total	248	0.156			1	

## Discussion

This study characterized the metacommunity structure of host microbial assemblages in the presence of a fungal pathogen. Overall, support was found for both of my hypotheses, I determined that the presence of *P. destructans* correlated with a change in cutaneous microbial metacommunity structure and loss of indicator OTUs from the core skin assemblage. Additionally, I found that the presence of *P. destructans* correlated with a change in relationship between community structure and an environmental structuring variable. These results suggest that the presence of *P. destructans* alters cutaneous microbial metacommunity structure by intensifying local processes, such as species sorting mechanisms or antagonistic species interactions.

The cutaneous microbial assemblages of *P. destructans* negative bats were characterized by a nested metacommunity structure with clumped species loss. The presence of numerous indicator taxa within negative bats further supported the inference of a nested metacommunity structure. Nested metacommunities have been observed in a variety of organisms, including Bryophytes (Heino *et al.* 2015), macroinfauna (Alves *et al.* 2020), and bats (Presley *et al.* 2012), and likely represent variation in species-specific characteristics such as dispersal ability and tolerance to environmental conditions (Presley *et al.* 2010). This is supported by previous work, which has shown the importance of host environment in shaping the cutaneous microbial assemblage (Walker *et al.* 2019) and suggests that OTU-specific tolerances to host environmental conditions might drive the clumped OTU loss seen in *P. destructans* negative bats.

The core microbiome is defined as the taxonomic identity of the most common bacterial taxa within a system (Risely 2020). Pairing of the EMS and indicator analysis

results for *P. destructans* positive bats suggested a loss of bacterial OTUs from the core microbiome. This loss might suggest alteration in community function and host defense against pathogens (Harris *et al.* 2009; Lemieux-Labonté *et al.* 2017; Grisnik *et al.* 2020). Nucleotide BLAST searches (based on ~250 bp region) revealed that indicator taxa identified in this study were not genetically identical to cultured bacteria with *in vitro* anti-*P. destructans* activity identified in Grisnik *et al.* (2020). However, seven of 363 indicator taxa were identified to the same genera of anti-*P. destructans* bacteria identified previously (Grisnik *et al.* 2020), including *Nocardia*, *Rhodococcus*, *Streptomyces*, *Luteibacter*, *Lysobacter*, and *Sphingomonas*. Each of these bacterial genera were detected on both positive and negative bats. Alternatively, bacteria with antifungal activity could have been gained to form the core microbiome of *P. destructans* negative bats, but additional work is required to mechanistically explain the correlational patterns found here. It is also important to acknowledge that approaches to understand assemblage function *in vitro* likely oversimplify complex inter- and intra-specific interactions at the community level, and further work to understand how bacterial function relates to fungal pathogenicity is warranted.

The cutaneous microbial assemblage of *P. destructans* positive bats exhibited turnover with boundaries clumped along an environmental gradient (Clementsian structure). Clementsian structure is known to be common in both free living (Heino *et al.* 2015) and host-associated microbial assemblages (Hernández-Gómez *et al.* 2017). Clementsian metacommunities can arise from antagonistic interactions preventing the coexistence of some taxa (Leibold and Mikkelsen 2002; Alves *et al.* 2020). Interestingly, previous work showed an inverse relationship between *P. destructans* positive bats and

bacteria that inhibited growth of *P. destructans* (Grisnik *et al.* 2020), suggesting that antagonistic interactions might drive the shift to Clementsian metacommunity structure in microbial assemblages of positive bats.

The lack of a distance-decay relationship in microbial assemblages suggests either a lack of dispersal limitation or absence of species sorting mechanisms driving the assembly of bat cutaneous microbial assemblages. Since bat host environment (ecoregion) had a significant impact on average assemblage structure and there was no significant distance-decay relationship, I can conclude that dispersal limitation does not have a predominant role in the assembly of the cutaneous microbial assemblages of *P. subflavus*. Bacterial dispersal limitation is consistent with previous work that has shown a lack of population structure in Appalachian bat species (Martin 2015; Wilder *et al.* 2015). This suggests that frequent roost switching and host dispersal may provide opportunities for microbial dispersal, and therefore, homogenization of bacterial assemblages across the region. Barriers to microbial dispersal between individual bats might be low, suggesting that the level of selection for microbial assemblage formation might be occurring at the colony level rather than the individual level (Kolodny *et al.* 2019). Other studies have attributed environmental heterogeneity as the underlying driver of distance-decay relationships in microbial assemblages (Hillebrand *et al.* 2001; Reche *et al.* 2005; Fierer and Jackson 2006; Liu *et al.* 2015). The lack of a distance-decay pattern driven by environmental heterogeneity could be due to the similarity of cave environments across my study system, as bats were sampled during the winter hibernation period, and not on a variety of summer/winter roost sites. Alternatively, variation within cave environments across the study system could result in a patchy distribution, rather than a geographically

constrained gradient of environmental heterogeneity. The overall influence of host environment and species sorting mechanisms have been observed in the literature, as other studies have shown an influence of site on cutaneous microbial assemblage structure for a variety of host taxa (Avena *et al.* 2016; Lemieux-Labonté *et al.* 2016; Walker *et al.* 2019). These results suggest the role of the host environment in shaping microbial communities through species sorting regardless of *P. destructans* status. The presence of *P. destructans* does not alter the rate (slope) of distance-decay in microbial assemblages across geographic space. In the context of community assembly, I found a lack of a *P. destructans* mediated change in dispersal limitation and/or species sorting in bacterial assemblage formation. Previous work has suggested an inverse pattern showing that as levels of disturbance increase, the rate of turnover within assemblages decreases, suggesting that disturbances can act as ecological filters (Goldenberg Vilar *et al.* 2014).

Results of permutational models indicated the role of the environment in shaping the bat cutaneous microbial assemblage. The PERMANOVA analysis indicates that the presence of *P. destructans* correlates with a difference in average community composition. Additionally, analysis of multivariate dispersion indicates that there is a significant interaction between *P. destructans* status and the environment, which suggests that the presence of *P. destructans* can alter the relationship between community structure and structuring variables, specifically the ecoregion where a bat is located. Of particular interest is the lack of significant differences in dispersion across ecoregions for *P. destructans* positive bats, despite significant differences for negative bats. In general, *P. destructans* positive bats have higher dispersion than negative bats. The presence of *P. destructans* within the Interior Plateau correlates with increased dispersion in the

turnover component of beta diversity compared to negative bats within that ecoregion. When the analysis of multivariate dispersion is coupled with the lack of a distance-decay relationship, it suggests that local processes (such as antagonistic interactions or species sorting) may be stronger in the presence of *P. destructans*. Previous work has suggested that disturbance increases the importance of species sorting mechanisms through the filtering of species that cannot persist within the disturbed environment (Chase 2007).

I assessed metacommunity structure in cutaneous assemblages as they responded to the progression of fungal disease. There was no significant relationship between community similarity and fungal load, which serves as a proxy for disease progression. This suggests that the presence of *P. destructans* alone might be enough to alter the average microbial assemblage. Previous work has shown the opposite pattern with increasing fungal load being positively correlated with assemblage dissimilarity (Muletz-Wolz *et al.* 2019). However, this study was done on salamanders infected with a chytrid fungus in a mesocosm setting, which could explain the conflicting results. Alternatively, due to the hierarchical structure of these data (bats nested within caves), the patterns I observed could be a result of site level averages rather than being representative of bacterial-fungal interactions on individual bats. While this is a valid concern, it has been shown that colony-level dynamics rather than individual identity better explain bat cutaneous microbial assemblage structure (Kolodny *et al.* 2019) suggesting valid ecological patterns observed during this study. The presence of *P. destructans* may drive the formation of a unique assemblage through deterministic processes, but within a disease state category (*P. destructans* positive or negative) the variation might be best explained by stochastic or species-specific factors. While this study failed to find a

relationship between assemblage-level similarity and fungal load, previous work has shown a correlation between pathogenic fungal load and specific bacterial taxa on bats (Grisnik *et al.* 2020). *Pseudogymnoascus destructans* load may induce OTU-specific abundance responses but not influence overall assemblage similarity in terms of species presence. Future research at a fine-scale temporal resolution and quantifying microbial relative abundances is necessary to understand the effects of disease progression on microbial assemblage structure.

In order to understand interactions between host-associated microbial assemblages and pathogens it is important to take scale into account. The goal of this study was to elucidate if the presence of a fungal pathogen correlates with changes in metacommunity structure and the variables that structure these communities as they relate to assembly mechanisms. Results suggest that invasion of these communities by a fungal pathogen correlate with a shift in metacommunity structure likely driven by intrinsic factors that alter community assembly mechanisms. I hypothesize that the change in community structure is caused by increased strength of local processes within assemblages. Future work should aim to better understand potential antagonistic interactions within microbial assemblages as they may help describe observed shifts in metacommunity structure and role in pathogen defense. Additionally, future experimental work in a controlled setting is required to confirm the processes structuring bat skin assemblages. Lastly, this study was conducted exclusively on bacterial communities, future work should incorporate other members of the host associated microbiome including viruses and fungi.

**Acknowledgements**

I would like to thank TWRA, TNC, and TVA for field work assistance. This work was approved by IACUC TTU-16-17-003 and USFWS 2009-038. Funding and support for this research project was provided by Tennessee Wildlife Resources Agency as State Wildlife Grant 32801-00803 to DMW. I thank the four anonymous reviewers for their helpful comments to improve this manuscript. All sequence data were submitted to GenBank SRA under the accession number PRJNA691025.

## References

- Alves AT, Petsch DK, Barros F. Drivers of benthic metacommunity structure along tropical estuaries. *Sci Rep* 2020;**10**:1–12.
- Anderson MJ, Walsh DC. PERMANOVA, ANOSIM, and the mantel test in the face of heterogeneous dispersions: what null hypothesis are you testing? *Ecol Monogr* 2013;**83**:557–74.
- Avena CV, Parfrey LW, Leff JW *et al.* Deconstructing the bat skin microbiome: influences of the host and the environment. *Front Microbiol* 2016;**7**:1–14.
- Baselga A, Orme CDL. betapart: an R package for the study of beta diversity. *Methods Ecol Evol* 2012;**3**:808–12.
- Bates D, Maechler M, Bolker B *et al.* Package lme4. R package version 1.1-7. <https://cran.r-project.org/web/packages/lme4/index.html>.
- Belden LK, Harris RN. Infectious diseases in wildlife: the community ecology context. *Front Ecol Environ* 2007;**5**:533–39.
- Blehert DS, Hicks AC, Behr M *et al.* Bat white-nose syndrome: An emerging fungal pathogen? *Science* 2009;**323**:227.
- Brown JJ, Mihaljevic JR, Marteaux L *et al.* Metacommunity theory for transmission of heritable symbionts within insect communities. *Ecol Evol* 2020;**10**:1703–21.
- Brown JH, Kodric-Brown A. Turnover rates in insular biogeography: effect of immigration on extinction. *Ecology* 1977;**58**:445–49.
- Caporaso JG, Lauber CL, Walters WA *et al.* Global patterns of 16S rRNA diversity at a depth of millions of sequences per sample. *PNAS* 2011;**108**:4516–22.
- Chase JM. Drought mediates the importance of stochastic community assembly. *Proc Natl Acad Sci USA* 2007;**104**:17430–34.
- Clements FE. *Plant succession: an analysis of the development of vegetation*. Washington DC: Carnegie Institution of Washington, 1916.
- Costello EK, Stagaman K, Dethlefsen L, Bohannan BJ *et al.* The application of ecological theory toward an understanding of the human microbiome. *Science* 2012;**336**:1255–1262.
- Dallas T. metacom: an R package for the analysis of metacommunity structure. *Ecography* 2014;**37**:402–05.
- De Caceres M, Jansen F, De Caceres MM. ‘indicspecies’. R package version 1.7.9. 2020. <https://CRAN.R-project.org/package=indicspecies> (10 October 2020, date last accessed).
- Ellison SL, English CA, Burns MJ *et al.* Routes to improving the reliability of low-level DNA analysis using real-time PCR. *BMC Biotechnol* 2006;**6**:33.
- Fierer N, Jackson RB. The diversity and biogeography of soil bacterial communities. *Proc Natl Acad Sci USA* 2006;**103**:626–31.
- Fox J, Weisberg S, Adler D *et al.* ‘car’. R package version 2.1-4. 2016. <https://CRAN.R-project.org/package=car>.
- Frick WF, Puechmaille SJ, Willis CKR. White-nose syndrome in bats. In: Voigt CC, Kingston T (eds.). *Bats in the Anthropocene: Conservation of Bats in a Changing World* New York City: Springer International Publishing, 2016, 245–262.

- Glassman SI, Martiny JB. Broadscale ecological patterns are robust to use of exact sequence variants versus operational taxonomic units. *mSphere* 2018, DOI:10.1128/mSphere.00148-18.
- Goldenberg Vilar A, van Dam H, van Loon EE *et al.* Eutrophication decreases distance decay of similarity in diatom communities. *Freshw Biol* 2014;**59**:1522–1531.
- Grice EA, Segre JA. The skin microbiome. *Nat Rev Microbiol* 2011;**9**:244–53.
- Grisnik M, Bowers O, Moore AJ *et al.* The cutaneous bat microbiome has antifungal activity against the white nose pathogen. *FEMs Microbiol Ecol* 2020, DOI: 10.1093/femsec/fiz193.
- Harris RN, Brucker RM, Walke JB *et al.* Skin microbes on frogs prevent morbidity and mortality caused by a lethal skin fungus. *ISME J* 2009;**3**:818–24.
- Heino J. The importance of metacommunity ecology for environmental assessment research in the freshwater realm. *Biol Rev* 2013;**88**:166–178.
- Heino J, Nokela T, Soininen J *et al.* Elements of metacommunity structure and community-environment relationships in stream organisms. *Freshw Biol* 2015; **60**:973–88.
- Hernández-Gómez O, Hoverman JT, Williams RN. Cutaneous microbial community variation across populations of eastern hellbenders (*Cryptobranchus alleganiensis alleganiensis*). *Front Microbiol* 2017;**8**:1379.
- Hillebrand H, Watermann F, Karez R *et al.* Differences in species richness patterns between unicellular and multicellular organisms. *Oecologia* 2001;**126**:114–24.
- Janicki AF, Frick WF, Kilpatrick AM *et al.* Efficacy of Visual Surveys for White-Nose Syndrome at Bat Hibernacula. *PLoS One* 2015, DOI:10.1371/journal.pone.0133390.
- Kolodny O, Weinberg M, Reshef L *et al.* Coordinated change at the colony level in fruit bat fur microbiomes through time. *Nat Ecol Evol* 2019;**3**:116–24.
- Langwig KE, Frick WF, Bried JT *et al.* Sociality, density-dependence and microclimates determine the persistence of populations suffering from a novel fungal disease, white-nose syndrome. *Ecol Lett* 2012;**15**:1050–57.
- Langwig KE, Hoyt JR, Parise KL *et al.* Resistance in persisting bat populations after white-nose syndrome invasion. *Philos Trans Royal Soc B* 2017;**372**:1–9.
- Leibold MA, Mikkelsen GM. Coherence, species turnover, and boundary clumping: elements of metacommunity structure. *Oikos* 2002;**97**:237–50.
- Leibold MA, Holyoak M, Mouquet N *et al.* The metacommunity concept: a framework for multi-scale community ecology. *Ecol Lett* 2004, DOI:10.1111/j.1461-0248.2004.00608.x.
- Lemieux-Labonté V, Tromas N, Shapiro BJ *et al.* Environment and host species shape the skin microbiome of captive neotropical bats. *PeerJ* 2016, DOI: 10.7717/peerj.2430.
- Lemieux-Labonté V, Simard A, Willis CKR *et al.* Enrichment of beneficial bacteria in the skin microbiota of bats persisting with white-nose syndrome. *Microbiome* 2017; **5**:115–30.
- Levin SA. The problem of pattern and scale in ecology. *Ecology* 1992;**73**:1943–67.
- Liu L, Yang J, Yu Z *et al.* The biogeography of abundant and rare bacterioplankton in the lakes and reservoirs of China. *ISME J* 2015;**9**:2068–77.

- Martin AM. Historical Demography and Dispersal Patterns in the Eastern Pipistrelle Bat (*Perimyotis subflavus*). *MS Thesis Grand Valley State University* 2014.
- Minich JJ, Sanders JG, Amir A *et al*. Quantifying and understanding well-to-well contamination in microbiome research. *MSystems* 2019, DOI: 10.1128/mSystems.00186-19.
- Muletz-Wolz CR, Fleischer RC, Lips KR. Fungal disease and temperature alter skin microbiome structure in an experimental salamander system. *Mol Ecol* 2019;**2**:2917–31.
- Muller LK, Lorch JM, Linder DL *et al* Bat white-nose syndrome: a real-time TaqMan polymerase chain reaction teste targeting the intergenic spacer region of *Geomyces destructans*. *Mycologica* 2013;**105**:253–59.
- Nekola JC, White PS. The distance decay of similarity in biogeography and ecology. *J Biogeogr* 1999;**26**:867–878.
- Oksanen J, Blanchet FG, Friendly M *et al*. Vegan: Community Ecology Package. R package version 2.5-2 2018. <https://CRAN.R-project.org/package=vegan> (10 October 2020, date last accessed).
- Patterson BD, Atmar W. Nested subsets and the structure of insular mammalian faunas and archipelagos. *Biol J Linn Soc* 1986;**28**:65–82.
- Presley SJ, Higgins CL, Willig MR. A comprehensive framework for the evaluation of metacommunity structure. *Oikos* 2010;**119**:908–17.
- Presley SJ, Cisneros LM, Patterson BD *et al*. Vertebrate metacommunity structure along an extensive elevational gradient in the tropics: a comparison of bats, rodents and birds. *Glob Ecol Biogeogr* 2012;**21**:968–976.
- Quast C, Pruesse E, Yilmaz P *et al*. The SILVA ribosomal RNA gene database project: improved data processing and web-based tools. *Nuc Acids Res* 2012, DOI: 10.1093/nar/gks/1219.
- Reche I, Pulido-Villena E, Morales-Baquero R *et al*. Does ecosystem size determine aquatic bacterial richness? *Ecology* 2005;**86**:1715–22.
- R Core Team. R: A language and environment for statistical computing. R Foundation for Statistical Computing, Vienna, Austria. 2020; <http://www.R-project.org/>.
- Risely A. Applying the core microbiome to understand host–microbe systems. *J Anim Ecol* 2020;**89**:1549–1558.
- Rognes T, Flouri T, Nichols B *et al*. VSEARCH: a versatile open source tool for metagenomics. *PeerJ* 2016, DOI:10.7717/peerj.2584.
- Schloss PD, Westcott SL, Ryabin T *et al*. Introducing mothur: open-source, platform-independent, community-supported software for describing and comparing microbial communities. *Appl Environ Microbiol* 2009;**75**:7537–41.
- Schloss PD, Westcott SL. Assessing and improving methods used in operational taxonomic unit-based approaches for 16S rRNA gene sequence analysis. *Appl Environ Microbiol* 2011;**77**:3219–26.
- Tornero I, Boix D, Bagella S *et al*. Dispersal mode and spatial extent influence distance-decay patterns in pond metacommunities. *PLOS ONE* 2018, DOI: 10.1371/journal.pone.0203119.
- Walker DM, Leys JE, Grisnik M *et al*. Variability in snake skin microbial assemblages across spatial scales and disease states. *ISME J* 2019;**13**:2209–22.

- Weiss S, Xu ZZ, Peddada S *et al.* Normalization and microbial differential abundance strategies depend upon data characteristics. *Microbiome* 2017;**5**:1–18.
- Wickham H. *ggplot2: Elegant Graphics for Data Analysis*. New York: Springer-Verlag, 2016.
- Wilber MQ, Jani AJ, Mihaljevic JR *et al.* Fungal infection alters the selection, dispersal and drift processes structuring the amphibian skin microbiome. *Ecol Lett* 2020;**23**:88–98.
- Wilder AP, Kunz TH, Sorenson MD. Population genetic structure of a common host predicts the spread of white-nose syndrome, an emerging infectious disease in bats. *Mol Ecol* 2015;**24**:5495–5506.

## Chapter V: Overall Conclusion

Recent estimates of extinction rates have indicated that Planet Earth is currently experiencing a period of biodiversity decline 1000-10,000 times the accepted background rate (De Vos *et al.* 2014). Drivers of biodiversity decline include infectious diseases, with pathogenic fungi emerging as one of the main causative agents (Fisher *et al.* 2012).

*Pseudogymnoascus destructans*, the causative agent of white-nose syndrome, has caused rapid population declines of bats across the eastern United States, and is a major biodiversity conservation concern (Blehert *et al.* 2009). This developing conservation crisis has led to an increase in interest in understanding how hosts defend themselves from fungal pathogens, with recent emphasis on understanding the role of host associated microbial assemblages (Belden and Harris 2007; Grice and Segre 2011). Previous work has identified a number of bacterial taxa within cutaneous microbial assemblages of a variety of organisms that have antifungal capabilities (Harris *et al.* 2009; Cheng *et al.* 2016; Hill *et al.* 2017; Grisnik *et al.* 2020).

A variety of factors correlate with overall assemblage structure, including host taxonomic relationships (Walker *et al.* 2019a), host behaviors (Tung *et al.* 2015), and host environment (Avena *et al.* 2016). Therefore, in order to better recognize potential interactions between fungal pathogens and host associated microbial assemblages, it is important to understand these assemblages within a metacommunity theory framework. Metacommunity theory provides a way to observe how assemblage patterns observed at a local level are influenced by interactions at a much larger regional level (Leibold *et al.* 2004). By incorporating drivers of assemblage formation, we can better understand and predict how fungal pathogens interact with host associated microbial assemblages. My

overall goal was to understand how the bat cutaneous microbial assemblage interacts with *Pseudogymnoascus destructans* across the state of Tennessee.

I found that the effect of *P. destructans* on the bat cutaneous microbial assemblage varies spatially. The importance of site has been observed in other studies (Avena *et al.* 2016; Walker *et al.* 2019b) and suggests the role of host environment or species sorting mechanisms in the maintenance of these complex assemblages. I found 18 bacterial taxa that had anti-*P. destructans* capabilities. These taxa were found ubiquitously in the cave environment, but were enriched within the bat cutaneous assemblage, suggesting the role of bat skin in selecting antifungal taxa. Interestingly, there was a higher richness of these anti-*P. destructans* taxa found on *P. destructans* negative bats, supporting the hypothesis that these assemblages play a role in host defense from fungal pathogens. This was consistent with previous work that has shown a similar pattern, with pathogen exposed hosts having an assemblage enriched with antifungal bacterial taxa (Lemieux-Labonté *et al.* 2017).

I found that *P. destructans* correlated with a shift in bacterial assemblage taxonomic structure, but this shift was not observed in overall function of the assemblage. This result is consistent with previous work that has shown a decoupling of taxonomic and functional assemblages (Burke *et al.* 2011; Louca *et al.* 2016). When a finer scale approach was taken, I observed variation between bacterial taxa metagenomes for orthologs hypothesized to play a role in host defense. Functional redundancy in the microbiome occurred at the broadest scale, specifically KEGG functional pathways, but some variation was observed within a pathway and dependent on *P. destructans* status. This suggests that if these assemblages are formed through environmental filtering or

species sorting of the functional, rather than the taxonomic, assemblage, it is likely that selection is acting at the functional pathway rather than the individual ortholog level.

Within a metacommunity context, I found that the presence of *P. destructans* correlated with a shift in metacommunity structure, with *P. destructans* negative bats having a nested metacommunity characterized by a group of shared taxa, and *P. destructans* positive bats having a Clementsian metacommunity, or one characterized by turnover between sites. I found that host environment, specifically ecoregion, likely plays a role in shaping host associated microbial assemblage structure. Additionally, there was a significant interaction between host environment and *P. destructans* status, suggesting that the presence of this pathogen influences how the bacterial assemblage interacts with the environment. I hypothesize that this interaction is caused by local processes, either species sorting or antagonistic interactions within assemblages invaded by *P. destructans*. Multiple other studies have noted the importance of host environment in the formation of host associated microbial assemblages (Lemieux-Labonté *et al.* 2016; Walker *et al.* 2019b).

In conclusion, I found that *P. destructans* has a differential influence on microbial assemblage taxonomic structure across the landscape. Within a metacommunity context, I found that the presence of *P. destructans* correlated with a shift in metacommunity structure. However, when looking at community function I found that, despite changes in taxonomic assemblage structure, at broad scales bacterial taxa are likely functionally redundant and that the presence of *P. destructans* does not correlate with a shift in community level functional capabilities. Additionally, I found that *P. destructans* negative bats had a microbial assemblage with a higher richness of anti-*P. destructans*

bacterial taxa than *P. destructans* positive bats. These results suggest the potential importance of local processes (species sorting/environmental filtering or antagonistic interactions) in maintaining assemblage structure in the presence of a fungal pathogen. It is important to note that without manipulative studies, the processes behind patterns cannot be discerned, therefore more work needs to be done within a controlled setting to better understand the role of these structuring processes.

## References

- Avena CV, Parfrey LW, Leff JW *et al.* Deconstructing the bat skin microbiome: influences of the host and the environment. *Front Microbiol* 2016;**7**:1–14.
- Belden LK, Harris RN. Infectious diseases in wildlife: the community ecology context. *Front Ecol Environ* 2007;**5**:533–39.
- Blehert DS, Hicks AC, Behr M *et al.* Bat white-nose syndrome: An emerging fungal pathogen? *Science* 2009;**323**:227.
- Burke C, Steinberg P, Rusch D. Bacterial community assembly based on functional genes rather than species. *PNAS* 2011;**108**:14288–93.
- Cheng TL, Mayberry H, McGuire LP *et al.* Efficacy of a probiotic bacterium to treat bats affected by the disease white-nose syndrome. *J Appl Ecol* 2016;**54**:701–08.
- De Vos JM, Joppa LN, Gittleman JL *et al.* Estimating the normal background rate of species extinction. *Conserv Biol* 2014;**29**:452–62.
- Fisher MC, Henk DA, Briggs CJ *et al.* Emerging fungal threats to animal, plant, and ecosystem health. *Nature* 2012;**484**:186–94.
- Grice EA, Segre JA. The skin microbiome. *Nat Rev Microbiol* 2011;**9**:244–53.
- Grisnik M, Bowers O, Moore AJ *et al.* The cutaneous bat microbiome has antifungal activity against the white nose pathogen. *FEMs Microbiol Ecol* 2020, DOI: 10.1093/femsec/fiz193.
- Harris RN, Brucker RM, Walke JB *et al.* Skin microbes on frogs prevent morbidity and mortality caused by a lethal skin fungus. *ISME J* 2009;**3**:818–24.
- Hill AJ, Leys JE, Bryan D *et al.* The potential of the snake cutaneous microbiome to inhibit *Ophidiomyces ophiodiicola*, the causative agent of snake fungal disease. *EcoHealth* 2017;**15**:109–20.
- Leibold MA, Holyoak M, Mouquet N *et al.* The metacommunity concept: a framework for multi-scale community ecology. *Ecol Lett* 2004, DOI:10.1111/j.1461-0248.2004.00608.x.
- Lemieux-Labonté V, Tromas N, Shapiro BJ *et al.* Environment and host species shape the skin microbiome of captive neotropical bats. *PeerJ* 2016, DOI: 10.7717/peerj.2430.
- Lemieux-Labonté V, Simard A, Willis CKR *et al.* Enrichment of beneficial bacteria in the skin microbiota of bats persisting with white-nose syndrome. *Microbiome* 2017;**5**:115–30.
- Louca S, Jacques SMS, Pires APF *et al.* High taxonomic variability despite stable functional structures across microbial communities. *Nat Ecol Evol* 2016, DOI: 10.1038/s41559-016-0015.
- Tung J, Barreiro LB, Burns MB *et al.* Social networks predict gut microbiome composition in wild baboons. *eLife* 2015, DOI:10.7554/eLife.05224.001.
- Walker DM, Hill AJ, Albecker MA *et al.* Variation in the Slimy Salamander (*Plethodon* spp.) Skin and Gut-Microbial Assemblages is Explained by Geographic Distance and Host Affinity. *Microbial Ecology* 2019a, DOI:10.1007/s00248-019-01456-x.
- Walker DM, Leys JE, Grisnik M *et al.* Variability in snake skin microbial assemblages across spatial scales and disease states. *ISME J* 2019b;**13**:2209–22.

APPENDICES

## APPENDIX A: MOTHUR COMMANDS

Linux version

Using ReadLine

Using Boost

Running 64Bit Version

mothur v.1.40.2

Last updated: 4/23/2018

by

Patrick D. Schloss

Department of Microbiology & Immunology

University of Michigan

<http://www.mothur.org>

When using, please cite:

Schloss, P.D., *et al.*, Introducing mothur: Open-source, platform-independent, community-supported software for describing and comparing microbial communities. *Appl Environ Microbiol*, 2009. 75(23):7537-41.

Distributed under the GNU General Public License

Type 'help()' for information on the commands that are available

For questions and analysis support, please visit our forum at

<https://www.mothur.org/forum>

Type 'quit()' to exit program

Interactive Mode

```
mothur > make.contigs(file=180607matt.txt, processors=12)
```

```
mothur > summary.seqs(fasta=current)
```

```
mothur > pcr.seqs(fasta=current, group=current, oligos=oligos.txt, rdiffs=3, pdiffs=1)
```

```
mothur > set.current(fasta=180607matt.trim.contigs.pcr.fasta, processors=12)
```

```
mothur > screen.seqs(fasta=current, group=current, maxambig=0, maxlength=253)
```

```
mothur > set.current(fasta=180607matt.trim.contigs.pcr.fasta,
```

```
group=180607matt.contigs.groups, processors=12)
```

```
mothur > screen.seqs(fasta=current, group=current, maxambig=0, maxlength=253)
```

```
mothur > summary.seqs(fasta=current)
```

```
mothur > unique.seqs(fasta=current, count=current)
```

```
mothur > summary.seqs(fasta=current)
```

```
mothur > count.seqs(name=current, group=current)
```

```
mothur > summary.seqs(fasta=current, count=current)
```

```
mothur > align.seqs(fasta=current, reference=silva.v4.fasta)
```

```
mothur > screen.seqs(fasta=current, count=current, start=1968, end=11550,
maxhomop=8)
```

```
mothur > summary.seqs(fasta=current, count=current)
```

```
mothur > filter.seqs(fasta=current, vertical=T, trump=.)
```

```
mothur > summary.seqs(fasta=current, count=current)
```

```
mothur > unique.seqs(fasta=current, count=current)
```

```
mothur > pre.cluster(fasta=current, count=current, diffs=2)
```

```
mothur > chimera.vsearch(fasta=current, count=current, dereplicate=t)
```

```
mothur > remove.seqs(fasta=current, accnos=current)
```

```
mothur > classify.seqs(fasta=current, count=current,
reference=trainset9_032012.pds.fasta, taxonomy=trainset9_032012.pds.tax, cutoff=80)
mothur > remove.lineage(fasta=current, count=current, taxonomy=current,
taxon=Chloroplast-Mitochondria-unknown-Archaea-Eukaryota)
mothur > summary.seqs(fasta=current, count=current)
mothur > cluster.split(fasta=current, count=current, taxonomy=current,
splitmethod=classify, taxlevel=4, cutoff=0.03)
mothur > remove.rare(list=current, count=current, nseqs=10, label=0.03)
mothur > get.oturep(list=current, count=current, fasta=current, method=abundance)
mothur >
set.current(fasta=180607matt.trim.contigs.pcr.good.unique.good.filter.unique.precluster.p
ick.pick.fasta,
count=180607matt.trim.contigs.pcr.good.unique.good.filter.unique.precluster.denovo.vse
arch.pick.pick.count_table,
list=180607matt.trim.contigs.pcr.good.unique.good.filter.unique.precluster.pick.pick.opti
_mcc.list, processors=12)
mothur > make.shared(list=current, count=current, label=0.03)
mothur > remove.rare(list=current, count=current, nseqs=10, label=0.03)
mothur > make.shared(list=current, count=current, label=0.03)
mothur > get.groups(shared=current, groups=negativelib2-Negativelib1-Negativelib3)
mothur >
remove.otus(shared=180607matt.trim.contigs.pcr.good.unique.good.filter.unique.preclust
er.pick.pick.opti_mcc.0.03.pick.shared, accnos=contam.csv)
mothur > classify.otu(list=current, count=current, taxonomy=current, label=0.03)
mothur > count.groups(shared=current)
mothur > sub.sample(shared=current, size=1300)
mothur > summary.single(shared=current, calc=sobs-coverage)
```

## APPENDIX B: qPCR Results

Swab Code	Avg Ct	Approx. # Copies
CCB001	29.16	754.4387729
CCB003	37.855	2.112379772
CCB033	35.4	11.10605961
CCB034	0	0
CCB036	30	427.5628862
CCB041	34.08	27.85197521
CCB043	0	0
CCB045	29.62666667	549.0754169
CCB047	29.81	486.1653471
CCB051	32.86	61.84491543
CCB053	31.71	134.5686824
CCB054	36.49	5.315400587
CCB056	33.328	45.01030958
CCB071	30.05	413.3519588
CCB074	31.45666667	159.3470398
CCB075	28.72	1015.799512
CCB076	31.37333333	165.9434061
CCB081	30.23666667	363.5264371
CCB082	31.64	141.0899242
CCB084	35.99	7.453083726
CCB087	27.22666667	2781.454756
CCB088	30.62333333	281.169365
CCB089	31.28666667	178.7540951
CCB129	31.74333333	131.5997911
CCB130	30.17	381.1430456
CCB131	35.10666667	13.60316607
CCB137	32.00666667	110.6114282
CCB138	30.40666667	326.2571214
CCB140	29.67333333	534.4265186
CCB141	31.5	155.0957867
CCB221	0	0
CCB222	0	0
CCB224	30.05	599.5149258
CCB231	34.96	14.95353942
CCB232	37.608	2.509805115
CCB233	31.46333333	159.3470398

<b>Swab Code</b>	<b>Avg Ct</b>	<b>Approx. # Copies</b>
CCB242	33.42666667	42.06801305
CCB244	0	0
CCB254	35.98333333	7.503640175
CCB255	33.10666667	52.58235102
CCB256	31.00333333	217.4703232
CCB261	38.91	0
CCB262	32.17333333	98.60251673
CCB264	31.36666667	169.6870892
CCB277	0	0
CCB280	30.984	220.4306595
CCB294	30.59	286.9300275
CCB295	32.72333333	67.98420135
CCB296	31.89333333	119.1505359
CCB297	35.36	11.41048226
CCB298	31.58666667	146.9305147
CCB305	32.02	109.1259406
CCB306	30.578	286.9300275
CCB307	28.94666667	869.5208494
CCB311	32.63	72.73911286
CCB312	34.912	15.57255954
CCB313	31.298	177.7899468
CCB314	35.31333333	11.88283317
CCB325	0	0
CCB331	35.41666667	10.95690762
CCB332	31.87666667	119.9587689
CCB333	33.89	30.82449711
CCB334	27.675	2051.880197
CCB335	36.01	7.352990418
CCB364	34.32	23.04878305
CCB365	27.53	2270.868573
CCB366	29.84666667	476.404659
CCB057	0	0
CCB309	0	0
CCB031	30.19	376.0243767
CCB032	30.53666667	297.4641733
CCB044	32.64666667	71.43954283
CCB052	35.26333333	12.18106704

## APPENDIX C: MOTHUR COMMANDS

Linux version

Using ReadLine

mothur v.1.42.1

Last updated: 01/09/2020

by

Patrick D. Schloss

Department of Microbiology & Immunology

University of Michigan

<http://www.mothur.org>

When using, please cite:

Schloss, P.D., *et al.*, Introducing mothur: Open-source, platform-independent, community-supported software for describing and comparing microbial communities. *Appl Environ Microbiol*, 2009. 75(23):7537-41.

Distributed under the GNU General Public License

Type 'help()' for information on the commands that are available

For questions and analysis support, please visit our forum at <https://forum.mothur.org>

Type 'quit()' to exit program

[NOTE]: Setting random seed to 19760620.

Interactive Mode

```
mothur > make.contigs(file=200109_stability.txt, processors=30)
mothur > pcr.seqs(fasta=current, group=current, oligos=oligos.txt, pdiffs=1, rdoiffs=3)
mothur > summary.seqs(fasta=current)
mothur > screen.seqs(fasta=current, group=current, maxambig=0, maxlength=256,
maxhomop=8, minlength=248)
mothur > summary.seqs(fasta=current)
mothur > unique.seqs(fasta=current)
mothur > summary.seqs(fasta=current)
mothur > count.seqs(name=current, group=current)
mothur > summary.seqs(count=current)
mothur > pcr.seqs(fasta=silva.bacteria.fasta, start=11894, end=25319, keepdots=F)
mothur > system(mv silva.bacteria.pcr.fasta silva.v4.fast)
mothur > system(mv silva.bacteria.pcr.fasta silva.v4.fasta)
mothur > system(mv silva.v4.fast silva.v4.fasta)
mothur > align.seqs(fasta=200109_stability.trim.contigs.pcr.good.unique.fasta,
reference=silva.v4.fasta)
mothur > summary.seqs(fasta=current, count=current)
mothur > screen.seqs(fasta=current, count=current, start=1968, end=11550)
mothur > summary.seqs(fasta=current, count=current)
mothur > filter.seqs(fasta=current, vertical=T, trump=.)
mothur > summary.seqs(fasta=current, count=current)
mothur > unique.seqs(fasta=current, count=current)
mothur > set.current(count=200109_stability.trim.contigs.pcr.good.good.count_table,
fasta=200109_stability.trim.contigs.pcr.good.unique.good.filter.fasta, processors=24)
mothur > unique.seqs(fasta=current, count=current)
```

```
mothur > summary.seqs(fasta=current, count=current)
mothur > pre.cluster(fasta=current, count=current, diffs=2)
mothur > summary.seqs(fasta=current, count=current)
mothur > chimera.uchime(fast=current, count=current, dereplicate=t)
mothur > chimera.uchime(fasta=current, count=current, dereplicate=t)
mothur > summary.seqs(count=current)
mothur > remove.seqs(fasta=current, accnos=current)
mothur > summary.seqs(fasta=current, count=current)
mothur > classify.seqs(fasta=current, count=current, reference=silva.nr_v132.pcr.align,
taxonomy=silva.nr_v132.tax, cutoff=80)
mothur > summary.seqs(fasta=current, count=current)
mothur > remove.lineage(fasta=current, count=current, taxonomy=current,
taxon=Chloroplast-Mitochondria-unknown-Archaea-Eukaryota)
mothur > summary.tax(taxonomy=current, count=current)
mothur > cluster.split(fasta=current, count=current, taxonomy=current,
splitmethod=classify, taxlevel=4, cutoff=0.03)
mothur > summary.seqs(fasta=current, count=current)
mothur > make.shared(list=current, count=current, label=0.03)
mothur > get.groups(shared=current, groups=Negativelib1-Negativeplate9-
Negativeplate8-Negativeplate6-Negativeplate5-Negativeplate4-Negativelib2-
Negativelib3-Negativelib4-Negativelib5-Negativelib6)
mothur > remove.rare(shared=current, nseqs=5)
mothur > classify.otu(list=current, count=current, taxonomy=current, label=0.03)
mothur > count.groups(shared=current)
mothur > sub.sample(shared=current, size=1200)
```

APPENDIX D: IACUC APPROVAL

TTU-IACUC-16-17-003

INSTITUTIONAL COMMITTEE FOR THE CARE AND  
USE OF LABORATORY ANIMALS IN EXPERIMENTATION

COMMITTEE ACTION FORM

Principal Investigator or Activity Director Donald Walker

Campus Address Department of Biology, Box 5063, TTU

College Arts and Sciences Department/Unit Biology

Project Title The probiotic microbiome of endangered Tennessee bats: implications for  
biodiversity conservation

The project referenced above has been reviewed. The decision is as follows:

Approved as presented (Date of Approval 2/3/2017)

Approved with stipulations which are: (Date \_\_\_\_\_)

\_\_\_\_\_  
\_\_\_\_\_  
\_\_\_\_\_

Not approved for the following reasons: (Date \_\_\_\_\_)

\_\_\_\_\_  
\_\_\_\_\_

Signatures:



Committee Chairperson  
Dr. Steve Hayslett